BACTERIOPHAGE T4 LYSIS AND LYSIS INHIBITION:

MOLECULAR BASIS OF AN ANCIENT STORY

A Dissertation

by

TRAM ANH THI TRAN

Submitted to the Office of Graduate Studies of
Texas A&M University
in partial fulfillment of the requirements for the degree of

DOCTOR OF PHILOSOPHY

May 2007

Major subject: Biochemistry

BACTERIOPHAGE T4 LYSIS AND LYSIS INHIBITION:

MOLECULAR BASIS OF AN ANCIENT STORY

A Dissertation

by

TRAM ANH THI TRAN

Submitted to the Office of Graduate Studies of
Texas A&M University
in partial fulfillment of the requirements for the degree of

DOCTOR OF PHILOSOPHY

Approved by:

Chair of Committee,	Ryland F. Young
Committee Members,	Deborah Siegele
	Paul Fitzpatrick
	Michael Polymenis
Head of Department,	Gregory D. Reinhart

May 2007

Major subject: Biochemistry

ABSTRACT

Bacteriophage T4 Lysis and Lysis Inhibition: Molecular Basis of an Ancient Story.

(May 2007)

Tram Anh Thi Tran, B.S., Stephen F. Austin State University;

M.S., Stephen F. Austin State University

Chair of Advisory Committee: Dr. Ryland F. Young

T4 requires two proteins: holin, T (lesion formation and lysis timing) and endolysin, E (cell wall degradation) to lyse the host at the end of its life cycle. E is a cytoplasmic protein that sequestered away from its substrate, but the inner membrane lesion formed by T allows E to gain access to the cell wall. T4 exhibits lysis inhibition (LIN), a phenomenon in which a second T4 infection occurs ≤ 3 min after primary infection results a delay in lysis. Mutations that abolish LIN mapped to several genes but only *rV* encoding the holin, T, and *rI,* encoding the antiholin, RI, are required for LIN in all hosts which support T4 replication. Antiholin RI inhibits T-mediated lysis by direct interaction with the holin. T has at least one transmembrane domain with its N-terminus (T_{NTD}) in the cytoplasm and C-terminus in the periplasm (T_{CTD}). In contrast, the N-terminus of RI (RI_{NTD}) is predicted to function as a cleavable signal sequence allowing the secretion of the RI C-terminal domain (RI_{CTD}) into the periplasm. Most of RI mutations which abolish LIN occur in the RI_{CTD}, suggesting RI inhibits T-mediated lysis by interacting with T via RI_{CTD}. Topological analysis of RI and T showed that

fusion of PhoA signal sequence (^{ss}PhoA) to RI_{CTD} is necessary and sufficient for LIN and $^{ss}PhoA\Phi T_{CTD}$ interferes with RI-mediated LIN, indicating T and RI interact via periplasmic C-terminal domains.

In T4 infection, LIN is observed only when superinfection takes place, indicating either the antiholin or the LIN signal must be unstable. Both RI and $RI_{NTD}\Phi$PhoA are localized to both the inner membrane and the periplasm suggesting that the RI_{NTD} is a Signal-Anchor-Release (SAR) domain. Protein stability studies indicated that the SAR domain is the proteolytic determinant of RI, and DegP is the protease that is responsible for RI degradation.

To date, how T_{NTD} participates in lysis and LIN is not known. Modifications and deletion of the N-terminus of T change the lysis time, indicating this domain is involved the in timing of lysis. GFP fusion to holin T allowed microscopic visualization of fluorescent patches on the membrane at the time of lysis.

DEDICATION

This dissertation is dedicated to my dearest grandma and to my parents.

ACKNOWLEDGEMENTS

I would like to thank my mom, grandparents and aunts who raised me and gave me a wonderful childhood in Vietnam. I would like to thank my dad, who drives me crazy with his expectations, but I guess his strategy worked in some way. I also want to express my gratitude to Mr. and Mrs. Thornhill (I call them my American parents) who have helped me a lot, especially when I first started school here in the U. S.

I especially wish to thank Dr. Douglas K. Struck for his almost daily discussions and supervision. Without his moral support and genius strategies, I do not think I would get this far for this project. Thanks, Dr. Struck!

I would also like to thank all the members of the Young lab, past and present. Dr. Min Xu, a friend and a teacher, taught me so much about cloning. Dr. John Deaton taught me about protein purification, specifically membrane protein purification. Brenley McIntosh let me stay with her while I wrote my dissertation. It would be difficult to do this on the street. Carrie Langlais listened to all of my complaints. These are just some examples. The list goes on. Their friendship made the lab a fun place to work.

Last, I want to thank my PI, Dr. Ry Young, for giving me the opportunity to study in his laboratory. The "SWIM" with him every other week was fun, helpful and fruitful. He is serious about science and also very considerate about each student. Thanks, Ry!

TABLE OF CONTENTS

CHAPTER Page

LIST OF FIGURES

FIGURE Page

LIST OF TABLES

CHAPTER I

INTRODUCTION

The discovery of bacteriophages

Viruses were first recognized in 1899 by M. W. Beijerinck. He reported that the tobacco mosaic virus could not be retained by ceramic filters or seen with a light microscope, or grown on artificial media (129). At that time, the common perception of viruses was that they were very small and difficult to grow bacteria. However, it was thought that viruses would grow if a proper novel medium was presented to them (129).

Bacterial viruses were first reported by F. W. Twort in 1915 (129). Twort was among bacteriologists seeking the "novel" media on which viruses could grow. The rationale of his approach was that pathogenic viruses were descendants of non-pathogenic viruses, and non-pathogenic parents would be less difficult to grow *in vitro*. The virus he chose to study was smallpox (129). Despite hundred of attempts, Twort never succeeded in growing smallpox virus. However, when he inoculated the agar with the unfiltered liquid containing small pox virus, micrococcus, a contaminant in the solution, grew (32,129). Upon prolonged incubation, these micrococcus colonies became transparent and watery-looking. Twort called this phenomenon "glassy transformation" (129). To summarize his observations, (i) the glassy transformed

---

This dissertation follows the style of Journal of Bacteriology.

colonies would not grow on any medium, (ii) examination of the transparent area showed small granules and no bacteria, (iii) a healthy colony eventually became transparent if contacted by a glassy colony, (iv) the glassy material retained its ability to cause the glassy transformation after filtration, and the glassy transformation could be conveyed for an indefinite number of generations or after a million fold dilution, (v) and the glassy material retained its activity after being stored for more than six months but lost its activity when heated to 60^{o}C for one hour (32,129). Twort explained these observations as follows: (1) the glassy transformation might be a stage of the life cycle of the micrococcus itself that could pass to a non-glassy micrococcus culture and could stimulate the new culture to transform into the glassy stage; (2) micrococcus might have secreted an enzyme that led to its own destruction, (3) and the glassy transformation was the destruction of micrococcus as the result of viral infection (129).

At about the same time, another scientist, Felix d'Herelle, studied a similar phenomenon. In 1910, d'Herelle was studying an invasion of locusts in Mexico and how to eliminate them. He found locust coccobacilli, the bacterial pathogens of locusts. In the following years, he was invited to several other countries to terminate locust invasions using coccobacilli. In the process of getting pure coccobacilli cultures, he noticed clear and circular zones, 2-3 mm in diameter, within the bacterial lawn. When he examined these clear zones under the microscope, he could not see anything. He concluded that the agents causing clear zone formation were too small for microscopic observation. In addition, these clear zones were not reproducibly obtained, making further studies difficult (129).

In 1915, Felix d'Herelle returned to Paris and was asked to investigate an epidemic of dysentery. On various occasions, he obtained clear zones when the filtered emulsion from the feces of men suffering dysenteric infection was spread on the culture of dysentery bacilli. This led d'Herelle to test the effect of filtered stool on a turbid culture of dysentery bacilli from a newly admitted dysentery patient. On the fourth day, the once turbid broth culture was perfectly clear and all of the bacteria vanished like "sugar dissolved in water". As for agar spread with bacteria, there was no growth. He speculated that if the same thing happened within the intestine of the dysenteric patient, the patient would be cured. D'Herelle ran to the hospital to check on that patient, and the patient's general condition was improved overnight and recovery had begun. D'Herelle called this curing agent an "anti-microbe". In 1917, d'Herelle published these observations, stating that in the absence of dysentery bacilli, the anti-microbe could not grow on any media, and the anti-microbe could not attack heat-killed bacilli whereas they grew perfectly well on saline washed bacilli. He concluded that the anti-dysentery microbe was an obligatory "bacteriophage", literally meaning bacteria-eating and also known as phage (32,129). Throughout this dissertation, the terms bacterial virus, bacteriophage or phage will be used interchangeably.

In 1918, d'Herelle published a second note presenting the case histories of thirty-four dysentery patients. His conclusion was that the pathology of dysentery was dominated by two opposing factors: the dysentery bacillus as the pathogenic agent and the filterable bacteriophage as the agent of immunity (129). If the bacteria were "winning", the condition of the patient became worse. If the phage took over, the patient

was on the road of recovery. D'Herelle generalized his observations and quickly found similar phenomena in patients recovered from typhoid fever and in chicken infected with avian typhosa (129). After a period of disbelief and criticism, numerous medical bacteriologists joined d'Herelle in finding bacteriophages that could cure bacterial infections (129). It is clear that d'Herelle gave bacteriophages a glamorous role in bacteriology in the 1920's as an agent to control bacteria borne diseases (17). By the middle of 1930, this glamorous role began to fade because the idea of using bacteriophage therapeutically failed to materialize. Why bacteriophage, so virulent *in vitro*, were impotent *in vivo* was a mystery at that time. The problems with phage therapy were mostly due to ignorance, such as a lack of a systematic testing of virulence of phages against infectious bacteria and of the knowledge of proper dosage used in patients (53).

D'Herelle was interested in bacteriophage not only as an agent to control bacterial infections but also as a material for studies of basic science. D'Herelle developed an assay to determine concentration, or titer, of bacteriophage in a filtrate (also known as lysate) by limiting dilution in liquid culture. In other word, he identified the dilution at which the bacteriophage could no longer lyse the bacterial host consistently. For example, he found only 3 out of 10 tubes of turbid cultures lysed upon addition of 10^{-11} mL of the original lysate, meaning the lysate contained between 10^{10} to 10^{11} bacteriophage per mL. He also took advantage of the appearance of clear zones on the dense bacterial lawns, or **plaques**, to calculate the number of phage in a lysate. The total number of plaques per mL was inversely proportional to the dilution of the

bacteriophage lysate mixed with bacterial culture. Therefore, he proposed that each of the plaques represented a bacteriophage colony descended from a single parental virus. He also demonstrated that bacteriophage first **fixed**, or attached to, the bacteria it later destroyed, and is now termed phage **adsorption**. After incubation of bacteriophage with its host for a few minutes, the bacteria were pelleted and the supernatant was titered for phage concentration. The results showed that the titer in the supernatant was much less than the titer of input lysate suggesting that the phage loss was due to the adsorption of phage to the host cells. However, this observation was only true when bacteriophage was incubated with its respective host, indicating the adsorption was **specific** (129).

Bacteriophage life cycle

Like all other viruses, phages are not living organisms. They are pieces of genetic material protected by protein or protein-lipid shells called capsids, and they are able to utilize host machinery to replicate. There are five major stages in the bacteriophage life cycle or phage vegetative growth:

1. Infection of a new host (adsorption and penetration of its genetic material)
2. Expression of the bacteriophage genes ("early genes")
3. Replication of bacteriophage DNA or RNA
4. Expression of late genes and assembly of new virions
5. Escape from the host cell by lysis

Phages that replicate exclusively by vegetative growth, like T4, are termed "virulent" or "lytic" (26,49,79,87). Some bacteriophages, such as lambda (λ)-like phages, can alter this life cycle by becoming a prophage. This involves integrating the phage genomic DNA into the host genome and replicating along with the host genome or alternatively, becoming a stably replicating plasmid (18). For both cases, this state is known as lysogeny, and the phage genes are generally not expressed, except for the lysogenic repressor. Phages that can undergo lysogeny like λ are known as "temperate" or "lysogenic" phage.

Strategies of progeny release from infected host

Once an infection is successful and virus particles are assembled, phages must escape from the host to find new prey. Progeny release into the medium is prevented by the cell wall. The cell wall, or peptidoglycan, is a continuous mesh of glycan strands that are cross-linked together by di-isopeptides (55). This layer protects bacteria from osmotic lysis and also is the shape-determinant of bacterial cells. Phages use several strategies to release the phage progeny from the infected host. Due to their unique morphogenesis, filamentous phages, such as M13, can extrude themselves through the host envelope without fatal consequences to the host (93,137). All other known phages release progeny by lysis of the host (146).

Lysis by small phages

To lyse the host, phages have to compromise the peptidoglycan layer. There are two ways to accomplish this: actively degrade the cell wall or inhibit peptidoglycan synthesis. The cell wall is not a static, rigid structure but a highly dynamic structure that constantly undergoes biogenesis when the cell is growing (101). The most accepted current model of peptidoglycan growth is the "three-for-one" model proposed by Höltje as shown in Fig 1.1 (55). During elongation, three new glycan strands replace one old glycan strand in the peptidoglycan layer (Fig 1.1A). At the constriction site (developing septum), three new glycan strands also replace one old glycan chain in the peptidoglycan layer, but the formation of constriction is the result of repeated additions of new glycan strands at the same site (Fig 1.1B)(55). Insertion of new glycan strands requires removing the cross-linker peptide and then re-establishing new cross-links. Inhibition of peptidoglycan biogenesis, coupled with turn over and/or recycling, during active growth, weakens the cell wall and eventually results in cell rupture from the osmotic pressure difference between the internal and external environment of the bacterium. This is the strategy that some small single stranded (ss) DNA and ssRNA phages utilize to elicit host cell lysis. For example, the A_2 protein of ssRNA phage Qβ and the E protein of ssDNA phage ϕX174 inhibit cell wall synthesis at different steps but with the same terminal phenotype, lysis when the cell is growing. A_2 inhibits MurA, the first enzyme in the dedicated peptidoglycan precursor biosynthesis pathway, and E inhibits MraY, the only membrane-embedded enzyme in the same pathway (7-10).

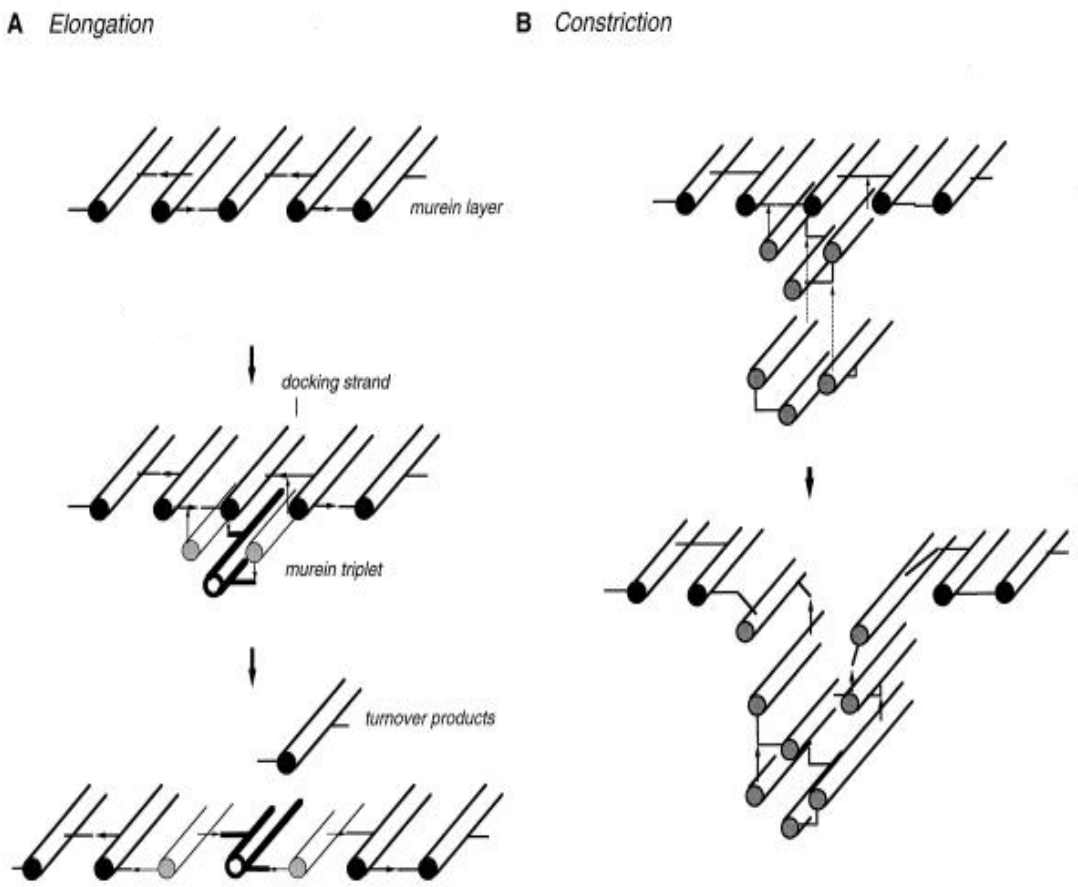

FIG. 1.1. Peptidoglycan growth according to the three-for-one model. (A) Peptidoglycan synthesis during cell elongation. Free preexisting glycan strands form a murein triplet. The triplet is then attached to the peptide bridges on the right and the left of the docking strand in the peptidoglycan layer. Removal of the docking strand by murein hydrolase results in the insertion of 3 glycan strands in place of 1 strand. This is proposed to occur all over and at different sites of an elongated cell. (B) Peptidoglycan synthesis at the constriction site. Similar proposed mechanism as in peptidoglycan growth of the elongated cell, but instead of uniform insertion at different sites of the cell wall, the repeated addition of glycan strands at one site is proposed to result in the constriction of the cell (55).

Lysis by large and double stranded DNA phages

According to the classical lysis paradigm, large double stranded (ds) DNA phages require two proteins for lysis, the endolysin and the holin (146). The endolysin is an enzyme that degrades the cell wall, but it is sequestered in the cytoplasm. This is why the holin is required for lysis. The holin is a membrane protein that accumulates in the cytoplasmic membrane, without harming the cells, until a genetically programmed time, when they trigger to form lesions in the membrane. The hole needs to be large enough to allow the endolysin to pass through the membrane and into the periplasm where it has access to the cell wall. At this point, the endolysin degrades the cell wall and lysis occurs (146). Hole formation also causes the collapse of membrane potential. However, recent findings suggest a more general role of holin in lysis. The endolysin of phage P1 and phage 21 were found to have an N-terminal SAR (signal anchor release) domain (145). The SAR domain allows the endolysin to be translocated and anchored in the membrane in an inactive form. Hole formation by holin collapses the membrane potential which facilitates the release and activation of the SAR endolysin. The endolysin is then free in the periplasm to degrade the cell wall and cause lysis (145). In both systems, hole formation by the holin frees the endolysin from an inactive state, but the mechanisms are different. In the classical paradigm, hole formation by the holin opens a path for active, sequestered endolysin and allows it to gain access to its substrate. In the new paradigm, hole formation allows the release of the endolysin from the membrane, resulting in activation of the enzyme. In either case, the holin controls the timing of lysis. It should be noted that SAR endolysins can spontaneously be

released from the membrane at a slow rate. Therefore, holins are not essential for lysis or plaque formation in phages with a SAR endolysin (145).

Endolysins

To be classified as a lysozyme, Salton (117) stated that a protein should catalyze an enzymatic reaction that results in: (1) the liberation of glucosamine and muramic acid from bacterial cell wall, (2) the generation of reducing groups and (3) the lysis of bacteria under proper conditions (69). An enzymatic activity was found in the phage-free T2 and T6 lysates that was able to lyse chloroform-killed bacteria. The material released from the cell wall was similar to that from a reaction using lysozyme. Thus, the conclusion was that the enzyme mediating this reaction was a phage lysozyme (68). Later, the word endolysin was used to described the lytic substance in the phage λ lysate (59). This term was later broadened and used for any phage-encoded enzyme that was required for host lysis (146). An endolysin can possess one or more of the four following enzymatic activities: glycosidase, transglycosylase, endopeptidase and amidase, as illustrated in Fig 1.2. A glycosidase, or true phage lysozyme, such as T4E, hydrolyzes β(1, 4)-glycosidic bonds (134). A transglycosylase, such as λR, also attacks glycosidic bonds, but instead of generating reducing ends, it forms a cyclic 1,6-disaccharide product (11). Endopeptidases, such as PLY118 and PLY500 of *Listeria monocytogenes* phages A118 and A500, respectively, cleave between amino acid residues in the cross-linking oligopeptide (81). Finally, an amidase, such as the bacteriophage T7 amidase, cleaves the amide bond between aminoglycosidic subunits

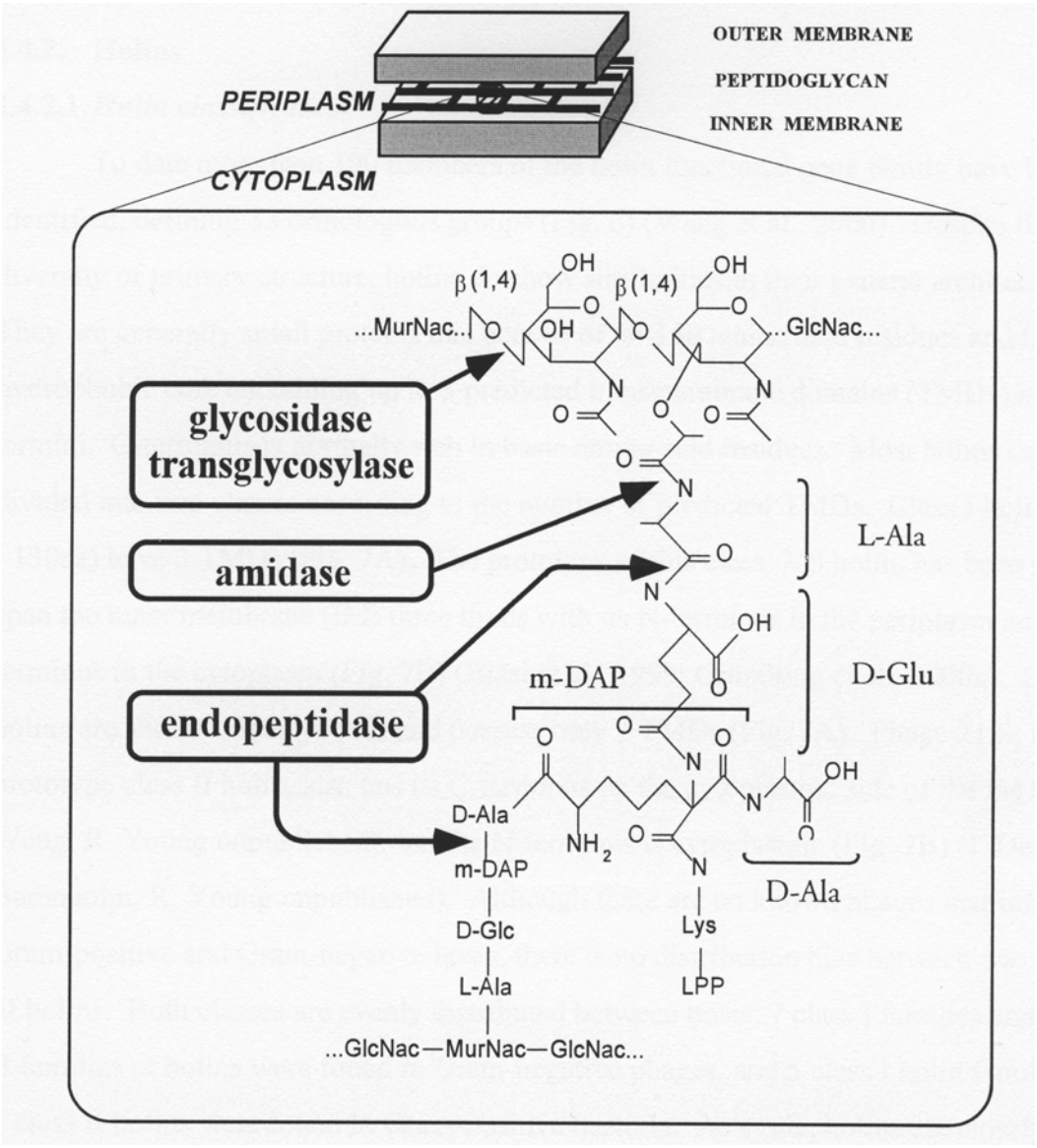

FIG. 1.2. Gram-negative bacterial peptidoglycan structure and sites of cleavage by various endolysins. Abbreviation: GlcNac, N-acetylglucosamine; MurNac, N-acetylmuramic acid; L/D-Ala, L/D alanine, D-Glu, D-glutamic acid; m-DAP, meso-diaminopimelic acid; Lys, lysine; LPP, Braun's lipoprotein (107)

and the tetrapeptide chain (56). The crystal structures of T4E glycosidase, λR transglycosylase and T7 amidase have been determined. T4E glycosidase (142) and λR transglycosylase (38) have similar folds with their active sites located in a crevice between two lobes connected by a helix (39). The structure of T7 amidase is very different compared to the structure of T4E and λR, as it has only one lobe (20). While T4E and λR have critical acidic residues on the opposite sides of the catalytic cleft (E11/D20 of T4E and E19/D34 for λR), no acidic residues are found in the catalytic cleft of T7 amidase (20,39). Instead, the residues important for catalytic activity of T7 amidase are lysine 128 at the top of the catalytic cleft and tyrosine 46 and histidine 17 at the base of the catalytic cleft (20).

Holins

The best studied holin is the holin of bacteriophage λ, S105, a product of the *S* gene. S105 has 105 amino acids with three transmembrane domains (TMD) arranged with the N-terminus out and C-terminus in (Fig 1.3) (46). The formyl group at the N-terminus of S105 is retained, indicating that TMD1 is integrated into the membrane rapidly and before cytoplasmic deformylase can act (R. White et al., manuscript in preparation). The wild type S105 holin mediates lysis at ~ 50 min after infection. Raab (106) isolated a number of *S* mutants with single amino acid changes that delayed the lysis time. In addition, there is another set of mutants that were completely defective in lysis (105) even though the proteins were expressed at the wild-type level (47). In cross-

linking experiments using cells expressing wild type *S* gene, S protein oligomers were detected up to a hexamer (149). Additional cross-linking experiments with lysis defective mutants showed that $S105^{A48V}$ could not form dimers while several others, $S105^{A52V}$, $S105^{A23V}$, $S105^{D60N}$ or $S105^{R33L}$, could not form higher order oligomers. Another mutant, $S105^{R59C}$, could form oligomers but could not lyse the host, indicating lesion formation was defective (47,105). Together, these results suggested that to form a hole, S105 has to dimerize, oligomerize and then undergo a concerted conformational change at the tertiary or quaternary level (47).

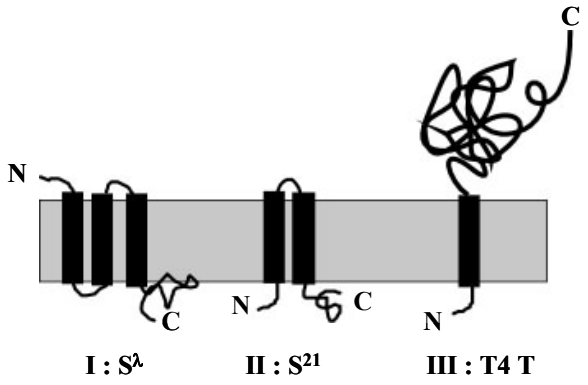

FIG. 1.3. Topology of class I, II and III holins (133).

The holes formed by S105 were big enough for cmycRΦLacZ to cross the membrane and degrade the cell wall (139). The cmycRΦLacZ was a fusion of N-terminal cmyc (EQKLISEEDL) tagged λR endolysin to the N-terminus of the entire LacZ (β-galactosidase) protein (139). The molecular weight of this fusion protein is ~ 119 kDa (139). When LacZ is folded properly, it exists as a tetramer in solution (60) with ~ 500 kDa molecular weight. The cmycRΦLacZ chimera was found to be fully

active and had a ~ 0.5 MDa molecular mass as judged by size exclusion chromatography (139). From the crystal structure, the dimension of a β-gal tetramer is 17.5 x 13.5 x 9.0 nm (60). Lysis mediated by holin S105 and cmycRϕLacZ was almost identical, in term of kinetic, to the lysis mediated by S105 with cmycR. Thus, the hole formed must be larger than this dimension. Therefore, the hole formed by holin S105 should be significantly larger than 20 nm (139).

There are at least three classes of holin proteins, as shown in Fig 1.3. The prototype of class I is the bacteriophage λ holin with three TMDs (46). Class II, with two TMDs, can be divided in to two subclasses, IIA and IIB. An example of class IIA is S68 of phage 21. Although S68 has two predicted TMDs, TMD1 has been shown to be a SAR domain and exits the membrane, leaving TMD2 in the membrane and the C-terminus in the cytoplasm (102). Even though there is no well-studied example for class IIB, the speculation is that class IIB members are S68 holin relatives that possess a TMD1 that remains membrane embedded (102). Most holins identified in phage genomics studies were of class I or II, based on the predicted transmembrane topology. Also, these holins are very diverse; more than 50 unrelated families of class I and II holins have been identified. Class III consist of a single family, the prototype of which is bacteriophage T4 holin T. T, encoded by T4*t*, is predicted to have the N-terminus inside and the C-terminus outside of the membrane with a single TMD (108).

T4 biology

T4 life cycle

Bacteriophage T4 is a large and complex bacterial virus as shown in Fig 1.4. The T4 particle consists of an icosahedral head that is attached to a contractile tail via a neck structure where six whiskers (gene product (gp) *wac*) are attached. The contractile tail is composed of a contractile tail sheath of gp*18* monomer units surrounding a non-contractile tail tube comprised of gp*19* monomer units (34). The end of the tail is attached to a hexagonal baseplate where the long and the short tail fibers are attached. The adsorption apparatus, composed of the contractile tail, long tail fibers, short tail fibers and the baseplate, makes T4 infection (i.e. absorption to the host and injection of its DNA) exceptionally efficient, 99% after 5 min of incubation with the host (22).

The T4 head contains a linear dsDNA of about 172 kb. The genome of T4 is 168,903 bp, encoding nearly 300 gene products, almost half of which have not been characterized (92). Only 63 genes are essential for phage growth (92). Over 65 kb of T4 genome is occupied by structural genes of the phage head, tail and tail fibers and genes necessary for phage particle assembly. More than 40 polypeptides are present in the phage particle, a large number compared to simple viruses where the capsid can be made from a single protein, such as tobacco mosaic virus or ΦX174 (33,34). T4 DNA replication generates concatemeric DNA molecules of multiple unit genomes. T4 packaging begins at a random site on the concatemer and proceeds by headful packaging. The T4 head can accept 102% of a unit genome length, so every T4 particle

contains a dsDNA with a 3.4 kb terminal redundancy (89). T4 DNA is circularly permuted in a population of particles, so the T4 genetic map is circular even though the genomic DNA in each virion head is linear.

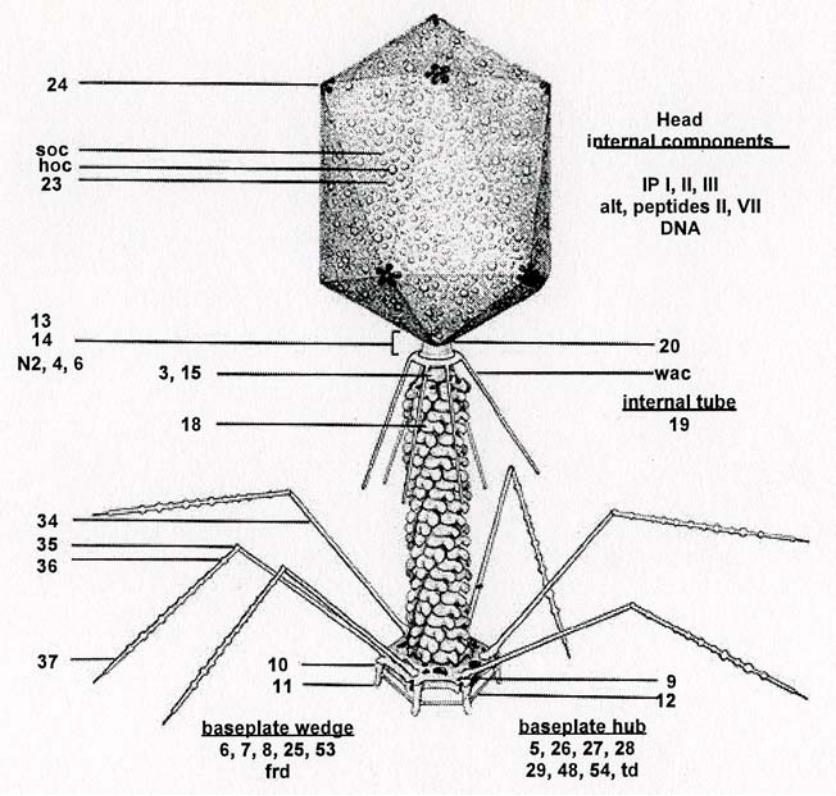

FIG. 1.4. Structure of bacteriophage T4, based on chemical cross-linking and on electron-microscopic structure analysis to a resolution of about 2 to 3 nm (43). Locations of known viral proteins are shown.

The T4 virion is more than just a container filled with viral genomic DNA. It undergoes a number of structural changes during infection. When a T4 encounters an *E. coli* cell, one or more long tail fiber binds reversibly to receptors on the surface of the host (either the diglycosyl residue of lipopolysaccharide (LPS) (43) or OmpC protein in

the exterior surface of the outer membrane (41)). Reversible binding of the long tail fibers allows T4 to "walk" on the surface of the host and eventually bring the baseplate closer to the cell surface. This event allows the short tail fibers to be released from their stored position and bind irreversibly to the surface of the host (114). This irreversible binding creates a tension that is transmitted to the closed conformation of the hexagonal baseplate and causes it to expand into the open hexagram (star) conformation (123). The star conformation induces a conformational change of gp*18*, which propagates in the manner of "falling dominos", and results in the contraction of the tail sheath (33,94). The sheath is contracted to approximately 37% of its length and drags the base-plate along with it. Because the baseplate is fixed to the cell surface, this process drives the tail tube downward into the bacterial cell (123). The tube penetrates through the cell wall with the help of gp*5*, a lysozyme and a part of the baseplate hub, and reaches the outer surface of the cytoplasmic membrane (64). Through an unknown process, a channel is formed in the cytoplasmic membrane and, subsequently, T4 DNA is released into the host cytoplasm through the tail tube (123).

The detailed mechanism of how DNA is released from the head into the host cytoplasm is not known, but DNA uptake requires the proton motive force, specifically the membrane potential and not the pH gradient (42). DNA ejection takes place only when the tube interacts with the cytoplasmic membrane (42). Although the tail sheath contraction can be induced by treatment with 6 M urea, formaldehyde or exposure to LPS, DNA ejection does not occur (42,43). In addition, ion leakage occurs during DNA injection, but stops when injection is complete (122). This suggests that the channel that

is formed by either host proteins, phage proteins or both is sealed after injection. Alternatively, Furakawa and Tarahovsky (41,42,95) proposed that the T4 tail tube protrusion penetrates the outer membrane by the mechanical force generated by the tail sheath contraction, and somehow induces a local fusion zone of inner and outer membranes. Then, the tail tube acts as a channel to deliver the DNA into the host through the fusion zone (95). In either case, ion leakage stops within a few minutes after infection, indicating that membrane lesion is sealed (122).

Injection of T4 DNA into the host starts the T4 vegetative cycle. The chronology of major events of T4 development is shown in Fig 1.5. T4 transcription utilizes three major classes of promoters, early (Pe), middle (Pm) and late (Pl), which broadly define the T4 developmental cycle. Many genes are served by multiple classes of promoters, and T4 relies entirely on host RNA polymerase for its transcription (92). Host replication, transcription and translation are blocked almost immediately after T4 infection (77). Gp*alt* is a protein that comes with the T4 DNA into the host cytoplasm and is responsible for host RNA polymerase (RNAP) modification. Gp*alt* ADP-ribosylates the α subunit of host RNAP to diverge it to transcribe T4 DNA. Genes involved in shutting down host metabolism are transcribed and translated to perform a number of functions. First, Gp*ndd* morphologically disrupts the host nucleoid while other phage encoded endonucleases, such as gp*denA*, gp*denB* and gp*46*/*47*, degrade host DNA to mononucleotides (95). T4 genomic DNA contains glucosylated hydroxymethyl cytosine, instead of cytosine, which allows the T4 nucleases to distinguish the difference between T4 genomic DNA versus host genomic DNA (95). Second, Gp*alc* is an RNAP

binding protein that diverts *E. coli* RNAP from transcribing the cytosine-containing host DNA to transcribe the glucosylated hydroxymethyl cytosine-containing phage DNA (95). Also, ModA and ModB ADP-ribosylate the α subunit of RNA polymerase so that transcription from the T4 middle promoter can take place later (92). Another protein, MotA, is a transcription factor that binds the Mot box at about the -30 position in the middle promoters and allows transcription of genes under control of these promoters to occur (92). Lastly, AsiA is an anti-sigma factor that activates middle mode transcription by forming an AsiA-σ^{70} dimer. The interaction of AsiA and σ^{70} interferes with recognition of early promoters, and stimulates T4 transcription from the middle promoters (92).

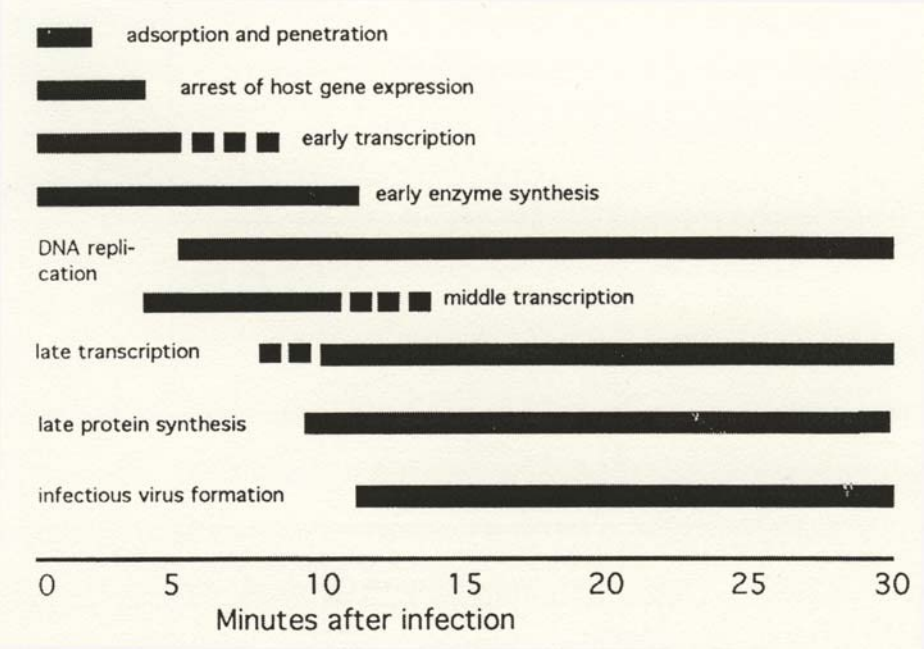

FIG. 1.5. Chronology of T4 development (89).

Mononucleotides obtained from the degradation of the host chromosome are only sufficient to synthesize about twenty T4 genome equivalents. The remaining deoxyribonucleotides necessary for T4 DNA synthesis come from *de novo* synthesis catalyzed by phage enzymes, which are also early gene products. Other proteins that are early gene products are involved in replication and recombination machineries, modification of the T4 DNA to protect it from restriction, tRNAs that decode codons abundant in the T4 genome, but not the host, and at least one sigma factor required for late gene transcription.

Once the T4 DNA replication machinery is made, DNA replication begins. At this time, transcription switches to the "late" mode. All late gene products are made including proteins involve in morphogenesis and lysis of the host to release phage progeny. T4 does not utilize the host σ^{70} factor for late gene transcription. Rather, late promoters are recognized by a T4-encoded sigma-factor, σ^{55}, which is not sufficient to initiate late transcription alone. T4 encodes another protein, gp*33*, which acts as a co-activator for late transcription by mediating the binding of σ^{55} and gp*45*. Gp*45* is the trimeric sliding clamp of the DNA replication complex, and once it is loaded, gp*45* slides on the DNA and enhances the opening of late promoters more than 1000 bp away from the loading site (92). Association with gp*45* allows σ^{55} to transcribe late genes. At the time of late gene expression, there is insufficient number of the σ^{55} molecules to compete for RNAP. However, late transcription out-competes middle transcription because of several factors. First, both α subunits of RNAP are ADP-ribosylated which enhances the affinity of σ^{55} for RNAP. Second, RpbA, a T4-encoded protein, is bound

to the RNAP core (70) and acts as a decoy to help σ^{55} compete for RNAP. Lastly, the T4 Srd protein resembles a segment of RNAP that interacts with σ^{70} and σ^{38} which helps σ^{55} compete for RNAP (92). Twenty-five minutes after infection, ~100 phage progeny are assembled inside the host, and the vegetative cycle of the T4 is terminated by lysis of the host cell.

T4 lysis

T4 utilizes the holin-endolysin strategy to lyse the host at the end of the infectious cycle (61,132,146). The holin of T4 is T, or gp*t*, and the endolysin is E, or gp*e*. Both of these genes were identified by genetics as mutants that failed to lyse the host but retained the ability to produce virions. T4$t^{+}e^{-}$ does not lyse the host, but the cell stops respiring at 25 min after infection, and there is no phage accumulation after the cell ceases to respire (96). T4$t^{-}e^{+}$ does not lyse the host; the cell continues to grow, and phage particles continue to accumulate indefinitely. Lysis of these mutants can be achieved by adding chloroform, which dissolves the membrane and releases the endolysin (61,62). Lysis mediated by wild type T4 at the end of the vegetative cycle is called lysis from within or LI.

Lysis mediated by the T4 holin and endolysin is rapid; the culture changes from turbid to clear in a few minutes. Premature lysis by T4 can be induced by the addition of chemicals that compromise the membrane potential or by switching to anaerobic growth late (~17.5 min after infection) in the latent period (28,62). However, compromising the

membrane potential early (~7.5 min after infection) in the latent period does not induce premature lysis (28), presumably because late gene expression has barely started and so little holin or endolysin is present.

Endolysin E

In 1961, Streisinger mutagenized T4 in order to isolate temperature-sensitive mutations that affected the lysozyme activity of T4 phage, and he called these mutations T4*e* (132). Gene *e* was mapped between 66.4 and 67.0 kb on the T4 map (78). Gene *e* is served by both early and late promoters as shown in 1986 by McPheeters and colleagues (90). Endolysin E is one of the most well-studied enzymes in terms of structure, mechanism and stability (88). E activity can be detected as soon as 8 min after infection, and accumulates in a fully folded form in the cytoplasm throughout morphogenesis (19). Because E lacks a secretory signal sequence, it cannot cross the cytoplasmic membrane to degrade the cell wall (146). Therefore, E-mediated lysis is subjected to the timing program of the holin T (141).

Gp5 as another muralytic enzyme

Infection of *E. coli* at a high multiplicity of infection (m.o.i.) (≥ 50 phages per cell) results in lysis and release of cell wall components. In addition, lysis also can be observed when *E. coli,* resuspended in PBS (phosphate saline buffer), are infected at a low m.o.i. with either T4 wild type or T4 “ghosts”, which are osmotically shocked T4

with empty heads (58). This kind of lysis is called lysis from without or LO. For some time, both of the above muralytic activities were believed to originate from T4 lysozyme E. However, an experiment by Loeb (1974) showed that cell wall fragments were released during the adsorption process, even when *E. coli* was infected with a T4*e* null mutant. This suggested that the cell wall degradation at the time of adsorption was not the result of E activity. In 1980, Kao and McClain isolated T4 mutants that allowed lysis in the absence of gene *e*. These mutations were mapped to gene *5*. Gene *5* is in the first cluster of tail genes between 75.3 to 92.1 kb in the T4 map (22), and it is served by the late promoter (78). The lysozyme activity of gp*5* was confirmed *in vitro* by Nakagawa et al. (98). In addition, Lin et al. (1989) found significant sequence homology between gp*e* and the middle region of gp*5*. Expression of gp*5* from a plasmid gave rise to a protein with an apparent molecular weight of 63 kDa, but the gp*5* isolated from T4 particles had an apparent molecular weight of 42 kDa, indicating the gp*5* incorporated into the phage particle is processed during morphogenesis (22). Among the revertants that suppressed the E defective phenotype, there were alleles that were temperature-sensitive for assembly of gp*5* into the baseplate hub (34,35,66). Cell wall degradation appeared to be better when gp*5* was free as compared to when it was in the hub complex (65). The simplest interpretation of these data was that the suppression of the lysis defect due to the absence of endolysin E could be accomplished by mutations in gp*5* that had conditionally lost the ability to incorporate into the baseplate hub complex. This way, there are some gp*5* that are free and some that are incorporated into the hub complex. Gp*5* that is incorporated into the hub complex allows the maturation

of infectious particles, and the free gp*5* with cell wall degrading activity replaces E to become the endolysin to restore lysis.

Spackle involved in lysis

Spackle (sp) mutations were isolated in 1968 by Emrich (35) as pseudorevertants that suppressed the loss of function of E. This suppression is temperature-sensitive, as T4 *e sp* gives plaques at 43^{o}C, but not at 30^{o}C (35). T4*sp* gave small wt (wild type) plaques at 30^{o}C, large *r* plaques at 43^{o}C, and at 37^{o}C, the plaque size was variable and intermediate between wt and *r* plaques (35). Even though the intracellular phage accumulation was about the same for T4 wt, T4 *e* and T4 *e sp*, phage liberation of T4 *e sp* was only 10% compared to the wt T4 (35). Because of the incomplete suppression of the loss of function of E, this gene was named spackle. Since E activity is required for lysis and spackle mutations restored lysis in T4*e* mutants, the speculation was that spackle mutations somehow increased lysozyme activity. However, the lysozyme activities of T4*e* and T4*e sp* were not different from each other (35). As mentioned in the gp*5* section, mutations in gene *5* also suppress T4*e* defective mutants, and free gp*5* seems to participate better in lysis compared to gp*5* in the hub complex (66). This led to the speculation that spackle inhibited the lysozyme function of gp*5*. In the absence of the spackle protein, the lysozyme function of gp*5* is no longer inhibited; thus, gp*5* can replace gp*e* to cause lysis from within (66).

As mentioned earlier, LO occurs when *E. coli* cells are infected with a high m.o.i. of T4 because of multiple punctures of the cell wall by gp*5* located on the base plate hub

complex. However, when the cells are infected by low m.o.i. and then superinfected with a high m.o.i., LO does not occur (138). This phenotype is possible because an infected cell produces proteins that change the cell envelope such that it becomes resistant to LO. One of these proteins is spackle. Cells infected with T4*sp* are more sensitive to LO than cells infected wild type T4 (35).

Spackle phenotypes are recessive based on the following evidence: (1) T4*e* does not lyse the host, but T4*e sp* does. In mixed infections of T4*e* and T4 *e sp*, no lysis is observed. (2) Cells pre-infected with T4 wild type are LO resistant while cells pre-infected with T4 *sp* are LO sensitive. Pre-infecting cells with a mixture of T4 *sp* and wild type T4 gives a culture that is LO resistant (35).

In 1988, the spackle gene was mapped to gene *40*, but Abedon invalidated this result in 1994 (63). In 1999, the spackle mutations were mapped to gene *61.3*. Mutations generated in gene *61.3* gave the same phenotype as the spackle mutants that Emrich isolated in 1968. In addition, the complementation experiment using gene *61.3* expressed from a plasmid in T4*sp* infected cells had a similar phenotype as coinfection of *E. coli* with T4 wild type and T4*sp* (63).

Holin T

Streisinger observed that T4*e* mutants failed to lyse the host at the normal lysis time, but the cells also stopped growing (96). T4*e* mutants failed to make plaques, but plates that were supplemented with 5 mM Tris pH 8, 0.25% citrate and 500 μg of egg white lysozyme complemented this defect (36). Based on this observation, Josslin

(1970) hypothesized that there were at least two components of T4 lysis, one which subverted the integrity of the cytoplasmic membrane, resulting in the cessation of host respiration of the infected cells and liberated the second, which was the phage lysozyme. Phage lysozyme then degraded the cell wall, resulting in lysis and release of progeny phage. Using 2-aminopurine (2-AP) and 5-bromodeoxyurindine (5-BUdR) as mutagens, he isolated two mutants, amA3 and amB5, that plated on the permissive amber suppressor host, but not on the restrictive non-suppressor host. In both mutants, phage lysozyme was synthesized; however, lysis was not observed, and phage accumulated beyond the normal lysis time. Josslin called the gene responsible for the lysis defective phenotype of T4 "*t*" for Tithonus. (Tithonus was the son of the dawn goddess Aurora and a Trojan prince. Since Tithonus was an "underbred" god, he was awarded a diminished sort of immortality, one that did not protect him from aging (61).) One possible explanation of T function was to inhibit cellular respiration, which somehow allowed E to degrade the cell wall. This interpretation led to another question, could chemicals or agents that inhibited cellular energy metabolism complement the lysis defect of T4t_{am}? Addition of cyanide or switching to anaerobic growth condition induced premature lysis of cultures infected with wild type T4. However, neither of the above restored lysis in *t*-defective T4 (62). The simplest interpretation was that inhibition of cellular respiration was not the function of T, but rather, was the result of the function of T. Josslin proposed a model in which T disrupted the cytoplasmic membrane, which then destroyed the electron transport chain (62).

Gene *t* was mapped at about ~ 160 kb in the T4 genome, between gene *38*, encoding a long tail fiber modifying protein, and gene *motA*, encoding the middle gene activator (113), and is served by a late promoter (78). The T amino acid sequence is shown in Fig 1.6. T is unusually large for a holin with 218 amino acids (a a). Most holins are about 60-120 a a; for example, the class I S105 holin of bacteriophage λ is105 a a and the class II holin of phage 21 is 68 a a.

```
    +       -       -+  +-     +     +                +
MAAPRISFSPSDILFGVLDRLFKDNATGKVLASRVAVVILLFIMAIVWYR
        10         20         30         40         50
    K                                     V

 -    -  +  + -    -  -+-+  + -     -          - -
GDSFFEYYKQSKYETYSEIIEKERTARFESVALEQLQIVHISSEADFSAV
        60         70         80         90        100
                          I

   + +       -     - +       -+        -+  --        +
YSFRPKNLNYFVDIIAYEGKLPSTISEKSLGGYPVDKTMDEYTVHLNGRH
       110        120        130        140        150

     +       ++    -              -             + -
YYSNSKFAFLPTKKPTPEINYMYSCPYFNLDNIYAGTITMYWYRNDHISN
       160        170        180        190        200

-+ -        +    + +
DRLESICAQAARILGRAK
       210
```

FIG. 1.6. Amino acid sequence of T. Underlined is the predicted TMD of T. Bold residues are mutations in T that makes it LIN insensitive (i.e., *rV* alleles of *t*).

Expression of the *t* gene from a high copy number pUC19 plasmid (500-700 copies/cell) under the lac repressor control was lethal (84). Induction of the *t* gene from the same plasmid with IPTG complemented the lysis defect of a λ*Sam7* lysogen although the complemented lysis was rather gradual (84) in contrast to lysis mediated by the S105 holin which was sharp and rapid. A chimera with mature OmpA replacing residues 1-35 of T was not toxic to cells. This chimera could be expressed abundantly for purification, and purified OmpA-T was used to raise antibodies against T. Detection of T using these antibodies was possible only when T protein was labeled with [^{35}S] methionine followed by immunoprecipitation prior to SDS-PAGE and autoradiography. Cellular fractionation of cells expressing T indicated that T was associated with the cytoplasmic membrane. This result was confirmed with the sodium hydroxide extraction of membrane from cells expressing T, where T protein ended up in the pellet of a sodium hydroxide wash (84). In addition, cross-linking experiments using DSP (dithiobis[succinimidyl propionate]), showed that T formed a dimer, trimer and tetramer with increasing concentration of cross-linker (84). These results suggested that T acted in an oligomeric form in the membrane.

The T-mediated lysis observed by Lu et al. in 1992 was very gradual making it unclear whether T really was functioning as a holin. However, a series of experiments were performed by Ramanculov to confirm that T was the holin of T4. In these experiments, *S105* was replaced by *t* in the λ lysis cassette, as shown in Fig 1.7, and this cassette was cloned into a pBR322-derivative plasmid called pER-T. This plasmid was used to recombine *t* onto λ to make the hybrid phage λ-*t*. Induction of the λ-*t* lysogen

resulted in the saltatory lysis at approximately 23 min (108,109). The extremely short latent period of λ-*t* reduced the burst size almost two orders of magnitude compared to the parental λ phage, and the plaque morphology was also reduced to pin-point size (108). The defect in plaque morphology of λ-*t* was exploited to isolate mutants that produced bigger plaques and had higher plating efficiencies, that is, plaque size increased as a result of mutations in *t* gene that delayed lysis (108). All mutants obtained, either from spontaneous or UV mutagenesis, had longer lysis times than wild type λ-*t*; they had point mutations that changed a single amino acid in T. Among these mutants, increasing plaque size correlated with increasing lysis time up to about 50 min, the normal lysis time of λ (108). The plaque size stayed constant with lysis time between 50 and 60 min but decreased rapidly with further increases in lysis time. Phage λ-*t* failed to make plaques when the lysis time was longer than 70 min (108).

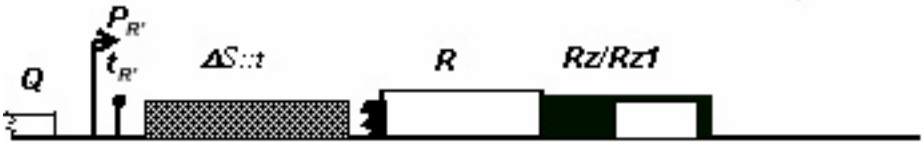

FIG. 1.7. λ lysis cassette with gene *t* substituted for *S* (133).

The membrane topology of holin T was investigated by Ramanculov using the periplasmic protein reporter alkaline phosphatase (PhoA) and cytoplasmic protein reporter β-galactosidase (LacZ) (108). In this study, PhoA-LacZ was inserted between residues in T creating a sandwich fusion (2). This strategy was used to avoid the loss of the downstream topology determinants and to ensure the essence of the results. A result

was only considered meaningful when it was Lac^+ and $PhoA^-$, indicating cytoplasmic localization, or Lac^- and $PhoA^+$, indicating periplasmic localization. Five fusions were made between codons 1 and 2 (*t1::pho-lac*), 26 and 27 (*t26::pho-lac*), 70 and 71 (*t70::pho-lac*), 146 and 147 (*t146::pho-lac*) and 218 and the stop codon (*t218::pho-lac*). Only *t1::pho-lac* and *t218::pho-lac* alleles retained holin activity. PhoA activity assays indicated that *t1::pho-lac* and *t26::pho-lac* were $PhoA^-$ while fusions at 70, 146 and 218 were $PhoA^+$. Weak β-gal activity was detected in fusions 1 and 26, but not for the other constructs. Based on the above criteria, fusions at 70, 146 and 218 gave meaningful results which implied that T had at least one TMD with the C-terminal domain from at least residue 70 to the end of the protein in the periplasm (108).

The domain of T responsible for lysis was also assessed using truncations and one deletion. All truncations, $T_{\boldsymbol{148}}$+R+27, $T_{\boldsymbol{148}}$+P+27, $T_{\boldsymbol{134}}$+23, $T_{\boldsymbol{96}}$+15 and $T_{\boldsymbol{96}}$+7, except $T_{\boldsymbol{96}}$+18, (the bold and italicized number following T represents the last parental residue and the number and following it was the number of vector-encoded amino acids added to T due to the deletion method) delayed lysis. The only internal deletion, $T_{\Delta(97\text{-}164)}$, also delayed lysis. Although the lysis times of these mutants were prolonged, they were not in a predictable trend (108). Thus, the only conclusion from this experiment was that T required at least the first 96 a a including the TMD to lyse the host (108).

Like S105, membrane lesions by holin T are large enough to allow cmycRϕLacZ to pass through the membrane and to enter into the periplasm (139). The lysis profile of the holin T with the fusion endolysin cmycRϕLacZ was almost identical to the lysis

profile of the holin T and cmycR (139). Therefore, the size of the hole formed by T is comparable to the hole formed by S105 (139).

T4 lysis inhibition

Many basic molecular biology concepts, such as the definition of a gene, the nature of the codon and recombination, were elucidated because of an interesting phenomenon exhibited in T4, called lysis inhibition or LIN. In the scenario of one T4 infecting one *E. coli* cell as shown by Doermann in 1948, lysis occurs at approximately 25 min after infection (27). This situation can be achieved by infecting a culture at a low m.o.i. (from 0.01 to 0.1), followed by a thousand-fold dilution, to create an environment in which there is no significant chance of physical contact between the infected cells and phages liberated during the infection cycle. However, following the lysis profile of a turbid culture (A_{550} ~ 0.4) infected with wild type T4 at m.o.i. ~ 5, a sudden decrease in turbidity is not observed (27). This is illustrated in Fig 1.8A, which shows the lysis profile of a turbid, T4-infected culture. There are three successive decreases in optical density (OD). The first decrease results from culture dilution when phages were added. The second drop corresponds to the lysis of the earliest infected cells, due to the non-synchronized nature of the infection process, and release of ~ 100 phages per lysed cell into the medium. These newly released T4 from the minority of lysing cells subsequently infected the surrounding infected cells, which caused the bulk of the culture to become lysis inhibited. This state of lysis inhibition is called LIN. These ideas were supported when the plaque forming unit (pfu) titer was determined from the

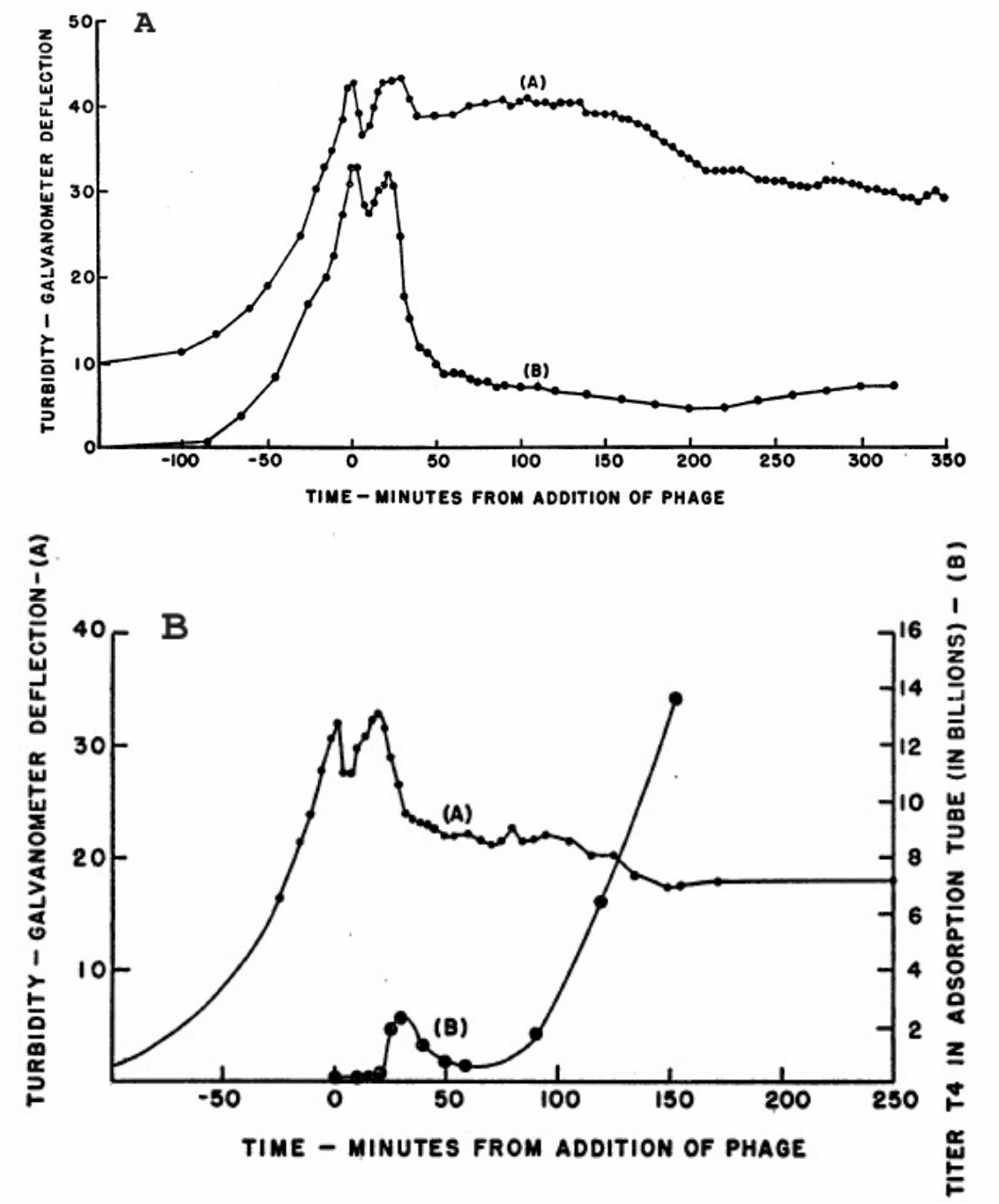

FIG. 1.8. Lysis profile of wild type T4 and T4*r*. (A) Lysis profile of wild type T4, curve A and T4*r*, curve B. (B) Lysis profile of wild type T4, curve A and the phage titer of cells in the same culture at the corresponding time.

culture manifesting the LIN phenotype as shown in Fig 1.8B (curve B) (27). Approximately 25 min after infection, there was a small increase in the number of phage due to lysis of cells that were infected a few minutes earlier. The decreasing phage titer after that point is due to the loss of these phages as they superinfect the rest of the culture. The increase in titer observed is due to the continued intracellular accumulation of phage particles. Because of LIN, wild type T4 makes small, fuzzy edged plaques while LIN-defective T4 mutants make large and sharp edged plaques. LIN-defective T4 mutants were termed T4*r*, in which "*r*" stands for rapid lysis, due to complete lysis of a turbid culture at 25 min after infection. T4 mutants that had lost the LIN phenotype were mapped to a number of loci, designated as *rI*, *rII*, *rIII*, *rIV* and *rV*. Later, the *rII* locus was shown to be a tandem array of two genes, *rIIA* and *rIIB* (6).

Genes that are involved in LIN

rI

Mutations in gene *rI* were among the original *r* mutants isolated in 1946 by A. D. Hershey (51,52) and characterized in 1957 by Seymour Benzer (6). T4*rI* mutants are one of two classes of *r* mutants that formed large and sharp edged plaques on *E. coli* B, *E. coli* K-12 and *E. coli* K-12(λ) (6). Gene *rI* and its mutated alleles were sequenced in 1998 (100) as shown in Fig 1.9A. This gene is served by both early and late promoters (100). Most of the *rI* mutated alleles had frameshift mutations, giving rise to non-functional, truncated RI proteins. Two exceptions were alleles *r*57 and *rp*10. Allele *r*57

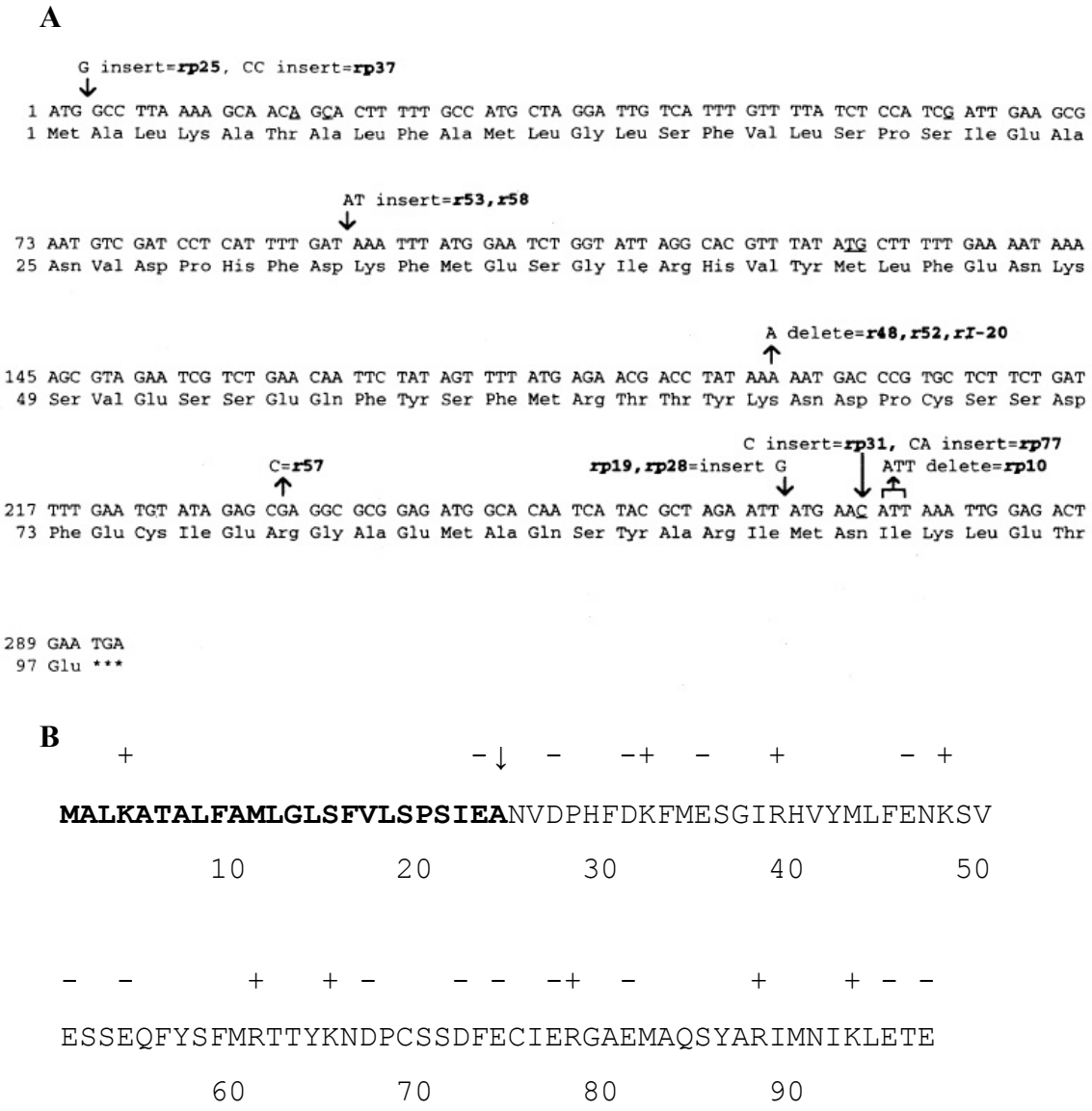

FIG 1.9. Amino acid and nucleotide sequence of *rI* gene. (A) Mutations in *rI* genes that result in the lost of LIN (100) are indicated on top of the nucleotide sequence. (B) Amino acid sequence of RI with annotated charges, predicted signal sequence (bold) and the predicted cleavage site (arrow).

has an R78P missense mutation, and allele *rp*10 is a deletion of codon 92 (100). It was not until 2001 that Ramanculov (110) cloned and studied the function of RI, demonstrating that RI functions as an antiholin that specifically inhibits T-holin

mediated lysis. The inhibition was shown to occur via a direct interaction with the holin T (110). In addition, it appears that RI is needed on all hosts to make wild type plaques.

rIIA and rIIB

T4*rII* mutants were also originally isolated by A. D. Hershey in 1946 (51,52). Because of the unique plating phenotype on different hosts (*r* plaques on *E. coli* B, wild type plaques on *E. coli* K-12 but no plaques on *E. coli* K-12(λ) (6), *rII* mutants were utilized for analysis of gene and codon structure, complementation, recombination, mutagenesis, transcriptional regulation and translational control (124). T4*rII* mutants were further grouped into two different classes, A and B (6), which later were shown to be two independent complementation groups. Currently, it is still unclear what the functions of RIIA and RIIB are (124), or, specifically, what is the contribution of *rII* gene products to LIN.

Gene *rII*A and *rII*B are under the control of a middle promoter (124). Both RIIA and RIIB are membrane-associated proteins (37,103,143), but the amino acid sequences of RIIA and RIIB are rich in charged residues (25,104), as shown in Fig 1.10, indicating they may associate with other membrane proteins, instead of being integral membrane proteins. RIIA and RIIB seem to be involved in multiple functions of T4 physiology (124), including:

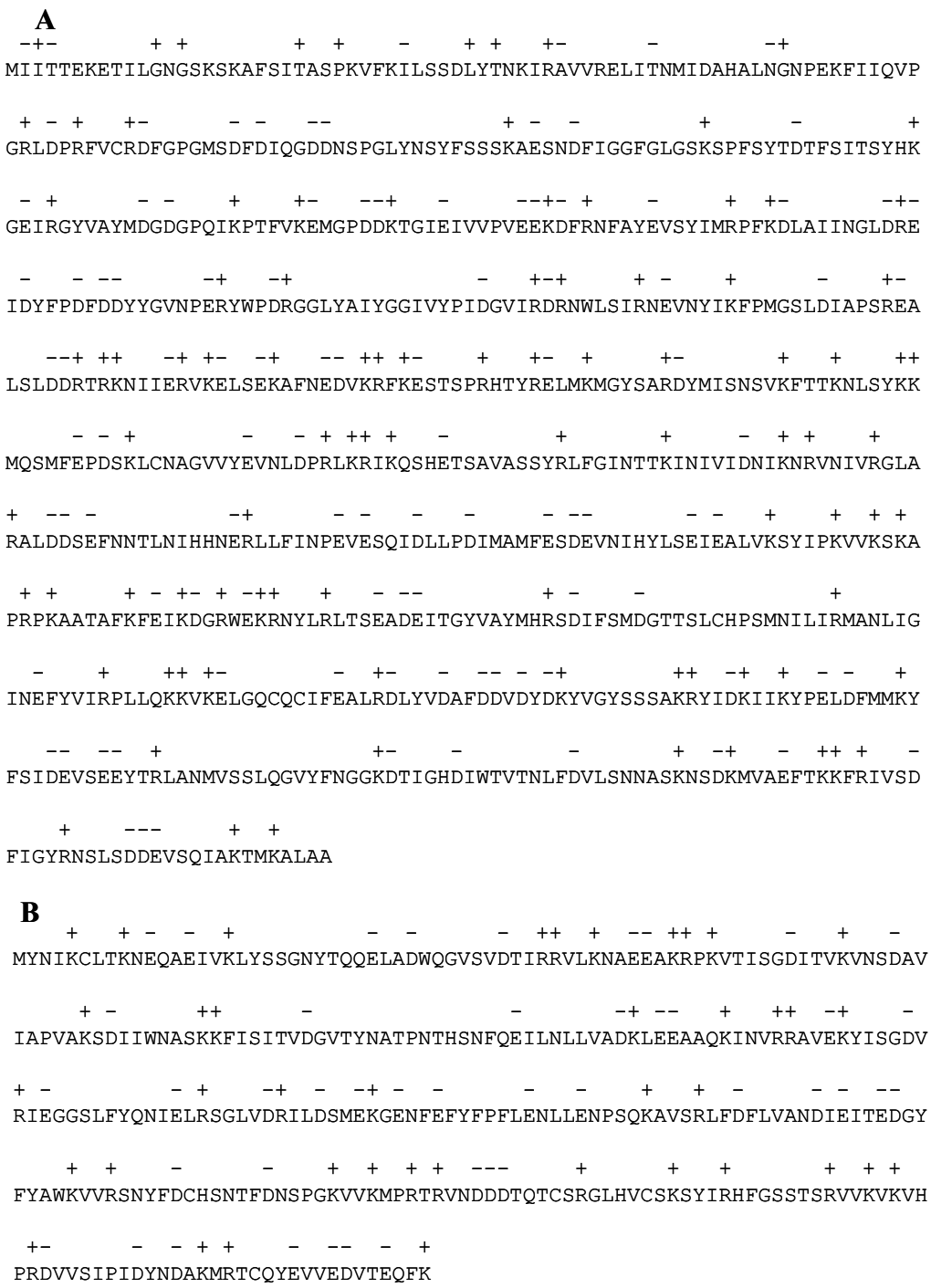

FIG 1.10. Amino acid sequence of RII proteins. (A) RIIA. (B) RIIB

- Mutations in T4*rII* suppress a mutation in T4DNA ligase as long as functional host ligase is available.
- Replication complexes in T4 infection are enriched for RIIA and RIIB
- They are essential for recombination in a λ-lysogenic host and may be involved in anchoring the replication/recombination complex to the membrane.
- Mutations in *rII* allow the maturation of unit size T4 genomes or even parental unreplicative DNA for packaging.

The most prominent phenotype of T4*rII* mutants is the Rex (*rII* exclusion) phenotype. The genes *rII* are absolutely required for T4 to have a successful infection in *E. coli* K-12 (λ) (5). T4*rII* mutants do not make plaques on *E. coli* K-12 (λ) lawns, but they do on *E. coli* K-12 lawns. While *E. coli* K-12 in liquid culture infected with T4*rII* produces progeny, no progeny is obtained when T4*rII* infects *E. coli* K-12 (λ) in liquid culture. Phage infection that does not produce plaques and progeny is called abortive infection. In an abortive infection, expression of phage genes occurs normally. However, about the time DNA replication starts (in T4 infection, this is ~ 5 min after phage DNA injection takes place), all gene expression is stopped (127). The abortive infection of T4*rII* on *E. coli* K-12 (λ) results of the activity of the RexA and RexB proteins, which are expressed from the *rex*A and *rex*B genes adjacent to the *cI* gene in the immunity region of λ (124). Rex^- lysogens do not restrict T4*rII* mutants (124). In addition, over-expression of RexA and RexB from a multicopy plasmid extends the Rex phenotype toward both T4 wild type and T4*rII* infections (119). Snyder and William (128) noted that over-expression of RexA relative to RexB gave a similar phenotype as

when a λ lysogen was infected with T4*rII* mutants. Together, it was hypothesized that the infection of a λ lysogen with T4*rII* mutants somehow altered the ratio of RexA and RexB in the cells and therefore resulted in the Rex phenotype (125,128). *E. coli* B (λ) also gives a similar restrictive phenotype as *E. coli* K-12(λ) (124).

T4*rII* makes *r* plaques on an *E. coli* B lawn but wild-type plaques on *E. coli* K-12 (6), on a Bc variant or BB (the Berkley) variant of *E. coli* B and *E. coli* K-12(P2) (116). Josslin (61) examined the release of phage from cells infected with T4*ΔrII*, T4t_{amA3} and T4t_{amA3} *ΔrII* mutants. He observed that cells infected with T4*ΔrII* or T4t_{amA3} *ΔrII* released phage while cells infected with T4t_{amA3} did not. This indicated that the deletion of both *rII*A and *rII*B suppressed *t* amber mutations and allowed phages to be released from one-step-growth experiments as shown in Fig 1.11 (61). Upon further examination of these data, phage released from T4*ΔrII* infected cells (~ 200 phage/cell) was completed at ~ 50 min after infection. However, at 50 min after infection, there were ~ 200 phage particles assembled in one T4t_{amA3} *ΔrII* infected cell, but only ~ 3 phage particles were released. At 90 min after infection, there were ~ 1000 phage particle in one T4t_{amA3} *ΔrII* infected cell, but only ~ 200 phage particles were released. Thus, the suppression was only ~ 1.5% at 50 min after infection and went up to ~ 20% at 90 min after infection. Together, it can be stated that this phenotype is not true suppression, but either a direct or indirect effect of RII proteins on T-mediated lysis.

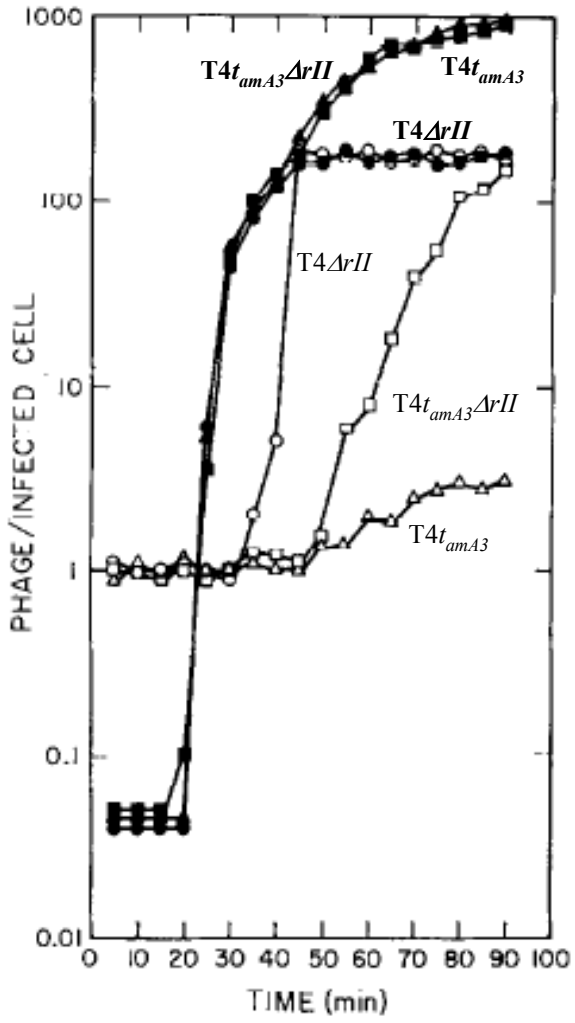

FIG 1.11. One step growth curves of cells infected with T4*ΔrII* (circle), T4t_{amA3} (triangle) or the double mutant (square). Open symbol was before and solid symbol was after the addition of $CHCl_3$. Samples collected before $CHCl_3$ addition represented phage released due to lysis, and samples collected after $CHCl_3$ addition represented total phages assembled intracellularly (62).

rIII

Like T4*rI* and T4*rII*, T4*rIII* mutants were also isolated by A. D. Hershey in 1946 (51,52) and characterized by Seymour Benzer in 1957 (6). They make *r* plaques on *E.*

coli B lawns but wild type plaques on *E. coli* K-12 and *E. coli* K-12(λ) (6). Gene *rIII* is the nearest downstream neighbor of gene *31* (111), and the *rIII* nucleotide sequence and its mutated alleles were published in 1993 (112). Gp*rIII* is predicted to be an 82 a a cytoplasmic protein (112). All of the *rIII* mutant alleles carry missense changes except rBB9, rCR28 and rCR24. Allele rBB9 harbors a nonsense mutation as a result of altering codon 16 to an opal stop codon. Allele rCR28 possesses a non-sense mutation that changes codon 12 to an ochre stop codon. Allele rCP24 is allele rCR28 with a second missense substitution, A70V (112). Using a *rIII::lacZ* fusion, β-galactosidase activity was detected as early as 5-6 min after infection until the end of the T4 vegetative cycle (30). The interpretation of this result was that *rIII* is under control of both early and late promoters (30).

rIV and rV

Another set of T4*r* mutants, identified as *rIV* and *rV*, were isolated later (76). T4*rV* mutants had an identical phenotype to T4*rI* mutants, that is, they make *r* plaques on *E. coli* B, *E. coli* K-12 and *E. coli* K-12(λ). However, they were mapped to a different location in the T4 genome, close to genes *38* and *t* (75). In 1999 (29), several *rV* mutants were sequenced and shown to be allelic to *t*; the mutations are shown in Fig 1.6. T4 *ts*64 is an R5K substitution, *r*2 is I39V and *r*3 is T75I. Two of these mutations are rather conservative, yet somehow these mutations make T insensitive to inhibition by antiholin.

Gene *rIV* has been suggested to be equivalent to the *sp* gene. As mentioned above, *sp* mutations suppress lysozyme mutations and allow release of progeny phages (35). The product of spackle plays an important role in resistance to lysis from without (66). T4*sp* mutations also have different plaque morphologies at different temperatures, wild type at 30^{o}C and *r* at 43^{o}C (35). The different morphologies indicated the temperature-sensitivity of the spackle gene towards LIN. Ramanculov (107) suggested that spreading of phages from lysed cells inside a plaque is limited by the rate of diffusion; thus, the local concentration of phage inside the plaque is high. In this condition, infected cells at the edge of a growing plaque are subjected to high multiplicity of superinfection. Therefore, mutations in the gene essential for LO resistance resulted in lysis from without, instead of a lysis inhibited zone. This gives rise to big and sharp edged plaques similar to T4*r* plaques. How spackle mutations give different plaque morphologies at different temperatures is not known, but the loss of LO resistance in T4*sp* is not temperature sensitive (66).

Factors that trigger LIN

If the expression of RI alone is sufficient for lysis inhibition, in principle, LIN should be observed all of the time. However, this is not what happens during T4 infection. LIN can only be observed when superinfection takes place; therefore, LIN is the result of superinfection. How superinfection causes LIN at the molecular level is not clear, but it occurs when there is a high concentration of free phage and a low concentration of uninfected cells. At this point, T4 has two choices: either undergoes

lysis, which produces more free phages, but free phage concentration does not increase after lysis occurs; or undergo lysis inhibition, which does not produce free phages, but accumulates phages intracellularly. From the standpoint of the phage, it is better to increase the number of progeny linearly within the cell rather than releasing progeny in a host-poor environment. Thus, high free phage concentration and low uninfected cell concentration provide a quorum sensing mechanism so that T4 can decide whether it is the optimal time to lyse the host. Proteins and phenotypes involved in superinfection are described below.

Immunity protein

In the early 1950s, it was reported that T2 ghosts, osmotically shocked T2 particles in with empty heads, had certain biological properties of intact T2 phage, such as (i) host range specificity, (ii) killing action, (iii) inhibition of host nucleic acid synthesis, (iv) induction of lysis and (v) induction of leakage of host phosphorus containing compounds (50). Later, it was shown that preinfection with ghosts inhibited infective center formation by T4, but preinfection with wild type T4 followed by T4 ghost infection had no or little effect on infective center formation as long as the preinfection with wild type T4 was 5 min or longer (31). T4 mutants that lost the ability to protect the host from the killing action of T4 ghosts were isolated in 1972 (136). This gene was named "*imm*", as in immunity to ghost superinfection (135). Gene *imm* was mapped between genes *42* and *43* in the T4 genome (21,24). The *imm* gene is under control of an early promoter, and the action of immunity protein can be observed as

early as 1 to 2 min after primary infection. In 1989, Lu and Henning (83) cloned T4*imm* and found that expression of the Imm protein from a plasmid protects 60% of a population of *E. coli* K-12 and 25% of *E. coli* B from wild type T4 infection at an m.o.i. of 6. Using isopycnic sucrose gradient fractionation and western blotting, Imm protein was found to associate with the plasma membrane (85). The amino acid sequence of Imm is shown in Fig 1.12A. Membrane topology analysis of the Imm protein using the positive inside rule predicts that Imm has two TMDs with both the N- and C-termini outside of the cell. These two TMDs would be unusually long, about 29 amino acid (85). TMpred (http://www.ch.embnet.org/software/TMPRED_form.html) supports this prediction, but TMHMM (http://www.cbs.dtu.dk/services/TMHMM-2.0/) predicts that Imm has two TMDs with both N- and C-termini inside the cell. Topological analysis of Imm using either PhoA or LacZ fusion was performed by Lu et al. in 1993. All Imm-PhoA fusions, starting from residue 5, gave about 4 fold lower activities than when PhoA is in the periplasm. In addition, fusion of the first 74 residues of Imm to mature PhoA allowed the detection of Imm in the inner membrane by immuno-labeled electron microscopy, and this fusion was protease resistant unless the cell was permeabilized with the detergent Triton X-100. In both of the above experiments, fusion protein was detected using PhoA antibodies. These results indicate that the PhoA fusions are cytoplasmic. In contrast, all Imm-LacZ fusions, starting at residue 32, had high β-gal activity indicating the proper localization of LacZ, or this region of Imm, in the cytoplasm. Together, these results indicated that Imm has a single transmembrane domain with N-terminus out and C-terminus inside the cell (85) as shown in Fig 1.12.

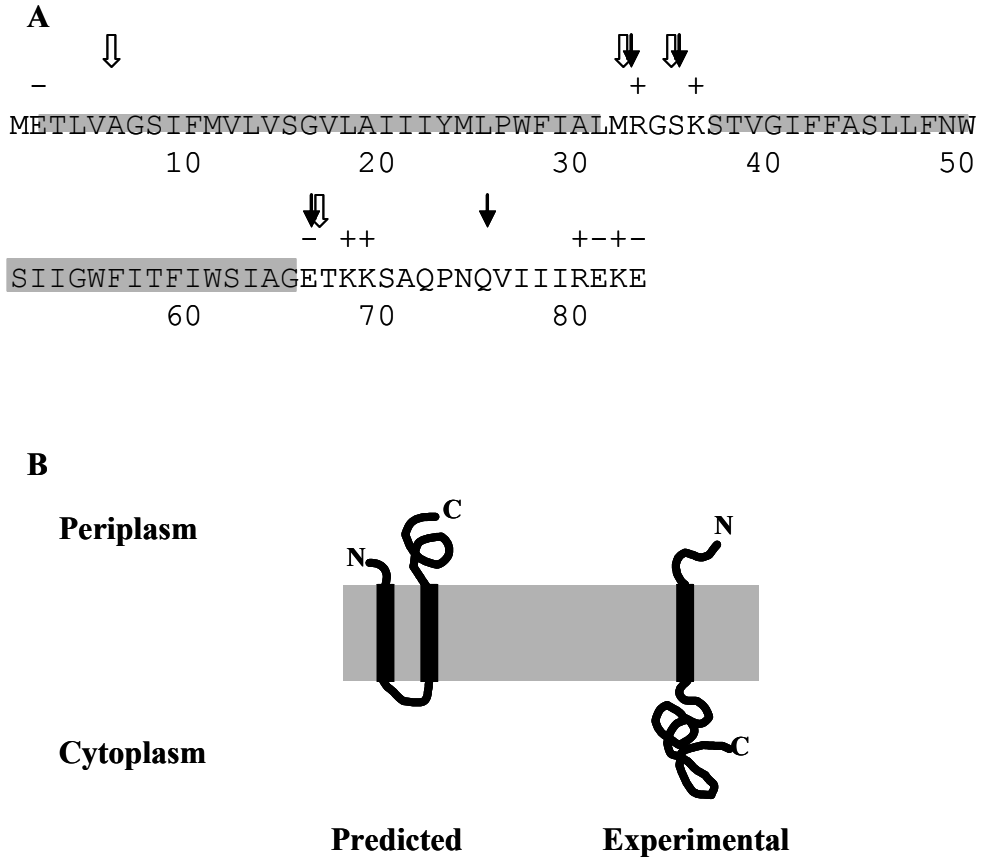

FIG. 1.12. Amino acid sequence and topologies of Imm protein. (A) Amino acid sequence of Imm protein. Gray shade, predicted TMDs by positive inside rule. Solid arrow, fusion join with LacZ. Open arrow, fusion join with PhoA. (B) Predicted topology and topology obtained from fusion studies.

Host proteins involved in LIN

EndA

LIN takes place only when the superinfecting phage is intact; i. e. T4 ghosts do not induce LIN. Thus, the signal for LIN is either the T4 genomic DNA or the internal

proteins that are carried in the head of superinfecting phages but missing from ghosts. During the primary infection, the phage DNA is injected into the cytoplasm and genetic markers from the primary phage are inherited in the progeny. However, as shown by Anderson et al. (4), DNA of the superinfecting phage ended up in the periplasm of the host, and thus cannot participate in the genetic make-up of the progeny. Gene *endA* of *E. coli* encodes periplasmic endonuclease I (23) and degradades DNA that ends up in the periplasm from the injection of superinfecting phage (3). The fact that genetic markers of superinfecting phage are not inherited in the progeny is called *superinfection exclusion*. This superinfecting phage DNA can be visualized by electron microscopy coupled with ^{32}P labeling and radiography when the host is $endA^-$ (4). The degradation of the DNA injected from the superinfecting phage by EndA is called *superinfection breakdown*. The length of LIN in $endA^+$ or $endA^-$ strains is not known, but both strains allow genetic exclusion from the superinfecting phage. It is thought that the presence of Imm protein from the primary infection or expressed from a plasmid alters the *E. coli* envelope so that the DNA of the superinfecting phage is diverted to the periplasm (83).

DegP

Internal proteins (IP) are proteins that are packaged into the T4 head along with T4 genomic DNA. In 1971, Black et al. determined the species and number of each species of the internal proteins from an osmotically shocked ^{14}C labeled T4 lysate by analytical chromatography. The results from this experiment showed that there were three different IPs: IPI, IPII and IPIII. In a single T4 particle, there are approximately

180, 90 and 30 molecules of IPI, II and III, respectively (12). In primary infection, both T4 genomic DNA and the internal proteins are injected into the cytoplasm of the host. In superinfection, since the T4 genomic DNA is injected into the periplasm, the internal proteins are presumably also injected into the periplasm, and serve as the LIN signal. The temporary nature of LIN, i.e. under controlled circumstances where only one round of secondary infection occurs, LIN lasts only for minutes instead of hours (14,27,115), gives rise to the hypothesis that the LIN signal should also be temporary. The easiest way to make the LIN signal temporary is to degrade it. The speculation is that the LIN signal ends up in the periplasm; thus, to degrade the LIN signal, a periplasmic protease is required. One obvious periplasmic protease is DegP. DegP, a member of the HtrA protease family, is a well-characterized periplasmic protease in *E. coli*. *E. coli* DegP was identified from a mutant hunt that isolated mutants lacking proteolytic enzyme activity. Analysis of the *degP*$^-$ strain showed that it grew poorly at high temperature (130,131). Later, Lipinska et al. (80) showed that DegP has endopeptidase activity using α and β casein. The endopeptidase activity of DegP can be inhibited by diisopropylfluorophosphate, a serine protease inhibitor (80), suggesting that DegP is a serine protease. In 1996, Kolmar et al. showed that the cleavage site for DegP is at V/A, V/S (Val/Xaa) and I/Y (Ile/Xaa) residues, and the activity of DegP does not require ATP, reducing agents or divalent cations (72). A number of natural substrates of DegP were described including colicin A lysis protein, K88 and K99 pilin subunits, MalS, and PapA pilin (67). DegP does not degrade folded proteins, but appears to cleave partially unfolded proteins. This finding is supported by the sequence of the cleavage site of

DegP, Val/Xaa and Ile/Xaa. These amino acids are hydrophobic and usually not exposed on the surface of a protein. However, these sites are often exposed when a protein is partially unfolded (72).

DegP also possesses a chaperone activity at low temperature (67). The crystal structure of DegP helped to explain the different activities of DegP at different temperatures. DegP possesses a protease domain at the N-terminus and two PDZ domains at the C-terminus (67,73). PDZ domains are involved in protein-protein interactions, specifically in interactions with a short peptide at the extreme C-terminus of the target protein. Within the protease domain, there is a Q-linker, which is either absent or shorter in other members of the HtrA family (67). The hexameric structure of DegP suggests DegP may have limited access to its substrate (73). PDZ domains of DegP have two orientations, a closed state that denotes the chaperone activity and an open state that denotes protease activity (73). It is thought that the PDZ domains function as a proteolytic regulator, much like a gatekeeper, to either restrict or allow substrate access to the proteolytic chamber (67).

Goals and specific aims

Lysis inhibition is the only known example of real time control, signal transduction in holin regulation. In addition, this phenomenon is historically significant in that it was used in the founding experiments of modern molecular genetics. The long

term goal of this project is to determine the detailed mechanism of LIN at the molecular level.

I. Determination of the interacting domains of antiholin RI and holin T

Ramanculov established that the antiholin RI inhibits T-mediated lysis by direct interaction using formaldehyde cross-linking. However, the specific interaction domains are not known. Thus, the first step in understanding the mechanism of LIN is to determine which domains of T and RI interact.

II. Characterization of antiholin RI

To date, the only thing known about RI is its predicted amino acid sequence and the sequence of the mutant *rI* alleles with LIN defects. Nothing is known about the physical characteristics of RI. Even though it was predicted to be a secreted protein by Paddison in 1991, no experimental data are available to support this prediction. In addition, Ramanculov had difficulty in detecting RI tagged with a c-myc tag, suggesting the protein is unstable, a very small amount of protein is made, or the tag is removed by proteolytic cleavage. The only time tagged-RI was detected was when it was cross-linked to T. Since RI is one of the two major players of LIN, understanding its physical characteristics may help to elucidate the molecular mechanism of LIN.

III. Characterization of holin T

In addition to its role in LIN, T is a large protein compared to other known holins and has a unique topology. In this specific aim, I propose to determine the topology of T, the domain important for oligomerization, and the localization of T in the *E. coli.* membrane when lysis occurs.

CHAPTER II

PERIPLASMIC DOMAINS DEFINE HOLIN-ANTIHOLIN INTERACTIONS IN T4 LYSIS INHIBITION*

Introduction

An *E. coli* cell infected at 37ºC by a wt T4 phage undergoes lysis at about 25 min after infection and releases ~200 progeny virions. Lysis requires the muralytic activity of the T4 lysozyme, E, one of the best characterized soluble enzymes in terms of its structure, enzymatic mechanism, and thermodynamic stability (88). The precise timing of lysis, however, is not determined by E, which accumulates fully folded and active in the cytoplasm throughout the morphogenesis period. Instead, like all dsDNA phages, the timing of T4 lysis is controlled by its holin, T, an integral membrane protein that suddenly triggers to disrupt the bilayer at an allele-specific time (141,147). Membrane disruption allows the T4 lysozyme to attack the cell wall, after which the infected cell bursts and releases the progeny virions. T4 *t*, like the λ holin gene *S*, is genetically malleable, in that many missense alleles have been isolated, with lysis times either advanced or delayed relative to the wt allele (47,106,108,141,146). This malleability is significant, because it is thought that investing lysis timing exclusively in the holin gene

* Reprinted with permission from "Periplasmic domains define holin-antiholin interaction in T4 lysis inhibition" by Tran, T. A., D. K. Struck, and R. Young, 2005. Journal of Bacteriology, 187, 6631-6640. Copyright 2005 by ASM Press.

allows dsDNA phages to evolve rapidly in response to changed conditions. For example, an environment with reduced host numbers should favor phages with an extended latent period, allowing the intracellular accumulation of more progeny virions before they are released into the host-poor medium (140). Holin genes have enormous diversity, with more than 50 unrelated gene families having been described (141). However, compared to other known holins, the T4 holin has an unusual topology. All other characterized holins have either three (class I; e.g., the S105 product of phage λ gene *S*) or two (class II; e.g., the $S^{21}68$ product of S^{21}, the holin gene of lambdoid phage 21) TMDs (Fig. 1.3). In contrast, T and its orthologs in T4-like phages constitute a single protein family with bitopic topology and a single TMD (Figs. 1.3). T, at 218 residues, is substantially larger than other holins (e.g., the λ holin S105 is only 105 residues and the $S^{21}68$ is only 68 residues). The extra mass comes principally from its large C-terminal periplasmic domain of 163 residues (Fig. 2.1A).

In addition to its unusual topology and size, the function of the T4 holin is subject to a type of control not seen with the prototypical class I and II holins. Almost 60 years ago, in publications now considered landmarks in the history of molecular genetics, it was reported that T4-infected cells are subject to "lysis-inhibition", or LIN (27,52). The LIN state, in which the normal lysis timing of the holin is over-ridden, is established if a T4-infected cell undergoes super-infection by another T4 particle. The LIN state is unstable, requires continued super-infection to be maintained, and can be subverted by addition of energy poisons that collapse the membrane potential (1). In infected cultures at visible optical densities, the lysis of a small fraction of the cells

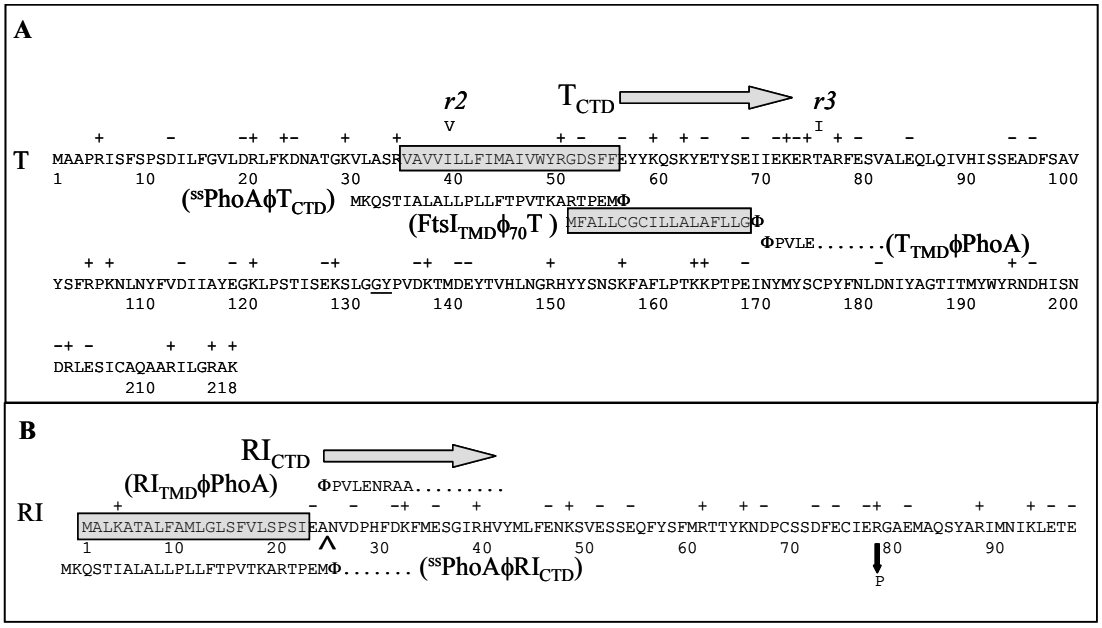

FIG. 2.1. Amino acid sequence of T and RI and their derivatives. (A) Amino acid sequence of T and its derivatives. The predicted TMD of T is boxed and shaded. The *rV* mutants *r2*(I39V) and *r3*(T75I) are indicated above the sequence. In T^{his}, a hexa-histidine tag (HHHHHHGG) was inserted between the residues G132 and Y133 (underlined). For the $^{ss}PhoA\Phi T_{CTD}$ construct, the signal sequence of PhoA, shown below the T sequence, was substituted for residues 1-55 of T. For the $FtsI_{TMD}\Phi T$ construct, the transmembrane domain of FtsI, shown in a shaded box below the T sequence, was substituted for residues 2-69 of T. For the $T_{TMD}\phi PhoA$ construct, residues 1-70 of T was substituted for residues 1-26 in the full-length primary gene product of *phoA*; the PhoA sequence begins with PVLE (PhoA residues 27 on, as indicated). (B) Amino acid sequence of RI and its derivatives. The predicted signal sequence of RI is boxed, with the leader peptidase I cleavage site predicted by the SignalP program (http://www.cbs.dtu.dk/services/SignalP/) {Bendtsen, 2004 133 /id} indicated by a carat. In the *cmyc*-tagged version of RI, the *cmyc* tag (QKLISEEDL) was inserted after the terminal glutamate at position 97, while in the $GFP\Phi RI^{cmyc}$ constructs, the entire GFP sequence was inserted after the initial Met residue. For the $^{ss}PhoA\phi RI_{CTD}$ construct, the signal sequence of PhoA, shown below the RI sequence, was substituted for residues 1-24 of RI. For the $RI_{NTD}\phi PhoA$ construct, the predicted signal sequence of RI replaced residues 1-26 in the uncleaved precursor to mature PhoA. The sole known *rI* missense mutation, R78P, is shown by a down arrow (133).

generates sufficient free virions in the medium to establish and maintain LIN throughout the bulk culture, allowing progeny to accumulate to $>10^3$ virions per cell over a period of hours. On agar lawns, LIN causes T4 to make small, indistinct plaques, and it is easy to isolate T4 mutants defective in LIN by virtue of their large, clearly defined plaque morphology (51). These mutants were called *r* mutants for "*r*apid lysis" and were mapped to multiple T4 loci, including *rI*, *rIIAB*, and *rV* depending on the host used (146). The *r* genetic system was exclusively exploited to establish many of the fundamental principles of molecular genetics (17). Ultimately, only two genes, *rI* (6) (100) and *rV* (74,75), later shown to be allelic to *t* (29), are required to maintain the wild-type plaque phenotype and to establish LIN with *E. coli* K-12. Nevertheless, despite the central importance of the *r* genetic system in the history of molecular biology, the molecular basis of LIN has remained obscure.

Recently, we have undertaken a molecular analysis of T4 lysis and the LIN phenomenon, as part of our study of the mechanisms of phage lysis and its regulation. We reported here the evidence that RI (Fig. 2.1B) is an antiholin that specifically binds to and inhibits the T holin. This clearly distinguishes T4 from bacteriophage λ whose antiholin, S107, is the product of an alternative translational start in its holin gene, *S*, which also encodes S105, the λ holin. Given its near identity with S105 and the fact that holins oligomerize in the process of forming membrane lesions, it is not surprising that S107 dimerizes with S105. The formation of these dimers is responsible for the ability of S107 to prevent the spontaneous triggering of S105. In contrast, RI has no sequence similarity to T (Fig. 2.1) that might support homotypic interactions of the type observed

in the λ S105/S107 system. Here we report experiments designed to identify the topological determinants of RI and T that lead to the LIN state. The results are discussed in terms of the unique ability of RI to respond to an environmental signal (i.e., a super-infecting T4 phage).

Materials and methods

Bacterial strains, bacteriophages, plasmids, and culture growth

The bacterial strains, bacteriophages, and plasmids used in this work are described in Tables 2.1, 2.2 and 2.3. T4 phage stocks were prepared as described previously (109). Bacterial cultures were grown in standard LB medium supplemented with ampicillin (100 μg/ml), kanamycin (40 μg/ml), chloramphenicol (10 μg/ml) when appropriate. Growth and lysis of cultures were monitored as A_{550} as previously described (109). When indicated, isopropyl β-D-thiogalactoside (IPTG), KCN, or $CHCl_3$ was added to give final concentrations of 1 mM, 10 mM, or 1%, respectively.

Standard DNA manipulations, PCR, and DNA sequencing

Isolation of plasmid DNA, DNA amplification by PCR, DNA transformation, and DNA sequencing were performed as previously described (145). Oligonucleotides listed in Table 2.4 were obtained from Integrated DNA Technologies, Coralville, IA, and were used without further purification. The Rapid DNA ligation kit from Roche

Molecular Biochemicals was used for ligation reactions. All other enzymes were purchased from New England Biolabs except for *Pfu* polymerase which was from Stratagene. Automated fluorescent sequencing was performed at the Laboratory for Plant Genome Technology at the Texas Agricultural Experiment Station.

TABLE 2.1. Phages

	Genotypes/features	Sources, references
T4 wt	T4D	I. Molineux
T4*rI*	*rI48*, single base deletion at position 195; N66-E97 replaced with MTRALLILNV	D. Hall
λ*kan*Δ(*SR*)	λb_{515} b_{519} *att::*Tn*903* cI_{857} *nin5* Δ(*SR)*	(105)
λ*kan* t^{his}	λb_{515} b_{519} *att::*Tn*903* cI_{857} *nin5* Δ*S::*t^{his}	This study
T4*ΔrI*	Deletion of *rI* gene from nt 59204 to nt 59496 in T4 genome	This study
T4e_{am}	M41, M41T4 with an amber mutation in *e* gene	Drake, J.
T4^{ss}*phoA*Φ*rI*$_{CTD}^{y42am}$	*rI* gene, from nt 59214 to nt 59496 in T4, replaced with ^{ss}*phoA*Φ*rI*$_{CTD}^{y42am}$	This study
λ-*t*	λb_{515} b_{519} *att::*Tn*903* cI_{857} *nin5* Δ*S::t*	(109)
λ*cam*Δ(*SR*)	λ*stf::cat::tfa* cI_{857} Δ(*SR)*; loss of l nt 45135-45815	(126)

Single base changes and small insertions were introduced using commercially synthesized primer in conjunction with the Quikchange kit from Stratagene. Larger insertions, replacements, and gene fusions were generated using a modification of the basic QuikChange site-directed mutagenesis protocol. Here, a donor sequence is PCR amplified using primers that have 5' ends that anneal to appropriate sequences in a target plasmid. The first PCR product is then used as the primer for a second PCR reaction using the target plasmid as a template. All subsequent steps are identical to those in the basic QuikChange protocol.

TABLE 2.2. *E. coli* strains

	Genotypes/features	Sources, references
CQ21	*E. coli* K-12 *ara leu lacI^{q1} purE gal his argG rpsL xyl mtl ilv*	(105)
CQ21λ*kan*Δ(*SR*)	Lysogen carrying λ*kan*Δ(*SR*) prophage	(105)
CQ21[λ*kan*Δ(*SR*)] *recA srl*::*Tn*10	Lysogen carrying λ*kan*Δ(*SR*) prophage	This study
CQ21(λ*kan t*^{his})	Lysogen carrying λ*kan t*^{his} prophage	This study
MG1655	F$^-$ *ilvG rfb50 rph1*	*E. coli* Genetic Stock Center
MDS12	MG1655 with 12 deletions, totaling 376,180 nt including cryptic prophages	(71)
MDS12 *tonA*::*Tn*10 *lacI^{q1}*		This study
XL-1Blue	*E. coli* K-12 *recA endA1 gyrA96 thi1 hsdR17 supE44 relA1 lac*[F' *proAB lacZ*$_{\Delta M15}$::*Tn*10]	Stratagene
BL21(DE3)	F$^-$ *ompT hsdS*$_B$ (r_B^- m_B^-) *gal dcm* (DE3)	Novagen
BL21(DE3) *tonA::Tn*5 *slyD::Tet^R*		This study
CQ21(λ-*t*)	Lysogen carrying (λ-*t*) prophage	This study
MG1655 *tonA::Tn*10 *lacI^{q1}*		(102)
KS474	F- *ΔlacX74 galE galK thi rpsL(strA) ΔphoA(PvuII) degP*	(91)
NJH110	F$^-$ *araD139 Δ(argF-lac) U169 rpsL150 relA1 flbB5301 deoC1 ptsF25 rbsR degP::Cm*	(57)
MDS12 *tonA*::*Tn*10 *lacI^{q1}degP::Kn^r*		This study
MDS12 *tonA*::*Tn*10 *lacI^{q1}degP::Cm^r*		This study
LE392	*E. coli* K-12 *hsd R574*, (r_k^-, m_k^+), *supE44*, *supF58*, Δ *(lac1ZY)6*, *gal K2*, *gal T22*, *metB1*, *trpR55*	(97)
LE392 *tonA::Tn*10		This study
MC4100	*E. coli* K-12 *F- araD139 Δ*(*argF-lac*)*U169 rpsL15 relA1flbB3501 deo pstF25 rbsR*	(121)
MC4100λ*cam*Δ(*SR*)	Lysogen carrying λ*kan*Δ(*SR*) prophage	Laboratory stock
C43(DE3)	F$^-$ *ompT hsdS*$_B$ (r_B^- m_B^-) *gal dcm* (DE3) with uncharacterized mutation that allows for toxic proteins to be induced at higher levels than BL21(DE3)	Avidis
C43(DE3)*tonA::Tn*10 *slyD::kn^R*		This study

TABLE 2.3. Plasmids

	Genotypes/features	Sources, references
pT4T	pBR322 derivative carrying late promoter and lysis cassette of λ with the *S* gene replaced by T4 *t*	I. N. Wang
pT4T^{132his} (pT4T^{his})	pT4T with a HHHHHHGG inserted between residues 132 and 133 of *t*	This study
pT4TRI	pT4T with *rI* gene inserted distal to *Rz1* gene	This study
pZA32-luc	p15A origin, $P_{LlacO-1}$ promoter, cam^R	(86)
pZA-RI	pZA32Δ*luc::rI*	This study
pZA-RI$_{CTD}$	pZA32Δ*luc::rI$_{CTD}$*, codons 25 to 97 of *rI*	This study
pZA-PhoA	pZA32Δ*luc::phoA,* codons 27 to 471 of *phoA*, encoding the mature PhoA	This study
pZA-^{ss}PhoAΦRI$_{CTD}$	Codons 1-24 of *rI* in pZA-RI replaced by codons 1-26 of *phoA*, encoding the signal sequence.	This study
pZA-^{ss}PhoAΦRI$_{CTD}^{cmyc}$	pZA-^{ss}PhoAΦRI$_{CTD}$ with 10 codons encoding QKLISEEDL inserted after codon 97 of *rI*	This study
pZA-RI$_{TMD}$ΦPhoA	The first 24 codons of *rI* inserted in front of codon 27 of *phoA* in pZA-PhoA	This study
pZA-T	pZA32Δ*luc*::*t*	This study
pZA-T$_{CTD}$	pZA32Δ*luc*::*t$_{CTD}$*, codons 56 to 218 of *t*	This study
pZA-^{ss}PhoAΦT$_{CTD}$	Codons 1-55 of *t* in pZA-T replaced by codons 1-26 codons of *phoA*, encoding the signal sequence	This study
pZA-^{ss}PhoAΦT$_{CTD}^{T75I}$	pZA-^{ss}PhoAΦT$_{CTD}$ carrying the T75I *rV* mutation	This study
pZA-T$_{TMD}$ΦPhoA	First 70 codons of *t* inserted before codon 27 of *phoA* in pZA-PhoA	This study
pZA-T $^{70-218}$	pZA32*Δluc*::*t$^{70-218}$*, codons 70 to 218 of *t*	This study
pZA-FtsI$_{TMD}$Φ70T	Codons 24 to 40 of *ftsI*, encoding the TMD, inserted before codon 70 of *t* in pZA-T$^{70-218}$.	This study
pZE12-luc	ColE origin, $P_{LlacO-1}$ promoter, amp^R	(86)
pZE-RI	pZE12 *Δluc::rI*	This study
pZE-RI^{cmyc}	pZE12 *Δluc::rI^{cmyc}* with codons encoding QKLISEEDL inserted after codon 97 of *rI*	This study
pZE-GFPΦRI^{cmyc}	DNA fragment encoding GFP inserted between codons 1 and 2 of *rI^{cmyc}* in pZE12-luc	This study
pDS439	pBR322 origin, P_{ara}BAD promoter amp^R, carrying *gfp^{mut2}*	(120)
pET11a-T$_{CTD}^{his}$	pBR322 origin, T7 promoter, amp^R, carrying DNA fragment encoding a Met residue, then residues 70 to 218 of T with the HHHHHHGG insertion between residues 132 and 133	This study
pER-T	Carrying lysis cassette of λ except *S* is replaced by T4 *t* gene, amp^R, kan^R	(109)
pPRI	pBR322 origin, λ $P_{R'}$ promoter, amp^R, carrying DNA fragment encoding RI	This study
pPRI^{his}	pPRI with 8 codons encoding GGHHHHHH inserted after codon 97 of *rI*	This study
pET11a-RI$_{CTD}^{his}$	pBR322 origin, T7 promoter, amp^R, carrying DNA fragment carrying a Met codon, then codons 25 to 97 of RI, followed by codons for the sequence GGHHHHHH.	This study
pZA-RI^{L}	pZA32 *Δluc::rIA7L*	This study
pZA-RI^{2L}	pZA32 *Δluc::rIA7L T6L*	This study
pZA-RI^{3L}	pZA32 *Δluc::rIA7L T6L A5L*	This study
pZE-Δluc	pZE12 *Δluc*	This study
pZE-RI^{L}	pZE12 *Δluc::rIA7L*	This study
pZE-RI^{2L}	pZE12 *Δluc::rIA7L T6L*	This study
pZE-RI^{3L}	pZE12 *Δluc::rIA7L T6L A5L*	This study
pZE-500RI	pZE12 *Δluc::500rI*	This study

TABLE 2.3. Continued

	Genotypes/features	Sources, references
pZE-500ΔRI	pZE12-500RI with in frame deletion of RI reading frame	This study
pZE-500RI-X	pZE12 *Δluc::500rI* with elimination of XbaI site	This study
pZE-500RI-X-K	pZE12 *Δluc::500rI* with elimination of XbaI and KpnI sites	This study
pZE-500-^{ss}PhoAΦRI$_{CTD}$	pZE12-500RI-X-K *ΔrI*::^{ss}*phoAΦrI*$_{CTD}$	This study
pZE-500-^{ss}PhoAΦRI$_{CTD}$-K	pZE12-500RI-X-K *ΔrI*::^{ss}*phoAΦrI*$_{CTD}$ with elimination of KpnI	This study
pZE-500-^{ss}PhoAΦRI$_{CTD}$ ^{Y42am}-K	pZE12-500-^{ss}PhoAΦRI$_{CTD}$-K with codon 42 of *rI* gene change to amber	This study
pJF118EH	ColE1 origin of replication, P$_{tac}$, *lac^{Iq}* and *amp^{R}*	(40)
pJF-FtsI^{cmyc}	pJF118EH harboring *ftsI^{cmyc}* gene	(145)
pJF-PhoA	pJF118EH harboring *phoA* gene	(145)
pZS-24*MCS	pSC101 origin of replication, P $_{lac/ara-1}$ and *kan^{R}*	(86)
pQ	pZS24* with *Q* gene insertion using Kpn1 and Cla1	(48)
pT4T^{5R6}	pT4T with an arginine residue inserted between residues 5 and 6 of *t*	This study
pT4T^{1RR2}	pT4T with two arginine residues inserted between residues 1 and 2 of *t*	This study
pT4T^{R5K}	pT4T with the arginine residue at position 5 was replaced by a lysine in *t*	This study
pT4T^{I39V}	pT4T with an isoleucine at position 39 was replaced by a valine in *t*	This study
pT4T^{T75I}	pT4T with a threonine at position 75 was replaced by an isoleucine in *t*	This study
pT4T^{28his}	pT4T with a HHHHHHGG inserted between residues 28 and 29 of *t*	This study
pT4T^{51his}	pT4T with a HHHHHHGG inserted between residues 51 and 52 of *t*	This study
pT4T^{148his}	pT4T with a HHHHHHGG inserted between residues 148 and 149 of *t*	This study
pT4^{cmyc}T^{his}	pT4T^{his} with EQKLISEEDL inserted between residue 1 and 2	This study
pT4^{au1}T^{his}	pT4T^{his} with DTYRYI inserted between residue 1 and 2	This study
pET11a	pBR322 origin, T7 promoter, a*mp^{R}*	Novagen
pET11a- T^{his}	pET11a harboring *t* gene with HHHHHHGG inserted between residues 132 and 133	This study
pETduet-1	pBR322 origin, two T7 promoter followed by two multiple cloning sites (NcoI-AflII) and (NdeI-AvrII), ampR	Novagen
pETduet-RI	pETduet-1 harboring RI in Nde1-AvrII multiple cloning site	This study
pETduet-RI-T	pETduet-RI harboring T^{his} in NcoI-AflII multiple cloning site	This study
pT4T$^{Δ2-28}$	pT4T with deletion of residue 2 to 28 in T	This study
pZA32-GFPΦT	pZA32 *Δluc::gfpΦt*	This study
pZA32-GFPΦAGSAGΦT	pZA32-gfp-T with a coding sequence for AGSAG inserted between residue 238 of GFP and residue 2 of T	This study

TABLE 2.4. Oligonucleotides

Oligo name	Sequence
HindIIIpR'for……	CATTAAAGCTTGAAGGAAATA
CRzNRIrev……	TGTATTTACTTTGTGCCGATGATGGGCAACTCTATCTGCACT
CRzNRIfor……	AGTGCAGATAGAGTTGCCCATCATCGGCACAAAGTAAATACA
ClaIRIrev……..	ATATATATCGATCTAGACCACTTTGTGAAAAGT
132-H6G2-133for….	GAAAAATCACTTGGAGGACACCACCACCACCACCACGGAGGAT ATCCTGTTGATAAAACT
132-H6G2-133rev….	AGTTTTATCAACAGGATATCCTCCGTGGTGGTGGTGGTGGTGTCC TCCAAGTGATTTTTC
Kpn1RIfor ……	GCGCGCGGTACCATGGCCTTAAAAGCAACAGCA
RIAvrIIrev…….	ATATATCCTAGGCTCTAGACCACTTTGTGA
25RIKpnfor ……..	ATATATGGTACCAATGTCGATCCTCATTTTGAT
ss25RIfor ……..	ATTAAAGAGGAGAAAGGTACCATGAAACAAAGCACTATTGCA
ss25RIrev……..	ATCAAAATGAGGATCGACATTCATTTCTGGTGTCCGGGCTTT
KpnItfor…….	ATATATGGTACCATGGCAGCACCTAGAATA
AvrIIt rev……...	ATATATCCTAGGAGCAGCGAACAAATAATTATT
56tKpnIfor…….	ATATATGGTACCGAGTACTATAAGCAATCAAAG
PhoAss70tfor…….	ATTAAAGAGGAGAAAGGTACCATGAAACAAAGCACTATTGCAC
56tssrev…….	CTTTAGTTGCTTATAGTACTCCATTTCTGGTGTCCGGGCTTT
KpnIphoAfor ……	ATATATGGTACCCCTGTTCTGGAAAACCGGGCT
AvrIIphoArev……	ATATATCCTAGGTTATTTCAGCCCCAGGGC
RItmphoAfor ……	ATTAAAGAGGAGAAAGGTACCATGGCCTTAAAAGCAACAGCA
RItmphoArev…….....	AGCCCGGTTTTCCAGAACAGGCGCTTCAATCGATGGAGATAA
KpnI70tfor …….....	ATATATGGTACCATTGAAAAGGAAAGAACTGCA
FtsITM70tfor ……	ATTAAAGAGGAGAAAGGTACCATGTTTGCGTTGTTATGCGGC TGT
FtsITM70trev……	TGCAGTTCT TTCCTTTTCAATTCCGAGCAGAAAAGCCAGCGC
T4TtmphoAfor……..	ATTAAAGAGGAGAAAGGTACCATGGCAGCACCTAGAATA TCA
T4TtmphoArev……..	AGCCCGGTTTTCCAGAACAGGAATTTCACTGTATGTTTCATA
KpnI-gfp-for …….	ATATATGTTACCATGAGTAAAGGAGAAGAACTT
N-RIC-gfprev……	AAGTGCTGTTGCTTTTAAGGCTTTTAAGGCTTTGTATAGTTCATC CATGCC
C-gfpN-RIfor…….	GGCATGGATGAACTATACAAAGCCTTAAAAGCAACAGCACTT
RI-XbaIrev……	GTCGACTCTAGACCACTTTGTGAA
NdeI70tfor…….	ATATATCATATGATTGAAAAGGAAAGAACTGCA
BamH1trev……	ATATATGGATCCAGCAGCGAACAAATAATTATT
25RINdeIfor……..	ATATATCATATGAATGTCGATCCTCATTTT
RIhisBamrev…….	ATATATGGATCCTCAGTGGTGGTGGTGGTGGTG
RIG2H6for…….....	AACATTAAATTGGAGACTGAAGGAGGACACCACCACCACCACC ACTGAAATTCAGCGACTTTTCAC
RIG2H6rev……	GTGAAAAGTCGCTGAATTTCAGTGGTGGTGGTGGTGGTGTCCTC CTTCAGTCTCCAATTTAATGTT
-500RIKpn1for……..	ATATATACCGACGTAGATATTTCCTTC
+500RIXba1rev…….	ATATATTCTAGAGCTAAGGACTGATTTCGC
RIA7Lfor……...	GCCTTAAAAGCAACACTACTTTTTGCCATGCTA
RIA7Lrev……..	TAGCATGGCAAAAAGTAGTGTTGCTTTTAAGGC
500delRIfor……...	AAAGGCCTCCTATCATTT
500delRIrev……...	TGAAATTCAGCGACTTTT
RIT6Lfor……...	ATGGCCTTAAAAGCACTACTACTTTTTGCCATG

TABLE 2.4. Continued

Oligo name	Sequence
RIT6Lrev……..	CATGGCAAAAAGTAGTAGTGCTTTTAAGGCCAT
RI5-6-7-Lfor……..	ATGGCCTTAAAACTACTACTACTTTTTGCC
RI5-6-7-Lrev…….	GGCAAAAAGTAGTAGTAGTTTTTAGGCCAT
RI-Y42am-for……	GGTATTAGGCACGTTTAGATGCTTTTTGAAAAT
RI-Y42am-rev……..	ATTTTCAAAAAGCATCTAAACGTGCCTAATACC
RI-end-XbaIrev…….	ATATATTCTAGATCATTCAGTCTCCAATTT
Kpn1-RI-up……...	ATATATGGTACCAAAGGCCTCCTATCATTTTTG
Xba1-RI-down……..	ATATATTCTAGAAGAATTATGAACATTAAATTG
Ss-PhoA-for……...	ATGAAACAAAGCACTATTGCA
RI-SDS-flanking-rev…….....	AAAGGCCTCCTATCATTTTTG
BamH1-pZE12-for…….....	ATATATGGATCCGCGGATAACAAGAT
T5-R-6for…….....	GGGTCTATGGCAGCACCTAGAAGAATATCATTTTCGCCCTCTGAT
T5-R-6rev……..	ATCAGAGGGCGAAAATGATATTCTTCTAGGTGCTGCCATAGACCC
T1-RR-2for……	ATCTTAAAAGGAGGGTCTATGAGAAGAGCAGCACCTAGAATATCATTT
T1-RR-2rev……...	AAATGATATTCTAGGTGCTGCTCTTCTCATAGACCCTCCTTTTAAGAT
28-G1H6-29-for……	AAAGATAACGCTACCGGGGGACACCACCACCACCACCACGGAGGAAAGGTTCTTGCTTCCCGG
28-G1H6-29-for……	CCGGGAAGCAAGAACCTTTCCTCCGTGGTGGTGGTGGTGGTGTCCCCCGGTAGCGTTATCTTT
51-G1H6G2-52-for...	ATTGTTTGGTATAGGGGAGGACACCACCACCACCACCACGGAGGAGATAGTTTCTTTGAGTAC
51-G1H6G2-52-rev……..	GTACTCAAAGAAACTATCTCCTCCGTGGTGGTGGTGGTGGTGTCCTCCCCTATACCAAACAAT
148-G1H6G2-149-for……..	CAGTTCATTTAAATGGAGGACACCACCACCACCACCACGGAGGACGTCATTATTATTCCAAC
148-G1H6G2-149-rev……..	GTTGGAATAATAATGACGTCCTCCGTGGTGGTGGTGGTGGTGTCCTCCATTTAAATGAACTG
Cmyc-tfor……..	ATCTTAAAAGGAGGGTCTATGGAGCAGAAACTGATCTCTGAAGAAGATCTGGCAGCACCTAGAATATCATTT
Cmyc-trev……..	AAATGATATTCTAGGTGCTGCCAGATCTTCTTCAGAGATCAGTTTCTGCTCCATAGACCCTCCTTTTAAGAT
AUI-tfor…….	ATCTTAAAAGGAGGGTCTATGGACACATACCGCTACATCGCAGCACCTAGAATATCATTT
AUI-trev……	AAATGATATTCTAGGTGCTGCGATGTAGCGGTATGTGTCCATAGACCCTCCTTTTAAGAC
ThisinpETfor…….	GCGCGCCATATGGCAGCACCTAGAATATCA
ThisinpETrev…….	GCGCGCGGATCCTTAGCAGCGAACAAATAATTA
RIcmycNde1for…….	ATATATCATATGGCCTTAAAAGCAACAGCA
Kpn1-RIrev……...	ATATATGGTACCCCACTTTGTCAAAAGTCG
TΔ2-28down…….	AAGGTTCTTGCTTCC
TΔ2-28up…….....	CATAGACCCTCCTTT
Fort-R5K……...	TCTATGGCAGCACCTAAAATATCATTTTCGCCC
Revt-R5K…….....	GGGCGAAAATGATATTTTAGGTGCTGCCATAGA

TABLE 2.4. Continued

Oligo name	Sequence
Fort-I39V…….....	CGGGTAGCTGCTGTAGTTCTTTTGTTTATAATG
Revt-I39V……..	CATTATAAACAAAAGAACTACGACAGCTACCCG
Fort-T75I……...	ATTGAAAAGGAAAGAATTGCACGCTTTGAATCT
Revt-T75I……..	AGATTCAAAGCGTGCAATTCTTTCCTTTTCAAT
CgfpNt-rev……	TGATATTCTAGGTGCTGCTTTGTATAGTTCATCCAT
CgfpNt-for…….	ATGGATGAACTATACAAAGCAGCACCTAGAATATCA
AG-T-for……...	GCAGGTGCAGCACCTAGAATATCA
Gfp-AGS-rev…….	ACTTCCAGCTTTGTATAGTTCATCCAT

Construction of plasmids

Plasmid pT4T was derived by removing the *aphI* (kanamycin-resistance) gene from pER-t (109) and was a gift from I.-N. Wang. It carries a hybrid lysis cassette in which the T4 *t* gene (Fig. 2.2; nt160204 to 160884 of the T4 genome) replaces the λ *S* gene (nt 45157 to 45465 of the λ genome) in a DNA segment comprising pR', the λ late promoter, the downstream genes *SRRzRz1*, and a deletion of the *bor* gene (Fig. 2.2). This lysis cassette is flanked by unique *Hind*III and *Cla*I sites (not shown). The plasmid, pT4TRI, was constructed by PCR amplifying the lysis cassette from pT4T using the forward and reverse primers HindIIIpR'for and CRzNRIrev. In a separate PCR reaction the *rI* gene was amplified using the forward and reverse primers CRzNRIfor and ClaIRIrev. The *rI* gene in the template used for this reaction had its internal *Cla*I site destroyed by the introduction of the silent mutation G63A by site-directed mutagenesis. Since the primers CRzNRIrev and CRzNRIfor were complementary, it was possible to fuse the *rI* gene sequence (nt 59540 to 59177 of the T4 genome) to the 3' end of the hybrid lysis cassette (after the base corresponding to 46437 of the λ genome, beyond the

end of the *Rz* gene; Fig. 2.2) by using the two PCR products as templates in an SOE (splicing by overlapping extension) reaction (54) using the HindIIIpR'for and ClaIRIrev primers. The product from this reaction was digested with *Hind*III and *Cla*I and ligated into the vector backbone produced by digesting pT4T with the same enzymes. The plasmid pT4T^{his} was generated by introducing a hexahistidine tag between codons 132 and 133 of the *t* gene (Fig. 2.1A, underlined residues) in pT4T, using a pair of oligonucleotides, 132-H6G2for/rev, encoding His_6Gly_2.

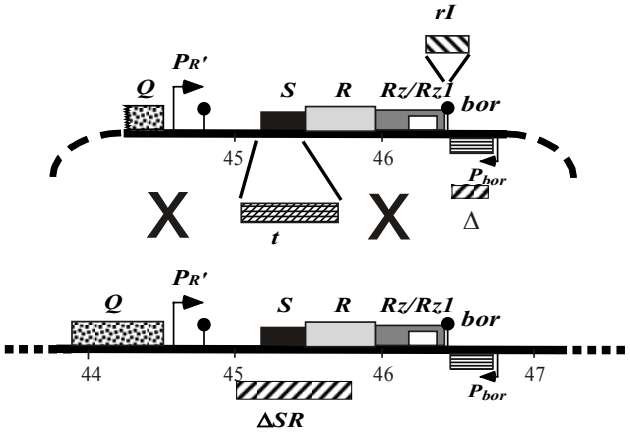

FIG. 2.2. Features of plasmid and phage constructs. All plasmids used for inductions are based on the structure of pS105 (109)(upper structure), with the λ late promoter and the promoter-proximal genes of the late transcriptional unit (lower structure), except that in the plasmid pT4T, the *S* gene in the λ *SRRzRz1* lysis cassette of pER157 (47) is replaced by the phage T4 *t* gene. In the plasmid pT4TRI, the *rI* gene is inserted 13 nucleotides downstream of the *Rz* gene of pT4T. "X" designates areas where homologous recombination can occur for generation of λ*t* recombinants (133).

Two plasmids were constructed for overexpression of the his-tagged C-terminal domain of RI (RI_{CTD}^{his}) and T (T_{CTD}^{his}). For the T_{CTD} plasmid, the DNA fragment encoding T_{CTD}^{his} was PCR amplified from pT4T^{his} using the primer pair NdeI70 for and

BamH1trev. The doubly-digested PCR product was inserted into the multiple cloning site of plasmid pET11a to generate the plasmid pET11a-T_{CTD}^{his}. To construct the RI_{CTD} plasmid, a fragment carrying gene *rI* was produced by cleaving pZE-RI with EcoRI and XbaI. The plasmid pER-t was digested using the same enzymes to generate the backbone for the plasmid pPRI, and this backbone fragment was ligated to the EcoRI-XbaI fragment carrying *rI* to produce pPRI. The plasmid $pPRI^{his}$ was made by inserting hexahistidine tag after codon 97 of the *rI* gene (Fig. 2.1B) in pPRI, using the primer pair, RIG2H6for/rev, encoding Gly_2His_6. The DNA fragment encoding the RI_{CTD}^{his} PCR was amplified from $pPRI^{his}$ using 25RINdeIfor and RIhisBamH1rev with NdeI and BamH1 restriction sites at their 5' ends, respectively. The doubly-digested PCR product was inserted into the multiple cloning site of pET11a to yield pET11a-RI_{CTD}^{his}.

Phage λt^{his} was generated by homologous recombination between $pT4T^{his}$ and the lysis-defective phage λ*kan*Δ(*SR)* (formerly designated as λΔ*SR* (105); Fig. 2.2). Recombinants were identified by their plaque-forming ability and the presence of the hybrid lysis cassette was verified by DNA sequencing. Lysogens were prepared by infecting cells with λt^{his} and plating at 30ºC for survivors on media containing kanamycin.

The T4 *t* and *rI* genes and their derivatives were also expressed from the *lac* promoter of the pZA and pZE plasmids from the family of modular pZ vectors (86). To construct pZA-RI and pZA-RI^{cmyc}, the primer pair, Kpn1RIfor and RIAvrIIrev was used to PCR amplify the *rI* gene from pZE-RI or pZE-RI^{cmyc}, respectively. After digestion with *Kpn*I and *Avr*II, these PCR products were used to replace the *luc* gene in pZA32-

luc. The plasmid, pZA-RI_{CTD}, carrying a DNA fragment encoding the C-terminal domain (residues 25-97; Fig. 2.1B) of the RI protein was similarly constructed using the PCR product from a PCR reaction with primers 25RIKpnIfor and RIAvrIIrev and pZE-RI as the template. The signal sequence of alkaline phosphatase (PhoA) was fused to the RI fragment in pZA-RI_{CTD} by the modified site-directed mutagenesis procedure described above. In the first PCR reaction, the PhoA signal sequence was amplified using the ss25RIfor and ss25RIrev primers. The second PCR reaction used the above PCR product as the primer and pZA-RI_{CTD} as the template yielding pZA-^{ss}PhoAΦRI_{CTD}. The identical reactions were used to generate pZA-RI_{CTD}^{cmyc} and pZA-^{ss}PhoAΦRI_{CTD}^{cmyc} from pZE-RI^{cmyc}. A similar strategy was used to generate the complementary series of plasmids, pZA-T, pZA-T_{CTD} and pZA-^{ss}PhoAΦT_{CTD}, using the primer pairs, KpnItfor/AvrIItrev, 56tKpnIfor/AvrIItrev, and ss25RIfor/56tssrev, respectively. Here, the T_{CTD} consists of residues 56 to 218 of T (Fig. 2.1A).

The sequence encoding residues 27-471 of the *phoA* gene was PCR amplified using the forward and reverse primers KpnIphoAfor and AvrIIphoArev, with *Kpn*I and *Avr*II restriction sites at their 5' ends, respectively. The doubly-digested PCR product was used to replace the *luc* gene in pZA32-luc to yield pZA-PhoA. To fuse the N-terminal domain (residues 1 to 24, RI_{NTD}) of RI to the mature form of PhoA, the DNA encoding the RI_{NTD} was PCR amplified using the primers RItmphoAfor and RItmphoArev. The PCR product was then used to conduct a modified site-directed mutagenesis reaction using pZA-PhoA as the template to generate pZA-RI_{NTD}ΦPhoA. The plasmid pZA-T_{TMD}ΦPhoA in which residues 1 to 70 of T are fused to the mature

sequence of PhoA was constructed in a similar fashion using the primers T4TtmphoA for and T4TtmphoArev.

The *ftsI*$_{tmd}$*ϕt* chimera, encoding a protein with the TMD of FtsI (Fig. 2.1A) replacing the TMD of T, was constructed in two steps. First, a DNA fragment encoding residues 70 to 218 of T was PCR amplified using the forward and reverse primers AvrIItrev and KpnI70tfor, with *Avr*II and *Kpn*I restriction sites at their 5' ends, respectively. The doubly digested PCR product was used to replace the *luc* gene in pZA32-luc generating the intermediate plasmid, pZA-T$^{70\text{-}218}$. Then, a DNA fragment encoding a methionine codon followed by the transmembrane segment of FtsI (residues 24 to 40) was PCR amplified using the forward and reverse primers, FtsITM70tfor and FtsITM70trev The PCR product was then used to conduct a modified site-directed mutagenesis reaction by using the with pZA-T$^{70\text{-}218}$ as the template to generate pZA-FtsI$_{TMD}$ΦT.

GFP was fused to cmyc-tagged RI (Fig. 2.1B) by another SOE reaction. First, a DNA fragment encoding GFP was PCR amplified from pDS439 (120) using the primers KpnIgfpfor and N-RIC-gfprev. Separately, a DNA fragment encoding residues 2-106 of the cmyc-tagged RI protein was PCR amplified from pZE-RI^{cmyc} using the primers C-gfpN-RIfor and RI-Xbarev. The PCR products from the two reactions were combined and amplified using the primers KpnIgfpfor and RI-Xbarev. The fusion product was digested with *Kpn*I and *Xba*I and ligated into pZE12 digested with the same enzymes, yielding pZE-GFPΦRI^{cmyc}.

Subcellular fractionation

To prepare total membrane and soluble fractions, cell pellets from 150 ml cultures were resuspended in 1 ml of French press buffer (100 mM Na_2HPO_4, 100 mM KCl, 5 mM EDTA, pH 8.0, 1 mM PMSF, 25 mM $MgCl_2$, 50 μg/ml DNAse, 50 μg/ml RNAse) and 2.5 μl of Protease Inhibitor Cocktail (4-(2-aminoethyl)benzenesulfonyl fluoride, bestatin, pepstatin, E-64 and phosphoramidon; Sigma). The cells were disrupted by passage through a French pressure cell (Spectronic Instruments, Rochester, N.Y.) at 16,000 psi (1 psi = 6.89 kPa). The unbroken cells were removed by centrifugation in a Damon-IEC Spinette clinical centrifuge at 1000 x g for 10 min. The membrane and soluble fractions were separated by centrifugation at 100,000 x g for 60 min at 4ºC. To identify periplasmic proteins, cells from 30 ml cultures were collected by centrifugation and the pellets were resuspended in 250 μl of 25% sucrose, 30 mM Tris-HCl, pH 8.0. Then, 10 μl of 0.25 M EDTA, 10 μl of lysozyme (20 mg/ml in water), and 250 μl of distilled water were added, sequentially (16). When microscopic examination showed that ~95% of the cells had formed spheroplasts, the samples were centrifuged at 9000 x g for 10 min to separate the periplasm from the spheroplasts (membrane and cytosol).

SDS-PAGE and Western blotting

SDS-PAGE and Western blotting were performed as previously described (46). To generate antibodies against RI and T, BL21(DE3) *tonA::*Tn*5 slyD::*Tet^r cells

harboring either pET11a-T_{CTD}^{his} or pET11a-RI_{CTD}^{his} were grown in 1 liter of LB-ampicillin to A_{550} ~ 0.5; then the cultures were induced with IPTG for 3 hrs. The cell pellets was resuspended in 20 ml of 20 mM BES (N,N-bis[2-hydroxyethyl]-2-aminoethanesulfonic acid; Sigma), 0.5 M NaCl pH 7.5 supplemented with 20 µl Protease Inhibitor Cocktail, 700 µl $MgCl_2$ (1M), 100 µl RNase (10 mg/ml), 100 µl DNase (10 mg/ml), and 20 µl DTT (1 M). The cells were lysed by passage through a French pressure cell (Spectronic Instruments, Rochester, N.Y.) at 16,000 psi (1 psi = 6.89 kPa). Inclusion bodies were collected by centrifugation of the French press lysates at 17,500 x g for 30 min. The pellets were extracted with 20 ml of 20 mM BES, 6 M guanidine hydrochloride pH 7.5 for 3 hrs. The extracts were cleared by centrifugation at 17,500 x g for 10 min. The supernatant was used as the starting material for purifying T_{CTD}^{his} and RI_{CTD}^{his} using Talon metal affinity resin (Clontech). The 5 ml resin bed is equilibrated with 20 mM BES, 6 M guanidine hydrochloride (United States Biochemical) pH 7.5 and the bound proteins were eluted with 20 mM BES, 6 M guanidine hydrochloride, 0.5 M imidazole (Sigma), pH 7.5.

Antibodies against the purified, C-terminal domains of T^{his} and RI^{his} were prepared in rabbits by ProSci Incorporated, Poway, CA. Antibodies against the *cmyc* epitope were purchased from Babco (Richmond, CA). Reagents and methods for immunodetection have been described (145). Equivalent sample loadings were used whenever multiple fractions from the same culture were analyzed.

Immunoprecipitation of RI - T complexes

MDS12 *tonA*::Tn10 *lacI*^{q1} cells harboring the indicated allele of pZA-^{ss}PhoAΦT$_{CTD}$ and pZE-GFPΦRI^{cmyc} either alone or in combination were grown to an A_{550} ~ 0.4 and then induced with 1 mM IPTG for 30 min. A 30 ml volume of each culture was taken through the EDTA-lysozyme treatment used to prepare spheroplasts (16). Instead of centrifuging the samples after the addition of water, the spheroplasts were lysed by adding 5 µl of Protease Inhibitor Cocktail and 500 µl lysis buffer (100 mM Tris-HCl pH 8.0, 150 mM NaCl, 1% NP40). Next, 100 µl of 1M $MgCl_2$, 10 µl of 10 mg/ml DNase I, and 10 µl of 10 mg/ml pancreatic RNase were added and the samples incubated at room temperature for 15 min with occasional mixing.

To collect complexes containing the T_{CTD} and GFPΦRI^{cmyc} proteins, 200 µl of the indicated lysate was diluted with an equal volume of wash buffer (lysis buffer containing 1 mg/ml bovine serum albumin). Next, 2 µl of a pre-immune rabbit serum, rabbit anti-T, or mouse anti-GFP (Stressgen) were added and the samples were incubated for 2 hrs at 4^{o}C with slow agitation. Then, 50 µl of the appropriate iron-conjugated secondary antibody (Pierce) was added and the mixture incubated for an additional for 2 hrs at 4^{o}C. The immune complexes were collected magnetically and washed three times with 0.5 ml of wash buffer. The complexes were dissociated by boiling in SDS-PAGE sample buffer and analyzed by SDS-PAGE and Western blotting followed by immunodetection using anti-T or anti-*cmyc* antibodies, as indicated.

Phage accumulation during LIN

For the assessment of the LIN state, CQ21 cells lysogenic for λ*kan* t^{his} and harboring either no plasmid, pZA-RI or pZA-^{ss}PhoAΦRI_{CTD}, were grown at 30°C and induced both by adding IPTG and simultaneously shifting the growth temperature to 42°C for 15 min then to 37°C. At 30, 60, 90, 120, and 150 min after induction, 1 ml was taken from each culture and the cells lysed by the addition of $CHCl_3$. Debris was removed by centrifugation, and the plaque-forming titers in the cleared lysates determined in triplicate on MDS12 *tonA*::*Tn*10 $lacI^{q1}$.

Results

Domain analysis of the RI antiholin

Paddison et al. (100) used primary structure analysis algorithms to predict that RI has an N-terminal secretory signal and was thus a secreted periplasmic protein. Although RI has been visualized as a cross-linked complex with T, it had previously escaped detection as an independent polypeptide, which presumably was due to proteolytic lability (110). Thus, whether this N-terminal sequence serves as a signal anchor, leaving its periplasmic C-terminal domain (RI_{CTD}) tethered to the cytoplasmic membrane, or a cleavable signal allowing release of the RI_{CTD} into the periplasm was unclear. Sequence analysis of the classical *rI* alleles of Doermann (27) revealed that most were frame-shifts distal to the predicted secretory signal. Moreover, the single

missense allele, (R78P; listed as R78G in Paddison et al. (100); Fig 2.1B), also mapped there, implicating the RI_{CTD} as critical to the antiholin function of RI.

To resolve RI into topological components, we constructed two chimeric genes: one, $^{ss}phoA\phi rI_{CTD}$, with RI_{CTD} fused to the signal sequence of alkaline phosphatase (PhoA); the other, $rI_{NTD}\phi phoA$, with the N-terminal domain of RI (RI_{NTD}) fused to the periplasmic domain of PhoA (Fig. 2.1B). Using antibodies raised against RI_{CTD}, the $^{ss}PhoA\Phi RI_{CTD}{}^{cmyc}$ protein could be detected in whole cells (Fig. 2.3A). However, efforts to localize it using conventional subcellular fractionation were unsuccessful, again presumably due to rapid proteolysis after cell disruption. To provide evidence that $^{ss}PhoA\phi RI_{CTD}{}^{cmyc}$ was present in the periplasm, the $^{ss}phoA\phi rI_{CTD}$ gene was expressed in cells grown in the presence or absence of azide to inhibit SecA. A slower migrating species accumulated in the presence of azide, indicating that, when SecA is not inhibited, $^{ss}PhoA\Phi RI_{CTD}{}^{cmyc}$ is processed and localized to the periplasm (Fig. 2.3A). By contrast, the product of the $rI_{NTD}\phi phoA$ construct was stable, unprocessed and was found in both the membrane and soluble fractions (Fig. 2.3B). The dual localization of the unprocessed $RI_{NTD}\Phi$PhoA protein will be considered in the Chapter III. We next compared the ability of these chimeras to support LIN with that of wt RI. While the $rI_{NTD}\Phi phoA$ fusion had no biological function, the $^{ss}phoA\phi rI_{CTD}$ chimera blocked *t*-mediated lysis, as assessed by monitoring the turbidity of the induced culture (Fig. 2.4A). Moreover, in addition to preventing the loss of optical density, both *rI* and $^{ss}phoA\phi rI_{CTD}$ allowed the extended intracellular accumulation of virions and suppressed their release to the medium (Fig. 2.4B). Finally, the LIN state supported by both *rI* and

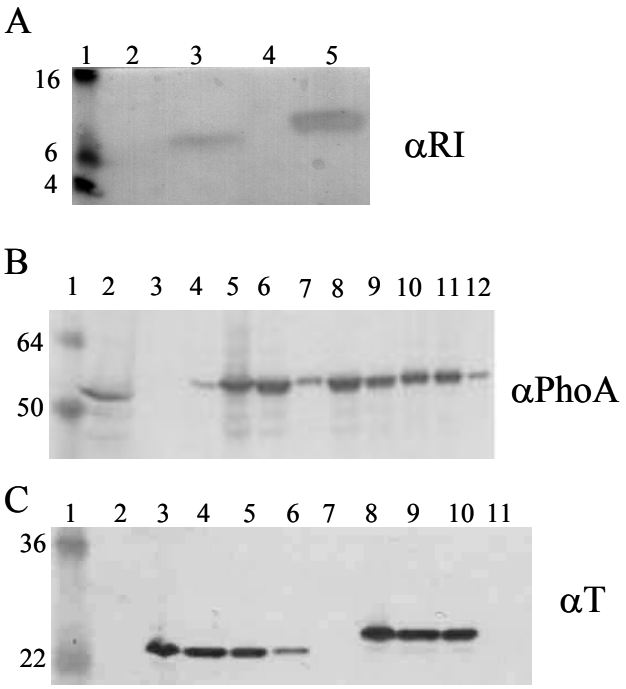

FIG. 2.3. Localization of T and RI chimeras. Subcellular fractions were prepared and analyzed by SDS-PAGE and Western blotting as described in *Materials and Method*. (A) Cells carrying pZA-^{ss}PhoAΦRI$_{CTD}^{cmyc}$ were grown in the absence (lanes 2 and 3) or the presence (lanes 4 and 5) of 1 mM azide for 10 min in advance of induction. Cells from these cultures were collected by TCA precipitation and centrifugation, resuspended in SDS-PAGE sample buffer and subjected to SDS-PAGE and Western blotting using anti-RI antisera as the primary antibody. Lane 1, molecular mass standards; lanes 2 and 4, samples from uninduced cultures; lanes 3 and 5, samples from induced cultures. (B) Cells carrying the pZA-RI$_{NTD}$ΦPhoA were induced, fractionated, and analyzed by SDS-PAGE and Western blotting using anti-PhoA as the primary antibody. Lane 1, molecular mass standards; lane 2, mature form of PhoA; lane 3, blank; lane 4, cells from an uninduced culture; lane 5, cells from an induced culture; lane 6, total cell lysate; lane 7, 1000 x g pellet; lane 8, 1,000 x g supernatant; lane 9, 100,000 x g supernatant (soluble fraction); lane 10, 100,000 x g pellet (membrane fraction); lane 11, detergent extractable (1% NP40) membrane fraction; lane 12, detergent insoluble fraction. (C) Cells carrying pZA-^{ss}PhoAΦT$_{CTD}$ were grown in the absence (lanes 2-6) or the presence (lanes 7-11) of 1 mM azide for 10 min in advance of induction, harvested, fractionated and analyzed by SDS-PAGE and Western blotting using anti-T antisera as the primary antibody. Lane 1, molecular mass standards; lanes 2 and 7, uninduced cells; lanes 3 and 8, induced cells; lanes 4 and 9, cells after spheroplasting; lanes 5 and 10, spheroplasts; lanes 6 and 11, periplasm (133).

$^{ss}phoA\phi rI_{CTD}$ could be subverted by the addition of energy poisons (Fig. 2.4A). We conclude that the periplasmic domain of RI is necessary and sufficient for authentic LIN. Indeed, the $^{ss}phoA\phi rI_{CTD}$ allele is more effective than the parental *rI* gene, as judged by the stability of the LIN phenotype (Fig. 2.4A).

RI-dependent LIN requires binding to the C-terminal domain of T

The unusually large C-terminal periplasmic domain of T (T_{CTD}) is a feature that distinguishes it from the numerous class I and class II holins (141). To determine whether this domain is the target for RI_{CTD}, we constructed an allele of *t* in which the sequences encoding the predicted cytoplasmic and transmembrane domains were replaced by the segment of *phoA* encoding its secretory signal sequence ($^{ss}phoA\phi t_{CTD}$; Fig. 2.1A). Like the RI_{CTD}, the T_{CTD} was also efficiently secreted by the PhoA signal sequence (Fig. 2.3C). This allele was lytically incompetent but exerted a weak dominant-negative phenotype in that it caused a short delay in T-mediated lysis (Fig. 2.4C inset), suggesting that homotypic interactions in the T_{CTD} are involved in the lytic function of T. The biological function of this chimera was assessed in a system in which *t* and *rI* are both expressed from the λ late promoter, shown in previous work to support physiologically meaningful lysis timing with the λ lysis cassette (47). The results clearly showed that supplying periplasmic T_{CTD} partially blocked the imposition of LIN (Fig. 2.4C). More dramatic results were obtained when cells producing the $^{ss}PhoA\Phi T_{CTD}$ were infected with T4 phage; LIN was completely subverted by the

FIG. 2.4. The C-terminal domains of T and RI are the determinants of LIN. (A) ^{ss}PhoAΦRI$_{CTD}$ is necessary and sufficient for LIN. CQ21(λ*kan*Δ*(SR)*) cells carrying the indicated plasmids were induced at time 0 and culture turbidity was followed as a function of time. ⊠, pT4T; ■, □, pT4T and pZA-RI; ○, ●, pT4T and pZA-^{ss}PhoAΦRI$_{CTD}$; ▲, pT4T and pZA-RI$_{NTD}$ΦPhoA; ◆, pS105; ◇, pS105 and pZA-RI; ▽, pS105 and pZA-^{ss}PhoAΦRI$_{CTD}$. To demonstrate premature triggering, KCN was added to two cultures (pT4T and pZA-RI, □ and pT4T and pZA-^{ss}PhoAΦRI$_{CTD}$, ○) at the time indicated by the solid arrow. (B) Phage accumulation during ^{ss}PhoAΦRI$_{CTD}$-mediated LIN. CQ21(λ-t^{his}) carrying the indicated plasmids was induced at time 0 and culture turbidity (solid symbols) and phage accumulation (open symbols) was followed as a function of time. ○, ●, no plasmid; ◇, ◆, pZA-RI; □, ■, pZA-^{ss}PhoAΦRI$_{CTD}$. (C) Periplasmic T$_{CTD}$ interferes with LIN. CQ21(λ*kan*Δ(SR)) cells carrying the indicated plasmids were induced at time 0 and culture turbidity was followed as a function of time. ●, pT4T; ○, pT4T and pZA-^{ss}PhoAΦT$_{CTD}$; □, pZA-^{ss}PhoAΦT$_{CTD}$; △, pT4TRI; ▽, pT4TRI and pZA-^{ss}PhoAΦT$_{CTD}$; ◇, pT4TRI and pZA-T$_{CTD}$; ▲, pT4TRI and pZAT$_{TCD}$; ▼, pT4TRI and pZA- FtsI$_{TMD}$ΦT$_{70\text{-}218}$; ■, pT4TRI and pZA-T$_{TMD}$ΦPhoA. . Inset: detail for growth of cells carrying pT4T alone (●) and pT4T and pZA-^{ss}PhoAΦT$_{CTD}$ (○). (D) Periplasmic T$_{CTD}$ blocks LIN during T4 phage infections. CQ21 cells carrying either pZA32-luc (solid symbols) or pZA- ^{ss}PhoAΦT$_{CTD}$ (open symbols) were induced at time 0 and were grown without infection (○, ●) or infected at a moi of 10 with either T4D (□, ■) or T4*rI* (△,▲). In all experiments, $CHCl_3$ was added at the time indicated by the dashed arrow (133).

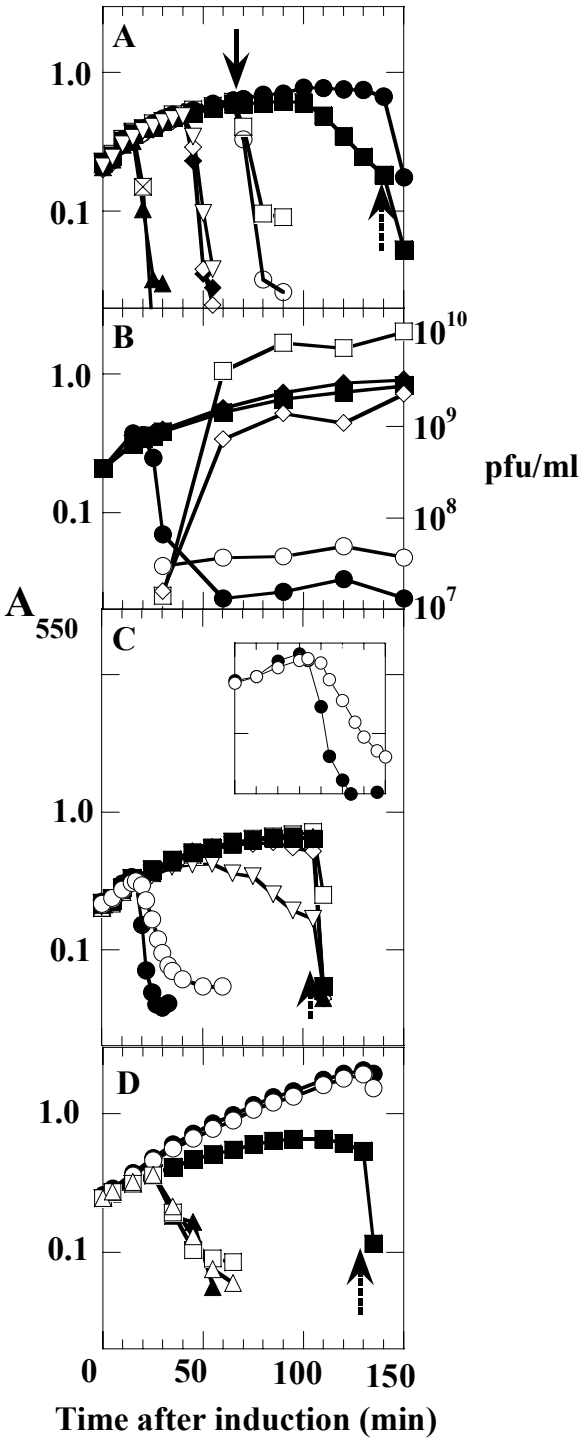
A
B
C
D
1.0
0.1
10^{10}
10^{9}
10^{8}
10^{7}
pfu/ml
A_{550}
0
50
100
150
Time after induction (min)

presence of the T_{CTD} (Fig. 2.4D). In a control infection, induction of $^{ss}phoA\phi t_{CTD}$ had no effect on the lysis kinetics of T4*rI* (Fig. 2.4D). When T4 phage were plated on bacteria secreting T_{CTD} to the periplasm, wt T4 (T4D) generated large, distinct plaques, which were nearly identical to the plaques produced by *rI* mutants (Fig. 2.5). We conclude that interactions between the periplasmic domain of RI and the periplasmic domain of T are required for LIN.

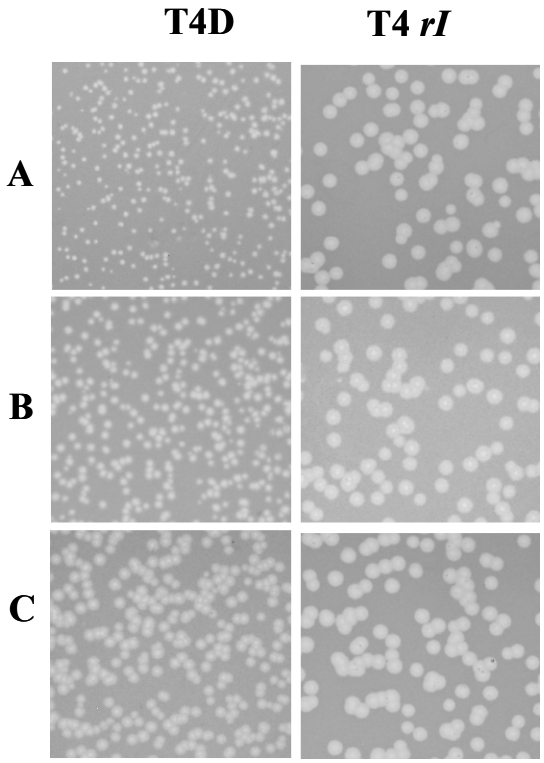

FIG. 2.5. Periplasmic T_{CTD} causes T4 to form *r*-type plaques. Lawns of MDS12 *tonA*::Tn*10 lacI*^{q1} (panel A), MDS12 *tonA*::Tn*10 lacI*^{q1} harboring uninduced pZA-^{ss}phoAΦT_{CTD} (panel B), or MDS12 *tonA*::Tn*10 lacI*^{q1} harboring induced ^{ss}PhoAΦT_{CTD} (panel C) were infected with either T4D or T4*rI* phage (133).

T and RI form a complex

To provide further evidence that the T and RI proteins interact, we performed co-immunoprecipitation experiments using lysates prepared from cells expressing ^{ss}PhoAΦT$_{CTD}$ and a GFPΦRI^{cmyc} chimera. The GFPΦRI^{cmyc} chimera was used since it was readily visualized by immunoblot, presumably because of decreased lability compared to either RI or ^{ss}PhoAϕRI$_{CTD}$, both of which were undetectable in immunoprecipitations. Using either anti-T or anti-GFP as the first antibody, the two proteins were found to co-precipitate (Fig. 2.6A). These complexes were also formed when detergent-solubilized extracts prepared from cells expressing T or GFPΦRI^{cmyc} separately were mixed and then subjected to immunoprecipitation (not shown). Identical results were obtained when the T75I mutation found in a *t* allele known to be insensitive to RI-mediated LIN was introduced into the ^{ss}PhoAϕT$_{CTD}$ protein (Fig. 2.6B). Since the R78P allele of *rI* is defective for LIN, we attempted to test the effect of this mutation on the ability of RI to form complexes with T. Unfortunately, the product of the R78P allele of *gfpϕrI^{cmyc}* does not accumulate in whole cells to levels detectable by Western blot.

Interestingly, the ratio of unprocessed ^{ss}PhoAΦT$_{CTD}$ to mature periplasmic T$_{CTD}$ was reproducibly higher when GFPΦRI^{cmyc} was present (Fig. 2.6AB, lanes 5 -7). This suggests that the binding of RI to the periplasmic domain can occur while T$_{CTD}$ is nascent and that this binding interferes with leader peptidase cleavage of the signal sequence.

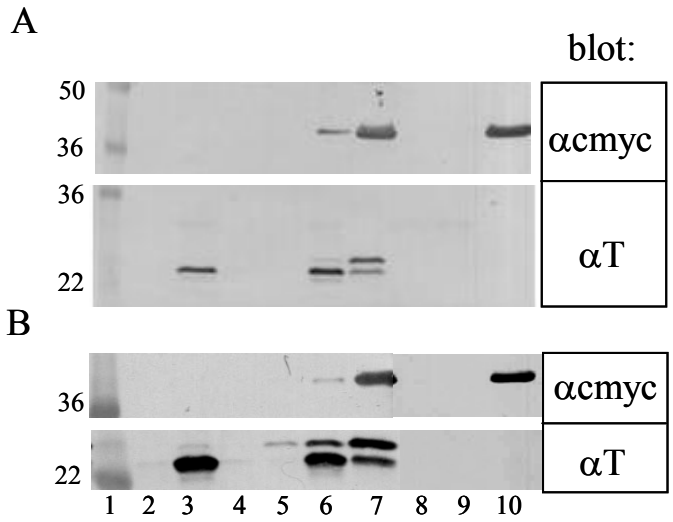

FIG. 2.6. T and RI form a complex. (A) Immunoprecipitations were performed with samples containing either ^{ss}PhoAΦT$_{CTD}$ (lanes 2 – 4), both ^{ss}PhoAΦT$_{CTD}$ and GFPΦRI^{cmyc} (lanes 5 – 7), or GFPΦRI^{cmyc} only (lanes 8 – 10), prepared from induced cells carrying either of the plasmids pZA-^{ss}PhoAΦT$_{CTD}$ or pZE-GFPΦRI^{cmyc}, or both. Primary antibodies for immunoprecipitations: lanes 2, 5 and 8, rabbit preimmune serum; lanes 3, 6, and 9, anti-T rabbit antibody; lanes 4, 7 and 10, anti-GFP monoclonal antibody. Samples were analyzed by SDS-PAGE and immunoblotted with either anti-T or polyclonal anti-cmyc, as indicated to the right. (B) Same as (A) except that the *rV* variant ^{ss}PhoAΦT$_{CTD}^{T75I}$, produced from the plasmid pZA-^{ss}PhoAΦT$_{CTD}^{T75I}$ was used. Molecular mass appears in lane 1 for each blot (133).

Discussion

Infections of T4 and the other T-even phages are the only examples where lysis timing has been demonstrated to be directly affected by the environmental conditions surrounding the infected cell. The classic LIN phenotype can be thought of as a "no quorum" signal, in the sense that an effector molecule (i.e., a super-infecting T4 phage) indicating the lack of available hosts binds to an infected cell and initiates an as yet unknown signal transduction pathway leading to activation of an effector, RI. The

simplest interpretation of our data is that activated RI directly binds to and inhibits the target molecule, T, so that lysis is blocked. Both RI and T have hydrophobic domains near their N-termini, but the results presented here demonstrate conclusively that the interactions essential for the transmission of the signal are entirely between the periplasmic domains of the two proteins. Moreover, we have shown that RI and T are present in a complex that can be recovered by immunoprecipitation without prior covalent cross-linking. Unlike class I and II holins which consist of two or three transmembrane domains, short interconnecting loops, and a 10-25 residue C-terminal cytoplasmic domain, T and its orthologs in T4-like phage have a single transmembrane domain and a relatively large C-terminal periplasmic domain (108). Our findings suggest that this periplasmic domain has evolved to serve as a receptor for the LIN signal provided by "activated" RI. This idea is consistent with the observation that large deletions within the T_{CTD} can be tolerated without entirely abolishing holin function (108). In addition, the co-immunoprecipitation experiments also suggest that RI binds to nascent T, since the presence of GFPΦRI^{cmyc} appears to reduce the efficiency of the maturation of ^{ss}PhoAΦT_{CTD} (Fig. 2.6 A, lanes 5-7). This idea that RI bind to nascent T is consistent with the finding that in T4 infections, T4 superinfection can confer RI-mediated LIN on a pre-existing pool of wt LIN-sensitive T molecules if the incoming phage has a wt, LIN-sensitive *t* allele, but not if it has an *rV*, LIN-insensitive *t* allele (109). The interference with signal sequence processing also suggests that conformational changes derived from binding of RI to the T_{CTD} can be transmitted to the

membrane, which is consistent with the fact that one of the classic *rV*, LIN-defective mutations is a subtle missense change, I39V, in the hole-forming TMD of T.

The classic LIN phenotype appears to involve a direct interaction between the periplasmic domains of RI and T and can be subverted by the collapse of the membrane potential by energy poisons. Thus, at a superficial level, the antiholin function of RI resembles that of S107 and $S^{21}71$, the antiholins of λ and lambdoid phage 21, respectively. The latter two proteins are identical to their cognate holins except for a short N-terminal extension. In both cases, antiholin-holin interactions are thought to prevent quaternary rearrangements that are required to convert holin oligomers into "holes". We suggest that in the energized membrane, the single TMD of T is unable to oligomerize into a functional "hole" in the absence of interactions between T_{CTDs} in the periplasm. The antiholin activity of RI would then be due to its ability to bind to the T_{CTD} preventing these interactions. Mutations that alter the periplasmic interactions between T_{CTD} molecules and between T_{CTD} and RI_{CTD} would allow for the genetic malleability of lysis timing for T4. For bacteriophages λ (13,44,45,106) and the lambdoid phage 21 (102), collapse of the membrane potential allows premature triggering of the holin by causing topological changes in the antiholin that lead to its inactivation. Moreover, in these cases, representing canonical class I and II holins respectively, these topological changes in the antiholin effectively convert it into the functional equivalent of its cognate holin. It seems unlikely that T and RI have the same relationship as is seen with the antiholin/holin pairs of phage λ and 21 for several reasons. First, the homotypic interactions that presumably characterize the S105/S107

and $S^{21}71$/ $S^{21}68$ systems are not possible since T and RI do not share amino acid sequence homology. Second, RI_{NTD} is not essential for its antiholin activity, indicating that RI does not directly interact with the hole-forming TMD of the T holin. Finally, in contrast to S107 or $S^{21}71$, RI appears to be a labile protein whose antiholin activity is only realized physiologically under conditions of superinfection.

While the mechanism of action of RI may be fundamentally different than that of S107 or $S^{21}71$, a feature common to the antiholin function of all three proteins is its abrogation by collapse of the membrane potential. Although the reason for this behavior is not obvious, we propose that it endows bacteriophage lysis systems with a "sentinel" function. Here, the injection of a heterologous phage DNA into a previously infected cell is detected by the resident holin as a transitory depolarization of the membrane, associated with the channel formed in the bilayer through which the DNA passes. The resident holin is thus triggered prematurely, aborting the new infection and allowing release of progeny from the initial infection.

The results presented here indicate that the large periplasmic domain of the T4 holin is fundamentally involved in real-time regulation by RI. In the T4 infection cycle, there is evidence that *rI* is transcribed from both early and late promoters (100). Moreover, the RI-dependent LIN phenotype is imposed by superinfections at 3 minutes after infection and beyond, before the first molecule of T, as a late gene product, is made. Given the temporal relationship between the expression of the *rI* and *t* genes, why does RI not inhibit T-mediated lysis in the absence of superinfection? The answer to this question may lie with the stability of RI. LIN is a transient phenomenon which requires

continual reinfection to significantly prolong the latent period of the initial T4 infection (1). This, in itself, suggests that the effector molecule that transmits the LIN signal to the T protein is unstable. In fact, we can detect RI in whole cells collected by TCA precipitation but not if cells are fractionated, which suggests that it is extremely labile. This leads to the parsimonious model that LIN is imposed only if RI reaches a certain level, which can be attained either by virtue of a stabilization signal provided by superinfection or by over-expression from induction of a multicopy plasmid. Our hypothesis is thus that RI function is regulated by its proteolytic instability in the periplasm. The nature of the stabilization signal is unknown but consideration of the molecular events during super-infection may provide a clue. It is thought that Imm, a small cytoplasmic membrane protein produced in quantity early in infection, causes secondary infections to fail, resulting in ectopic periplasmic localization of the capsid contents, which includes the 170 kb T4 chromosome and the more than 1000 molecules of internal head proteins (1,83,85,118). T4 “ghosts”, emptied of DNA and internal proteins, do not cause LIN, although the ability to undergo tail contraction and induce lethal channels in the cytoplasmic membrane is unaffected (1,42). The simplest model is that either the T4 DNA or the internal head proteins interfere in proteolysis of RI, thus indirectly activating the *r* system to block T holin. Recently Los et al. (82) reported that T4 wt, but not T4*rI*, exhibited delayed lysis in slow-growing cells cultured in chemostats, even when there were insufficient free phage to effect LIN by super-infection. This may reflect a significant stabilization of RI due to cellular responses to slow chemostat growth conditions rather than to the ectopic localization of the contents

of superinfecting phage. In any case, experiments to test our model and address other unanswered questions about T4 lysis and LIN that arose decades ago during the classical era of the Delbrück "Phage Church" (15,17), including the roles of the intensively studied *rIIAB* genes and also *rIII*, will be presented elsewhere.

CHAPTER III

THE T4 RI ANTIHOLIN HAS AN N-TERMINAL SAR-DOMAIN THAT TARGETS IT FOR DEGRADATION BY DEGP

Introduction

For dsDNA bacteriophages, the length of the infection cycle is controlled by a holin, which triggers to disrupt the membrane at an allele-specific time (141,146,148). This allows a phage-encoded endolysin to attack the cell wall, leading to the rupture of the cell and release of the progeny virions. Many phages also encode an antiholin which contributes to the timing of host lysis by inhibiting the holin. In phage T4, the holin, endolysin and antiholin are the products of genes *t*, *e*, and *rI*, respectively (61,84,107-110,132). Normally, *E. coli* cells lyse ~25 min after infection by T4 with a burst size of ~ 100. If the infected cell undergoes a secondary infection beginning at 3-5 min after the primary infection, lysis is inhibited and the infection cycle is extended. The lysis-inhibited (LIN) state is unstable; repeated superinfections are required to continue extension of the LIN state (1). In practice, this leads to a greatly prolonged phase of intracellular virus accumulation with each cell containing thousands of progeny virions. The LIN state can be terminated by depolarization of the membrane, after which lysis is essentially instantaneous (1). The LIN phenomenon, the T4 genes associated with it, and the interaction of these genes with host genes were the basis of the classic studies by which the fundamentals of genetic structure were defined (17). Nevertheless, nearly

sixty years after Hershey (51) first reported T4 "*r*" mutants ("*r*" for rapid lysis, or LIN-defective), the molecular basis of LIN is still obscure.

The mechanism of LIN began to be clarified in the past few years, when it was established that RI and T are the only phage proteins required for LIN in all *E. coli* hosts (B, K-12 and K-12(λ)) (29,100,107-110). T is unique among holins in that it has a large periplasmic domain and only a single transmembrane domain (TMD) (Fig. 2.1A), whereas other holins have two or more TMDs and no significant periplasmic component (141). RI is a small protein with a predicted signal sequence and a periplasmic domain of about 75 residues (Fig. 2.1B). As discussed in the previous chapter, LIN requires the interaction of the periplasmic domains of holin T and antiholin RI (133). A chimera in which the N-terminal domain (NTD) of RI was replaced by the cleavable signal sequence of periplasmic alkaline phosphatase, PhoA, (^{ss}PhoAΦRI$_{CTD}$) was found to be more effective at LIN than the wt RI. By contrast, a complementary chimera constructed of RI$_{NTD}$ and the periplasmic domain of PhoA (RI$_{NTD}$ΦPhoA) had no effect on T-mediated lysis (133).

Strikingly, the unprocessed RI$_{NTD}$ΦPhoA protein was found to be present in both the membrane and periplasmic compartments leading us to suspect that the RI$_{NTD}$ might be a SAR (signal-anchor release) domain. The first SAR domain to be characterized was the predicted N-terminal TMD of the bacteriophage P1 endolysin, Lyz (145). Xu et al. provided evidence that the N-terminal TMD of Lyz is initially retained in the bilayer and that this membrane-inserted form is enzymatically inactive (144,145). At a slow rate, the Lyz TMD exits the bilayer spontaneously, which activates the enzyme (145).

Although the mechanism by which the SAR domain of Lyz moves from the membrane to the periplasm is unknown, this process is accelerated by depolarization of the membrane, either artificially by the addition of exogenous energy poisons or physiologically by the action of the P1 holin (145). Similar SAR domains are found in many bacteriophage endolysins and are characterized by a high content of residues of reduced hydrophobicity. More recent studies have shown that SAR domains are not restricted to phage-encoded endolysins. The N-terminal TMD of the type II holin, S^{21}, is also a SAR domain and must exit the bilayer in order for the holin to trigger and form its lethal membrane holes (102). Here we report the results of experiments to determine whether the NTD of RI is also a SAR domain and incorporate them into a model for the molecular basis of LIN.

Materials and methods

Bacterial strains, bacteriophages, plasmids, and culture growth

The bacterial strains, bacteriophages, and plasmids used in this work are described in Tables 2.1, 2.2 and 2.3. T4 phage stocks were prepared as described previously (109). Bacterial cultures were grown in standard LB medium supplemented with ampicillin (100 μg/ml), kanamycin (40 μg/ml) or chloramphenicol (10 μg/ml) when appropriate. Growth and lysis of cultures were monitored as A_{550} as previously

described (109). When indicated, isopropyl β-D-thiogalactoside (IPTG), NaN_3, or $CHCl_3$ was added to give final concentrations of 1 mM, 1 mM, or 1%, respectively.

Standard DNA manipulations, PCR and DNA sequencing

Isolation of plasmid DNA, DNA amplification by PCR, DNA transformation, and DNA sequencing were performed as previously described (133). Oligonucleotides, listed in Table 2.4, were obtained from Integrated DNA Technologies, Coralville, IA, and were used without further purification. Enzymes were purchased from New England Biolabs except for *Pfu* polymerase which was from Stratagene. Automated fluorescent sequencing was performed at the Laboratory for Plant Genome Technology at the Texas Agricultural Experiment Station. Site-directed mutagenesis or modified site-directed mutagenesis on plasmids was performed as described (133).

Subcellular fractionation, SDS-PAGE and Western blotting

Subcellular fractionation, sodium dodecyl sulfate-polyacrylamide gel electrophoresis (SDS-PAGE) and Western blotting were performed as described in Chapter II. Rabbit polyclonal antibodies against polypeptide AQSYARIMNIKLETE of RI were obtained from Sigma-Genosys. The blocking solution for western blotting was a 1:16 dilution of 1% gelatin (Difco) and 1% BSA (ICN) in TBS (150 mM NaCl and 10 mM Tris pH 7.7).

Construction of plasmids and T4 mutants

In these constructions, vector backbone fragments were prepared by digestion with appropriate enzymes then isolated by gel purification. To generate pZE-500RI, the primers -500RIKpn1for and +500RIXba1rev were used to amplify the T4 genome from nucleotide 58681 to nucleotide 60000. The PCR product was digested with KpnI and XbaI then ligated into the pZE12-luc (86) backbone, which had been digested with the same enzymes. The DNA sequence coding for RI was deleted from pZE-500RI by PCR amplification using the primers 500delRIfor/ 500delRIrev. The PCR product was phosphorylated and ligated to make pZE-500ΔRI.

T4Δ*rI* phage was made by homologous recombination between pZE-500ΔRI and T4D. Plasmid pZE-500ΔRI was transformed into MDS12 *tonA::Tn*10 *lacI*^{q1}, and the transformants were grown to A_{550} of ~ 0.4. The culture was infected with T4D at an m.o.i. of ~ 10 for 3 hrs. The infected cells were lysed using $CHCl_3$ to make the recombinant lysate. T4*ΔrI* in the recombinant lysate was enriched three times as follows: a culture of MDS12 *tonA::Tn*10 *lacI*^{q1} at A_{550} ~ 0.3 was infected with the recombinant lysate at an m.o.i. of ~ 0.1 for 5 min. The infected culture was then superinfected with T4*Eam* at an m.o.i. of ~ 10 for 30 min. The infected culture was harvested, rapidly filtered through a 0.22μm syringe filter, and the filtrate was used for the next round of enrichment. At the end of the third enrichment, the filtrate was titered, plated and screened for large plaques. Phages were recovered from the large plaques, and the *rI* deletion was confirmed by PCR using primer pair -500RIKpn1for

/+500RIXba1rev. The PCR product from T4D should be 292 bp longer than the PCR product from T4Δ*rI*.

We wanted to replace the *rI* gene in pZE-500RI with $^{ss}phoA\Phi rI_{CTD}$. This process involved the use of XbaI and KpnI restriction enzymes; thus the XbaI and KpnI sites in pZE-500RI had to be removed. The XbaI site in pZE-500RI was eliminated by digestion of the plasmid with XbaI followed by end repair (Lucigen Corporation) then ligation. This step produced pZE-500RI-X. The integrity of this plasmid was confirmed by a diagnostic digest screen of candidates that had lost the XbaI site but retained the same molecular weight. Subsequently, plasmid pZE-500RI-X was treated with KpnI, end-repaired and religated to obtain pZE-500RI-X-K. This plasmid was confirmed by screening candidates that had lost the KpnI site but retained the same molecular weight. To obtain pZE-500^{ss}PhoAΦRI$_{CTD}$, two different PCRs were performed. First, KpnI and XbaI sites were introduced into this plasmid at the 5' and 3' ends of the *rI* gene in pZE-500RI-X-K using primer pair Kpn1-RI-up and Xba1-RI-down. This reaction also excluded the *rI* gene from the plasmid. Second, the DNA fragment coding for ^{ss}PhoAΦRI$_{CTD}$ was cloned by PCR using pZA-^{ss}PhoAΦRI$_{CTD}$ as the template and the primer pair BamH1-pZE12-for and RI-end-XbaI-rev. The PCR products obtained from these two reactions were digested with KpnI and XbaI then ligated resulting in pZE-500^{ss}PhoAΦRI$_{CTD}$. We wanted to compare the function of RI and ^{ss}PhoAΦRI$_{CTD}$ in T4D and T4$^{ss}phoA\Phi rI_{CTD}$ respectively; thus, we wanted to make these two phages as isogenic as possible which started at the level of materials used for the recombination. The KpnI site at the 5' end of $^{ss}phoA\Phi rI_{CTD}$ in pZE-500^{ss}PhoAΦRI$_{CTD}$ inserted four

nucleotides between the start codon and the Shine Dalgarno sequence, which might lead to a different level of translation once we recombined *$^{ss}phoA\Phi rI_{CTD}$* into T4. Thus, the KpnI site in pZE-500^{ss}PhoAΦRI$_{CTD}$ had to be eliminated. The KpnI site was excluded by PCR using primer pair Ss-PhoA-for and RI-SDS-flanking-rev followed by phosphorylation, ligation and DpnI digestion. The resulting plasmid was pZE-500^{ss}PhoAΦRI$_{CTD}$-K. An amber codon was introduced into this plasmid using primer pair RI-Y42am-for and RI-Y42am-rev resulting in pZE-500^{ss}PhoAΦRI$_{CTD}^{Y42am}$-K.

The plasmid pZE-500^{ss}PhoAΦRI$_{CTD}^{Y42am}$-K was transformed into MDS12 *tonA::Tn*10 *lacI*^{q1}. The transformants were grown to A_{550} of ~ 0.4 and infected with T4D at an m.o.i. of ~ 10. The culture was allowed to grow for 3hrs, $CHCl_3$ was added to terminate the infection, and the resulting recombinant lysate was collected. To enrich for T4*$^{ss}phoA\Phi rI_{CTD}^{y42am}$*, the non-suppressor strain MDS12 *tonA::Tn*10 *lacI*^{q1} was used as the host for infection by the recombinant lysate at an m.o.i. of ~ 0.1 for 30 min. The culture was quickly filtered with a 0.22 μm filter, and the filtrate was used for the next round of enrichment. The enrichment was repeated 3 times then plated on the non-suppressor host MDS12 *tonA::Tn*10 *lacI*^{q1}. Plaques with *r* morphology were picked and plated on both suppressor LE392 *tonA::Tn*10 and non-suppressor MDS12 *tonA::Tn*10 *lacI*^{q1} strains. The presence of *$^{ss}phoA\Phi rI_{CTD}^{Y42am}$* in the T4 genome of the enriched *r* plaque candidates was confirmed by PCR using the primer pair Ss-PhoA-for and RIend+874-rev.

The deletion of the *luc* gene in pZE12-luc was constructed by digesting the plasmid with KpnI and XbaI. The plasmid backbone was gel purified, and the overhang

was filled in with Klenow and then ligated. The deletion of the *luc* gene was confirmed by comparing single digest of the parental and candidate plasmids with AatII, which has a single site. The pZE-Δluc candidates were 1659 bp shorter than the parental plasmid.

Leucines were introduced into RI, as shown in Fig 3.1, via QuikChange using pZA-RI (133) as the template and RIA7Lfor and RIA7Lrev primers. This QuikChange reaction generated pZA-RI^{L}. Then, pZA-RI^{L} was used as the template to make pZA-RI^{2L} using RIT6Lfor and RIT6Lrev primers. Plasmid pZA-RI^{2L} was used as the template to make pZA-RI^{3L} using RI5-6-7-Lfor and RI5-6-7-Lrev primers. Plasmids pZE-RI^{L}, pZE-RI^{2L} and pZE-RI^{3L} were generated by digesting pZA-RI^{L}, pZA-RI^{2L} and pZA-RI^{3L} with KpnI and AvrII followed by ligation into the pZE12-luc (86) backbone digested with same enzymes.

The DNA fragment encoding RI_{TMD}ΦPhoA was cut out of plasmid pZA-RI_{TMD}ΦPhoA (133) by digestion with KpnI and AvrII. To make plasmid pZE-RI_{TMD}ΦPhoA, this DNA fragment was then ligated into the pZE12-luc (86) backbone digested with the same enzymes.

Complementation of T4*ΔrI* with *rI* alleles expressed from plasmids

Fresh transformants of the desired strains harboring either pZE-RI, pZE-^{ss}PhoAΦRI_{CTD} or pZE-Δluc were grown in 25 ml of LB-Amp to A_{550} ~ 0.2 and split into three 7 ml aliquots. Each aliquot was diluted with LB-Amp to make final volume of 25 ml; the cultures were grown until A_{550} ~ 0.3, and induced with IPTG for 10 min. One of

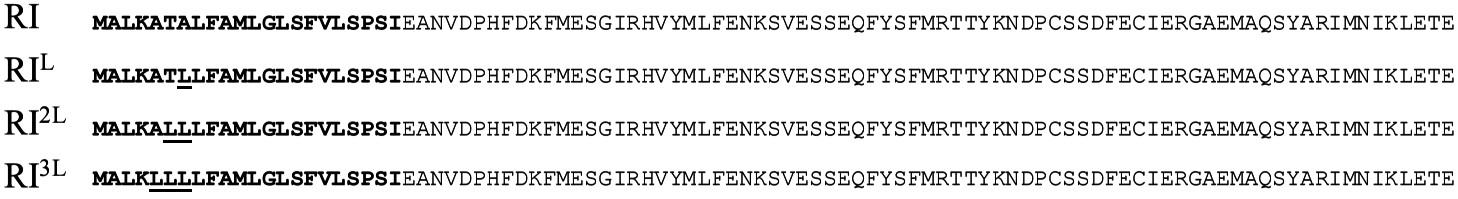

FIG 3.1. Amino acid sequence of RI and RI with leucine substitutions in the predicted signal sequence of RI. Bold: predicted signal sequence of RI. Underline: leucine substitutions.

these cultures was left uninfected while the other two were infected with either T4D or T4Δ*rI* at an m.o.i. of ~ 10, and the culture growth was monitored by A_{550}.

Stability of RI protein

The desired host strain harboring a plasmid with the indicated allele of *rI* was grown in 30 ml of LB-Amp to A_{550} ~ 0.4. The culture was then split into two 15 ml aliquots, and each aliquot was diluted to 60 ml with LB-Amp. These cultures were grown until A_{550} ~ 0.4 and induced with IPTG for 1 hr. Protein synthesis from one of the cultures was inhibited using chloramphenicol (Cam) (300 μg/ml final concentration). At ~ 1.5 min intervals for 10 min after addition of Cam, 5 ml from each culture was taken and added to 5 ml of 10% tri-chloroacetic acid (TCA). The TCA precipitates were collected by centrifugation and subjected to SDS-PAGE and Western blotting using anti RI antibodies. The intensity of the bands on the Western blot corresponding to RI was analyzed using the Image J program downloaded from NIH website (http://rsb.info.nih.gov/ij/).

Phage released assays

MDS12 *tonA*::*Tn*10 *lacI*^{q1} was grown to A_{550} ~ 0.4 and infected with the indicated T4 phage at an m.o.i. of ~ 10. To cultures infected with T4*ΔrI*, chemicals (chloramphenicol or the same volume of 95% ethanol) were added at 15 min after infection. To cultures infected with T4D, the same reagents were added at 30 min after

infection. The A_{550} of these cultures was followed for ~ 2hrs, and samples were collected at 1 hr after infection from T4D-infected cells. Total phage was assessed by titering a $CHCl_3$ treated aliquot of the infected culture. Free phage was determined in the filtrate collected through a 0.22 μm filter. The ratio of plaque forming units (pfu) in the filtrate to that in the total phage sample was used as percentage of phage released.

Azide inhibition of secretion

Fresh transformants of MG1655 *tonA::Tn*10 *lacI*^{q1} harboring pQ, pT4T with or without pZA-^{ss}PhoAΦRI$_{CTD}$ were grown at 37^{o}C until A_{550} ~ 0.2. The cultures were split into three 7 ml aliquots; then each aliquot was diluted with LB containing appropriate antibiotics to a final volume of 25 ml. The cultures were grown to A_{550} ~ 0.2, then NaN_3 at a final concentration of 1mM was added to one aliquot. Ten minutes after the addition of NaN_3, IPTG was added, and the A_{550} was followed until lysis occurred.

Results

The N-terminal TMD of RI is a SAR domain

Previously, we reported that the C-terminal periplasmic domain of RI, the T4 antiholin, was both necessary and sufficient to block lysis mediated by the T4 holin. In the course of these studies, we noted that the chimeric protein RI$_{NTD}$ΦPhoA (Fig. 2.1B)

existed in both soluble and membrane-associated forms indistinguishable by SDS-PAGE (Fig 2.3B). This species had a mass similar to that of the unprocessed form of PhoA that accumulates during inhibition of the *sec*-mediated translocation pathway by sodium azide (Fig. 3.2A, lane 3). Upon further examination, the soluble form of RI_{NTD}ΦPhoA was found to be present in the periplasm (Fig. 3.2A). Thus, by several criteria, RI_{NTD}ΦPhoA behaves like the endolysin of bacteriophage P1 Lyz. The N-terminal SAR domain of Lyz directs its *sec*-mediated integration into the cytoplasmic membrane and allows its subsequent release into the periplasm independent of proteolytic processing. Since commercially available anti-epitope antibodies were unable to reliably detect epitope-tagged RI in Western blots, we prepared antisera to a C-terminal peptide of RI. Using this reagent, we found that the RI protein was present in the soluble and membrane fractions of cells expressing the *rI* gene from a plasmid (Fig. 3.2 C). As with the RI_{NTD}ΦPhoA chimera, the soluble protein appeared to be periplasmic (Fig. 3.2B). Since the mass of the soluble and membrane bound forms of RI were indistinguishable, the former was not generated from the latter by proteolysis. As a control, a Western blot of the samples from cells expressing $FtsI^{cmyc}$ was probed with the antibodies for the *cmyc* tag; this inner membrane protein was only detected in the membrane and spheroplast fractions (Fig. 3.2D). The ability of both RI_{NTD}ΦPhoA and RI to distribute between the membrane and periplasmic fractions strongly argues that the N-terminal domain of RI functions as a SAR domain.

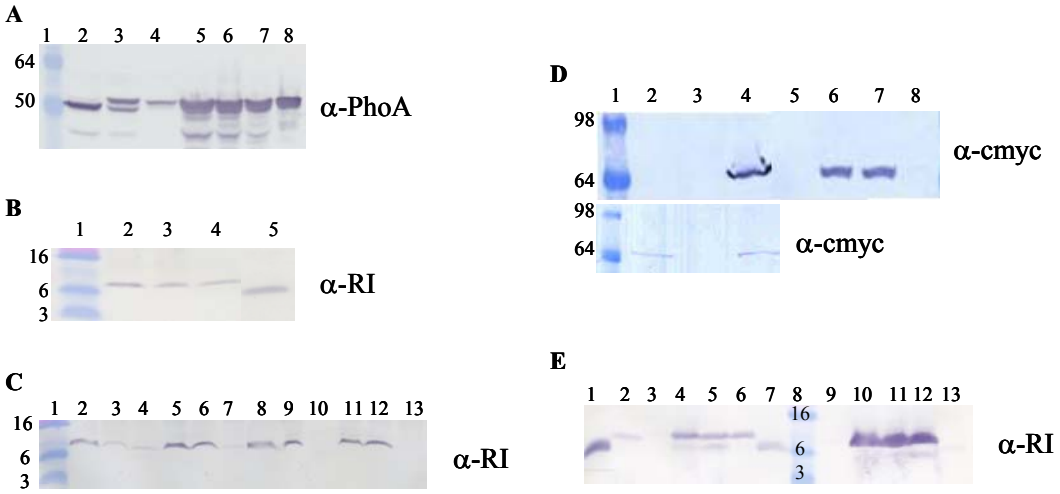

FIG. 3.2. Subcellular localization of RI and its derivatives. Subcelluar localization were prepared and analyzed by SDS-PAGE and Western blotting as described in the *Materials and Methods*. Antibodies were used Western blots as indicated on the right of each for panels. (A) Cells harboring pZE-RI$_{TMD}$ϕPhoA using spheroplasting method. Lane 1, molecular weight marker, lane 2 and 3, cells harboring pJF-PhoA grew in the absence (lane 2) or presence (lane 3) of 1 mM of azide in advance of induction, lane 4, uninduced, lane 5, induced, lane 6, cells after spheroplasting, lane 7, spheroplast (membrane and cytoplasm) and lane 8, periplasm. (B) Cells harboring pZE-RI were induced and fractionated using spheroplasting method. Lane 1, molecular weight marker, lane 2, cells after spheroplasting, lane 3, spheroplast, lane 4, periplasm, lane 5, partially purified RI$_{CTD}$ (C) Cells harboring either pZE-RI, pZE-RI^{L}, pZE-RI^{2L} or pZE-RI^{3L} were induced then fractionated using French press method. Lane 1, molecular weight marker, lanes 2, 3 and 4, RI, lanes 5, 6 and 7 RI^{L}, lanes 8, 9 and 10 RI^{2L} and lanes 11, 12 and 13 RI^{3L}. Lanes 2, 5, 8 and 11, total cell lysates, lanes 3, 6, 9 and 12, detergent extractable membrane, and lanes 4, 7, 10 and 13, 100,000 x g supernatant (soluble fraction). (D) Cells harboring pJF-FtsI^{cmyc} were induced then fractionated. Upper panel, fractionation using French pressing method. Lane 1, molecular weight marker, lane 2, uninduced, lane 3, induced, lane 4, total cell lysate, lane 5, 100,000 x g supernatant, lane 6, 100,000 x g perllet (membrane total), lane 7, detergent extractable membrane and lane 8, detergent insoluble fraction. Lower panel, fractionation using spheroplasting method. Lane 1, molecular weight marker, lane 2, cells after spheroplasting, lane 3 periplasm and lane 4, spheroplast. (E) Cells harboring pZE-^{ss}PhoAϕRI$_{CTD}$ were grown in the absence (lanes 3-7) or presence (lanes 9-13) of 1 mM azide 10 min before induction then harvested and fractionated using the spheroplasting method. Lane 1, partially purified RI$_{CTD}$; lane 2, whole cell RI sample; lanes 3 and 9, uninduced, lanes 4 and 10, induced; lanes 5 and 11, cells after spheroplasting, lanes 6 and 12, spheroplasts and lanes 7 and 13, periplasm; and lane 8, molecular weight marker.

The SAR domains of P1 Lyz and related endolysins have a high content of weakly hydrophobic and uncharged polar residues when compared to conventional TMDs. This suggested that this compositional feature is one factor allowing SAR domains to exit the membrane. For this reason, we tested the effect of increasing the hydrophobicity of the SAR domain of RI on its ability to distribute in the soluble fraction and on its function as an anti-holin. The progressive substitution of leucines for the Ala/Thr residues at positions 5-7 of RI (RI^{1L}, RI^{2L}, and RI^{3L}; Fig. 3.1) had the effect of increasing the fraction of RI that was membrane-associated upon separation of cellular contents into soluble and membrane fractions (Fig. 3.2C). Moreover, increasing hydrophobicity of RI_{NTD} resulted in decreasing the antiholin function of RI (Fig. 3.3A).

RI is an unstable protein

LIN is transient and requires continued reinfection for its maintenance. This could be explained if RI is an unstable protein that is rapidly degraded in the absence of a signal generated by repeated superinfections. As one test of this hypothesis, we determined the half-life of RI protein. In this experiment, the *rI* gene under the control of the *lac* promoter was induced by the addition of IPTG and one hour later chloramphenicol was added to block further protein synthesis. The level of RI present as a function of time after the addition of chloramphenicol was assessed by SDS-PAGE and Western blotting. In this case, the RI protein rapidly disappeared after the addition of the protein synthesis inhibitor showing a half-life of ~ 2 minutes (Fig. 3.4A, E). It was not possible to measure RI stability in T4-infected cells since the level of RI produced

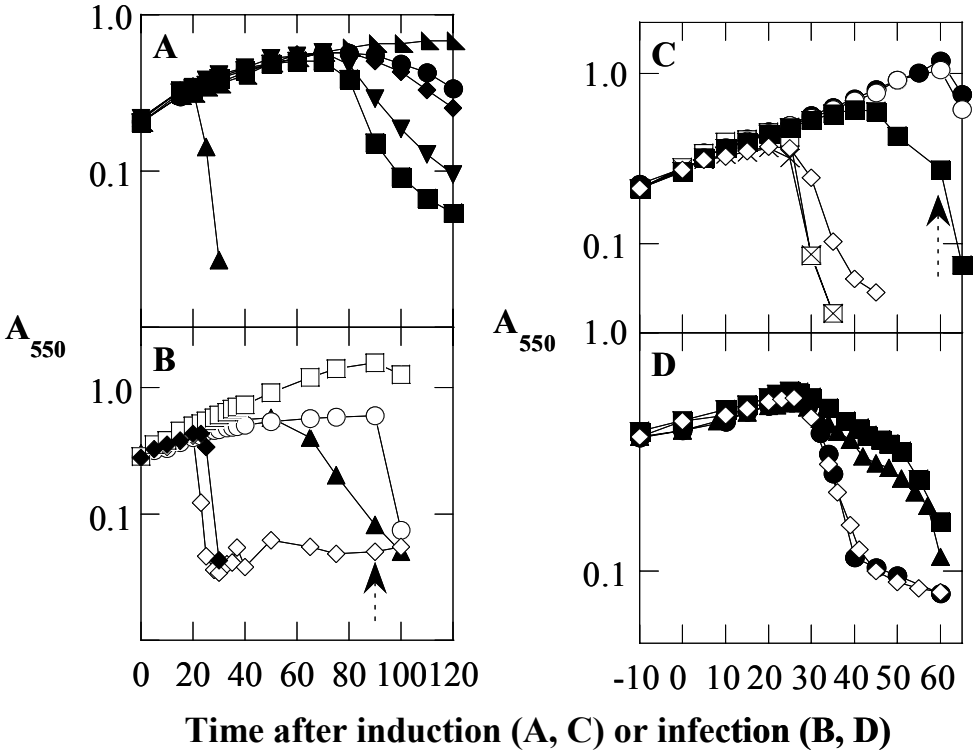

FIG. 3.3. Lysis inhibition by RI and its derivatives. (A) Effect of introducing lecines into the SAR domain of RI on LIN. ▲, host, CQ21(λ-t); ◣, host harboring pZE^{ss}phoAϕRI$_{CTD}$; ●, host harboring pZE-RI; ◆, host harboring pZE12-RI^{L}; ▼, host harboring pZE-RI^{2L} and ■, host harboring pZE12-RI^{3L}.
(B) Complementation of LIN defect in T4Δ*rI* infection with RI and ^{ss}PhoAϕRI$_{CTD}$. The host used was MG1655 *tonA::Tn*10 *lacI*^{q1}. ○, host harboring pZE-Δluc infected with T4D; ◇, host harboring pZE-Δluc infected with T4Δ*rI*; □, host harboring pZE12-Δluc without infection; ◆, host harboring pZE-RI infected with T4Δ*rI*; and ▲, host harboring pZE^{ss}PhoAϕRI$_{CTD}$ infected with T4Δ*rI*. The m.o.i for all infections was ~ 10. (C) Azide collapses ^{ss}PhoAϕRI$_{CTD}$ mediated LIN. The host used was MG1655 *tonA::Tn*10 *lacI*^{q1} pQ. ●, □ and ×, host harboring pT4T; ○, ■ and ◇, host harboring pT4T and pZA-^{ss}PhoAϕRI$_{CTD}$. ●, ○, uninduced cultures; ■, □, induced cultures and ◆, ◇, cultures pretreated with 1 mM azide 10 min before induction. Dashed arrow, 1% $CHCl_3$ was added. (D) Complementation experiments in absence of either DegP, CpxP or both. Hosts MDS12 *tonA::Tn*10 *lacI*^{q1} (parental), MDS12 *tonA::Tn*10 *lacI*^{q1}*degP::Cm*, MDS12 *tonA::Tn*10 *lacI*^{q1}*cpxP::Kn* or MDS12 *tonA::Tn*10 *lacI*^{q1}*degP::Cm cpxP::Kn* harboring pZE-RI were induced for 10 min then infected with T4*ΔrI* at an m.o.i of ~ 5. ◇, parental host;■, *degP::Cm* host, ●; *cpxP::Kn* host and ▲, *degP::Cm cpxP::Kn* host.

was below the limits of detection with our antibody, even when 5 ml of T4-infected culture at A_{550} ~ 0.5 was used for SDS-PAGE and Western blot. Instead, we added chloramphenicol to cultures undergoing LIN during the course of an infection with wild type T4. This treatment resulted in a gradual decrease in culture A_{550} beginning immediately after the addition of chloramphenicol (Fig. 3.5A). After 1 hour of infection, nearly 70% of the total phage present in the treated culture had been released to the medium compared to 10% of the phage in a parallel, untreated culture (Fig.3.5B). The ability of chloramphenicol to partially abrogate LIN is consistent with the rapid turnover of RI during phage infection.

The SAR domain is a major determinant of RI's instability

Previously, we had observed that when the periplasmic C-terminal domain of RI (RI_{CTD}) was fused to the cleavable signal sequence of alkaline phosphatase (PhoA), the resulting chimera (Fig. 2.1), $^{ss}PhoA\Phi RI_{CTD}$, was more effective at eliciting LIN than RI itself (Fig 2.4A). Induction of the *$^{ss}phoA\Phi rI_{CTD}$* gene resulted in the accumulation of two anti-RI reactive species (Fig. 3.2E, lane 4 and 5). The larger product with a mass approximately equal to that of RI was located while the smaller product with a mass approximately the same as that of a polypeptide fragment comprising residues 25-97 of RI was periplasmic (Fig. 3.2E lane 7). The latter product was not present in cultures treated with azide (Fig. 3.2E lane 10 to 12), an inhibitor of the *sec* translocation pathway, and represents the soluble, periplasmic RI_{CTD} released by cleavage of the $^{ss}PhoA\Phi RI_{CTD}$

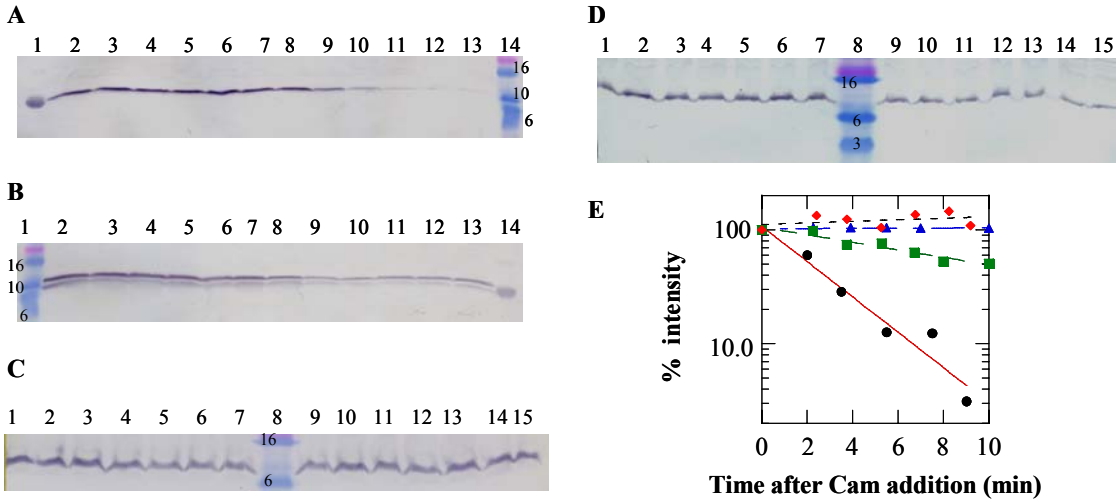

FIG. 3.4. Stability of RI. Panels, A- D show Western blots of samples taken from cultures expressing the indicated *rI* alleles. Samples were TCA precipitated, as described in *Materials and Methods*. (A) Wild type RI. Lane 1, purified RI_{CTD}^{his}, lanes 8-13: 0, 2, 3.5, 5.5, 7.5 and 9 min after addition of Cam. Lane 2-7: same time interval but no Cam added. Lane 14, molecular weight marker. (B) $^{ss}PhoA\Phi RI_{CTD}$. Lane 1, molecular weight marker and lane 14, purified RI_{CTD}^{his}. Lanes 8-13:0, 2.3, 3.9, 5.5, 7 and 10 min after Cam addition. Lanes 2-7: same time interval but no Cam added. (C) RI in a $DegP^-$ strain. Lanes 9-15: 0, 2.4, 3.8, 5.3, 6.8, 8.3 and 9.2 min after addition of Cam. Lanes 1-7: same time intervals but no Cam added. Lane 8, molecular weight marker. (D) RI^{3L}. Lanes 9-15: 0, 2.3, 3.7, 5.3, 6.7, 8.2 and 10 after Cam addition. Lane 1-7: same time interval but without Cam addition. Lane 8, molecular weight marker. (E) Kinetics of RI degradation. ●, RI, ▲, $^{ss}PhoA\Phi RI_{CTD}$, ■, RI^{3L} and ◆, RI in $DegP^-$.

precursor by signal peptidase. Since azide treatment also eliminated LIN (Fig 3.3), it was the periplasmic RI_{CTD} and not the precursor that inhibited the T holin. When cultures expressing the $^{ss}phoA\Phi rI_{CTD}$ gene were treated with chloramphenicol, the periplasmic RI_{CTD} polypeptide was found to be relatively stable (Fig. 3.4B and E). Moreover, the membrane-restricted RI^{3L} protein also had a half-life considerably longer than RI (Fig. 3.4D and E). These data indicate that the degradation of RI occurred after

its release from the membrane and was promoted by the exposure of its SAR domain to the periplasm.

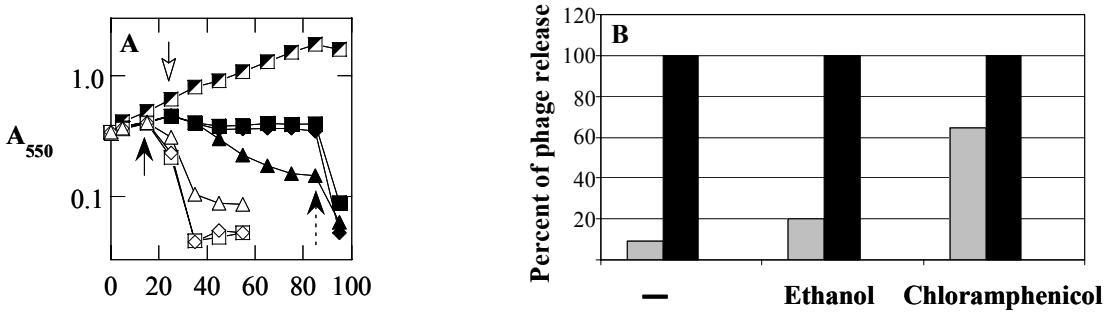

FIG. 3.5. Chloramphenicol collapses LIN. (A) Lysis profile. Host MDS12 *tonA::Tn*10 *lacI*^{q1} was infected with an m.o.i of ~ 10 using either T4D (solid symbols) or T4Δ*rI* (open symbols). ◩, no infection, ■ and □, infected cultures without chemical treatment, ◆ and ◇, infected cultures treated with 95% ethanol at the indicated time, ▲ and △, infected cultures treated with 300μg/mL of chloramphenicol at the indicated time at the times indicated by arrow (solid head: T4*ΔrI*, open head: T4D). Dashed arrow, 1% chloroform was added to the indicated cultures. (B) Percent of phage release. Chemicals added to the cultures are indicated in the figure. Black bar, total phage and gray bar, free phage.

Additional evidence for the destabilization of RI by its SAR domain was obtained by complementing the LIN defective phage, T4Δ*rI*, with plasmids carrying either the *rI* or the ^{ss}*phoAΦrI*$_{CTD}$ genes. In these experiments, the plasmids were induced ten minutes before infection with T4Δ*rI*. Since T4 infection results in the rapid destruction of host DNA, synthesis of RI or ^{ss}PhoAΦRI$_{CTD}$ should cease shortly thereafter. Attempts to complement the LIN defect of T4Δ*rI* with *rI* resulted in a 5

minute delay in lysis compared to the 30-40 minute delay seen with $^{ss}phoA\Phi rI_{CTD}$ (Fig. 3.3B). This result is consistent with the increased stability of the RI_{CTD} compared to RI with its N-terminal SAR domain.

The DegP protease is required for the rapid turnover of RI

We reasoned that the rapid degradation of periplasmic RI might due to the recognition of its exposed SAR domain by proteolytic machinery responsible for removing misfolded proteins from this compartment. Since DegP is known to be involved in the degradation of misfolded periplasmic proteins, we determined the effect of mutations that eliminate DegP activity on the half-life and function of RI. The RI protein was found to have a prolonged half-life in a *degP* mutant (Fig. 3.4C and E). Somewhat unexpectedly, no significant lysis delay was observed when T4Δ*rI* was complemented with *rI* expressed from a plasmid in this mutant (Fig. 3.3D).

Recently, Isaac et al. (57) showed that degradation of a subset of misfolded periplasmic proteins by DegP required the adaptor protein CpxP. We hypothesized that both DegP and CpxP were necessary for RI degradation. According to this idea, when DegP is absent, RI is stable, but no significant LIN could be observed because CpxP binds to RI and prevents the interaction of RI with T. To test this hypothesis, we performed the complementation experiments in the absence of CpxP, DegP or both. Lysis delay in the double mutant was not different from the *degP* mutant alone, indicating CpxP did not interfere with RI antiholin function (Fig.3.3D).

Lysis inhibition of ^{ss}PhoAΦRI$_{CTD}^{Y42am}$ in T4 infection

Since ^{ss}PhoAΦRI$_{CTD}$ was a better inhibitor than RI of T-mediated lysis in the plasmid context, we wanted to study its function in phage T4. Multiple trials to generate T4 *^{ss}phoAΦrI$_{CTD}$*, in which the *rI* gene is replaced with *^{ss}phoAΦrI$_{CTD}$*, failed. This suggested that T4 *^{ss}phoAΦrI$_{CTD}$* was not capable of forming a plaque. Therefore, we made a different phage, T4 *^{ss}phoAΦrI$_{CTD}^{Y42am}$*. In this phage, the *rI* gene was replaced with *^{ss}phoAΦrI$_{CTD}^{Y42am}$*, in which Tyr 42 of RI is replaced by an amber codon. We expected this phage to make *r* plaques on a non-suppressor lawn and no plaques on a suppressor lawn. However, T4*^{ss}phoAΦrI$_{CTD}^{y42am}$* made *r* plaques on both suppressor and non suppressor lawns (Fig 3.6A and B). In addition, the lysis profile of T4 *^{ss}phoAΦrI$_{CTD}^{Y42am}$* in liquid culture had an intermediate phenotype (Fig. 3.6 C). A likely explanation for this phenotype was that the efficiency of suppression was not 100%. In fact, *supF* is the best suppressor available, but the efficiency of suppression is ~ 50% in uninfected cells (99); T4 infection perturbs all aspects of protein synthesis, so it would not be surprising for suppression to be significantly less.

Discussion

Lysis inhibition (LIN) in T-even phage infection is a historically significant phenomenon that was used to elucidate many basic concepts of molecular biology. However, its molecular basis has been obscure. Recently, it was shown that holin T and antiholin RI play a major role in LIN. With T4 infected cells, LIN only occurs when

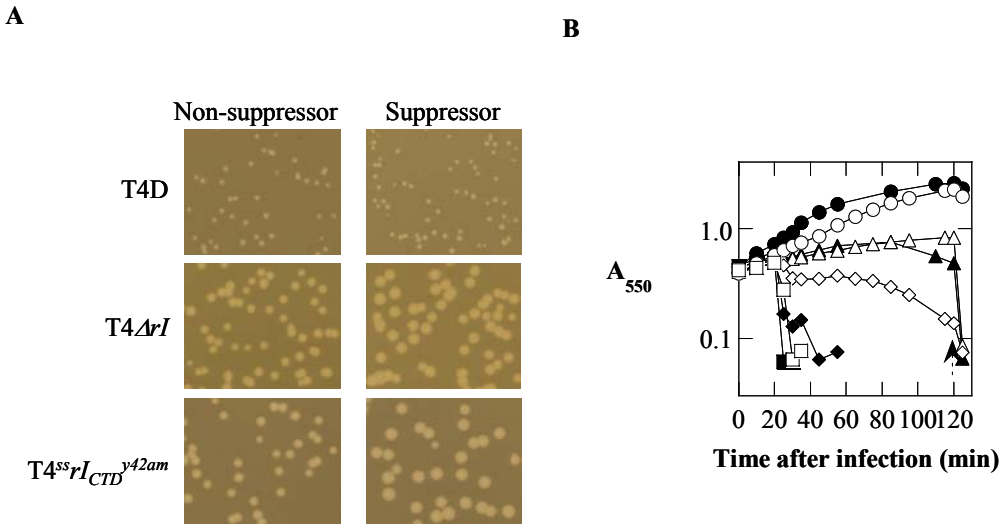

FIG. 3.6. Plating phenotypes. The hosts used were either non-suppressor MG1655 *tonA::Tn*10 *lacI*^{q1} or suppressor LE392 *tonA::Tn*10 *supE supF*. (A) Plaque morphology of indicated phages on indicated host. (B) LIN phenotypes. Non-suppressor host (●, ▲, ■ and ◆) or suppressor host (○, △, □ and ◇) were infected with either T4D (▲ and △), T4*ΔrI* (■ and □) or T4^{ss}*phoAΦrI*$_{CTD}$ (◆ and ◇) or not infected (● and ○). Dashed arrow indicates when $CHCl_3$ was added.

there is superinfection with intact T4 particles but not with T4 ghosts, indicating that the intact phages deliver some kind of signal to activate LIN. LIN can be reconstituted by expressing T and RI from plasmids. In this system, RI is expressed at much higher levels than in T4 infection suggesting that overexpression of RI compensates for the lack of the signal of LIN. In Chapter II, we showed that T and RI interact via their C-terminal domains, and the C-terminal domain of T could titrate the inhibition by RI, implicating the C-terminal domain of T as the receptor for the LIN signal. How does the LIN signal work? Here, we have established that RI possesses a N-terminal SAR domain, which allows it to be released into the periplasm. Anchoring RI in the

membrane by leucine substitutions in the SAR domain significantly reduced its antiholin function suggesting that it is the soluble periplasmic form of RI that normally participates in LIN. In addition, the SAR domain of RI facilitates its DegP-dependent degradation. Thus, while the release of RI into the periplasm is necessary for LIN, it is also responsible for the rapid degradation of RI. Based on these findings, we propose the model shown in Fig 3.7. When there is no superinfection, RI is made, is released into the periplasm, is inactivated and is degraded by DegP. Changing from the active to the inactive form, in the absence of superinfection, is rapid since the stability of RI in DegP mutants is not accompanied by a commensurate enhancement of LIN. Thus, there is no active RI available, there is no inhibition of T-mediated lysis; thus, lysis occurs at

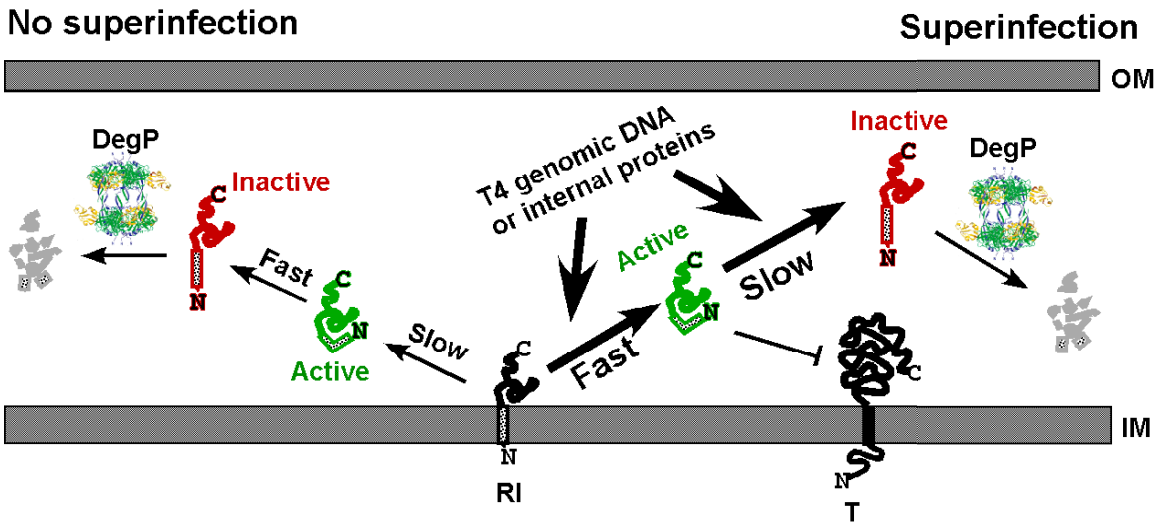

FIG 3.7. Model of how superinfection leads to LIN.

the time programmed into the holin. When there is superinfection, one or both of the following events may occur. (1) Superinfection signal enhances the release of RI into

the periplasm, or (2) superinfection signal slows down the inactivation of RI. Either or both of these processes increase the concentration of active RI in the periplasm; thus RI is now available to interact with T and inhibit lysis. Since both T4 genomic DNA and the internal proteins are ectopically-localized in the periplasm during superinfection, either or both of these elements can serve as the LIN signal.

Energetically, it would be difficult to release a TMD into the periplasm. In fact, we do not know how proteins with N-terminal SAR domain are released into the periplasm. It is possible that a protein with SAR domain is pulled out of the membrane by an unknown factor. If this is the case, the LIN signal enhances the activity of this factor, thus increasing the amount of RI being released into the periplasm. To slow down the inactivation of RI, the LIN signal can either interact directly with RI and prevents it to change into the inactive form or to inhibit an inhibitor of active RI. An alternative theory positing that the LIN signal inhibits the activity of active RI inhibitor is unlikely. If active RI inhibitor is a host protein, mutation in this protein would result in a host mutant that supports T4 infection and replication, but do not allow lysis to occur. This type of host mutant has never been isolated. If active RI inhibitor is a T4 protein, mutation in this protein would result in a T4 mutant that infects and replicate but fail to lyse the host. This type of T4 mutant has never been isolated either. Therefore, the most likely action that a superinfection signal allows LIN to occur is somehow to prevent the inactivation of active RI. To remove the LIN signal, internal proteins would be degraded by DegP protease, and the ectopically localized DNA would be degraded by the periplasmic endonuclease I. Once the LIN signal is removed, inactivation of RI is

rapid, no active RI is available, and lysis occurs, unless another superinfection occurs. This model would explain why superinfection has to occur continuously in order for LIN to persist.

Why should RI possess a SAR domain instead of a signal sequence or a transmembrane domain? We showed that ^{ss}PhoAΦRI$_{CTD}$, a version of RI with a cleavable signal sequence that allowed the secretion of the inhibiting domain into the periplasm, is a strong, stable inhibitor of T for the following reason. In the absence of the SAR domain, the process of changing into the inactive state is much slower, which explains the longer LIN time in the complementation where ^{ss}PhoAΦRI$_{CTD}$ was used. In addition, we could not obtain T4*^{ss}PhoAϕrI$_{CTD}$* as a plaque former, consistent with the idea that LIN imposed by the secreted RI$_{CTD}$ is too stable. Therefore, a metastable inhibitor is the best fit for a system that senses the availability of new hosts. A SAR domain serves two purposes. It allows the release of RI into the periplasm which can either inhibit lysis or be inactivated and degraded, depending on a signal that reflects the availability of new hosts.

CHAPTER IV

CHARACTERIZATION OF HOLIN T

Introduction

Holins are highly diverse: more than 50 unrelated families are known from phage genomics. All but one of these holin families are in two topological classes: class I, with three TMDs, N-out and C-in and class II, with two TMDs, N-in and C-in. The T holin of T4 is the prototype of class III holins. It is unique because of its large size, 218 a a, and large periplasmic domain. A topological study of T established that the C-terminal domain (CTD) of T is in the periplasm (108). When this domain is deleted, the truncated T holin is still partially functional. However, the truncated holin T is insensitive to lysis inhibition mediated by the antiholin RI (108). In Chapter II, we showed that the T_{CTD} interacts with the antiholin RI of T4. In addition, the expression of T_{CTD} also delayed holin T-mediated lysis, indicating that it may play a role in T-T oligomerization.

The topological study of T was carried out using PhoA-LacZ sandwich fusions (108). In such studies, the results are only meaningful when the fusion proteins are either $PhoA^+/LacZ^-$ or $PhoA^-/LacZ^+$. This result was found with three fusions, all in the C-terminal domain of T. The $PhoA^+$/LacZ- nature of these fusions unambiguously demonstrated the periplasmic localization of the T_{CTD}. This left unsolved whether the N-terminus was cytoplasmic or periplasmic. If T has two TMDs and an N-out and C-out topology, a PhoA-LacZ fusion at the N-terminus would likely be non-permissive for

translocation of the first TMD into the membrane. Thus, fusion analysis is not a good method for studying topology of the N-terminus lacking a signal sequence. Therefore, one objective of this chapter is to determine whether T has one TMD with N-in and C-out or two TMDs with N-out and C-out topology (Fig 4.1B).

In addition, we do not know the role of the N-terminal domain (NTD) of T in T-mediated lysis or the distribution of T molecules in *E. coli* cells at the time of lysis. It has been proposed that holin forms large aggregates in the membrane (48). These aggregates have been called "death rafts", and it was speculated that these death rafts act as the locations of hole formation. The second objective of this chapter is to analyze the function of the T_{NTD} in T-mediated lysis and to determine how T is localized during the lytic pathway.

Materials and methods

Bacterial strains, bacteriophages, plasmids, and culture growth

The bacterial strains, bacteriophages, and plasmids used in this work are described in Tables 2.1, 2.2 and 2.3. T4 phage stocks were prepared as previously described (109). Bacterial cultures were grown in standard LB medium supplemented with ampicillin (100 μg/ml), kanamycin (40 μg/ml), chloramphenicol (10 μg/ml) when appropriate. Growth and lysis of cultures were monitored by following the optical density of cultures at A_{550} as previously described (109). When indicated, isopropyl β-

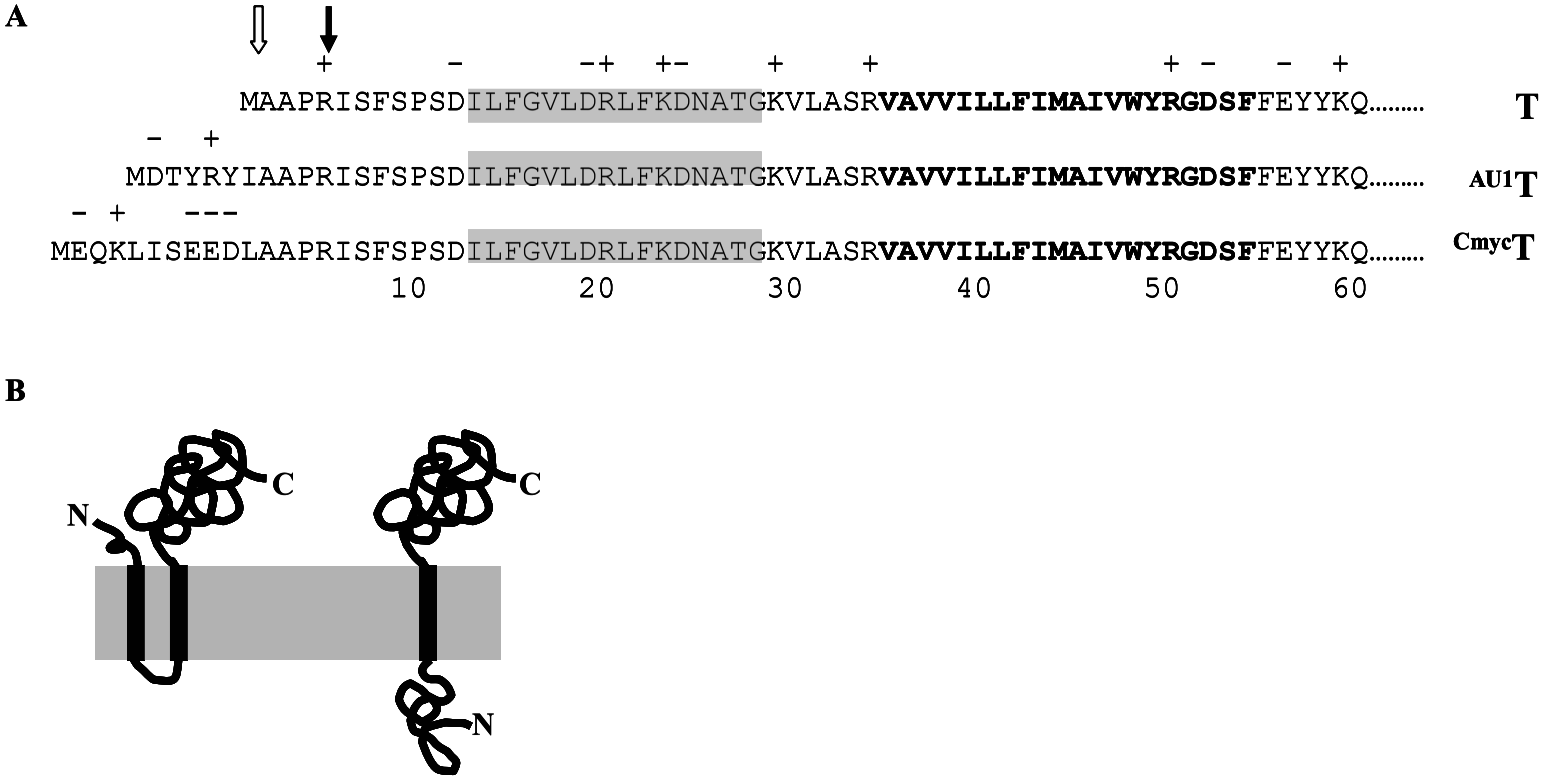

FIG 4.1. Amino acid sequence of T, its derivatives and possible topologies of T. (A) Amino acid sequence of T and mutant proteins. Bold, TMD as predicted by TMHMM. Gray shaded, second possible TMD. Solid arrow, insertion of one arginine residue, open arrow, insertion of two arginine residues. (B) Two possible topologies of T.

D-thiogalactoside (IPTG), KCN, dinitrophenol (DNP) or $CHCl_3$ was added to give final concentrations of 1 mM, 10 mM, 10 mM or 1%, respectively.

Standard DNA manipulations, PCR, and DNA sequencing

Isolation of plasmid DNA, DNA amplification by PCR, DNA transformation, and DNA sequencing were performed as previously described (145). Oligonucleotides, shown in Table 2.4, were obtained from Integrated DNA Technologies, Coralville, IA, and were used without further purification. Single base changes, small and large insertions were introduced using commercially synthesized primers in conjunction with the QuikChange kit from Stratagene. The Rapid DNA ligation kit from Roche Molecular Biochemicals was used for ligation reactions. All other enzymes were purchased from New England Biolabs except for *Pfu* polymerase, which was from Stratagene. Automated fluorescent sequencing was performed at the Laboratory for Plant Genome Technology at the Texas Agricultural Experiment Station.

Construction of plasmids

Positively charged residues and peptide tags were introduced into the N-terminal domain of T by site-directed mutagenesis of T using QuikChange. The following primer pairs, T5-R-6for/T5-R-6rev, T1-RR-2for/T1-RR-2rev, and pT4T (133) as the template were used to generate $pT4T^{5R6}$ and $pT4T^{1RR2}$. To generate plasmids harboring *t* alleles encoding T with a histidine tag at different positions, QuikChange reaction using pT4T

as the template and following primer pairs 28-G1H6G2-29-for/rev, 51-G1H6G2-29-for/rev, 132-H6G2for/rev and 148-G1H6G2-149-for/rev were performed to obtain $pT4T^{28his}$, $pT4T^{51his}$ and $pT4T^{148his}$, respectively. The nucleotide sequence coding for a cmyc tag and an AU1 tag was introduced between codon 1 and 2 of *t* gene in plasmid $pT4T^{his}$ (133)using the primer pairs cymc-Tfor/cmyc-Trev and au1-Tfor/au1-Trev respectively to generate $pT4^{cmyc}T^{his}$ and $pT4^{au1}T^{his}$.

The *rI* gene was amplified from pZA-RI (133) using primer pair cmycNde1-RIfor/Kpn1-RIrev. The PCR product was digested with NdeI and KpnI, and then ligated into pET-duet1 digested with same enzymes to make pET-duet-RI. The DNA sequence encoding T^{his} was amplified from $pT4T^{his}$ using the primers ThisinpETfor and ThisinpETrev. The PCR product was digested with NdeI1 and BamHI and ligated into pET11a digested with the same enzymes to make pET11a- T^{his}. The T^{his} coding sequence was cut out of pET11a- T^{his} using XbaI and BamHI and then ligated into pET-duet-RI digested with the same enzymes to make pET-duet-RI-T^{his}.

Residue 2 to 28 of T was deleted by a PCR reaction that excluded the coding region for these residues, using the primers TΔ2-28down and TΔ2-28up and pT4T as the template. The PCR product was phosphorylated and ligated to make $pT4T^{\Delta 2\text{-}28}$.

To fuse GFP to the N-terminus of T, the coding region of GFP was amplified using the primers Kpn1-gfp-for/CgfpNt-rev and pDS439 (120) as the template. Next, the coding region of T was amplified using the primers CgfpNt-for/AvrIItrev and pT4T as the template. The two PCR products were used as templates for an SOE PCR (54) using the primers Kpn1-gfp-for and AvrIItrev. The resulting PCR product was digested

with KpnI1 and AvrII then ligated into pZA32-luc digested with the same enzymes to make pZA-GFPΦT. An AGSAG linker was added between the coding region of GFP and T using primer pair AG-T-for/Gfp-AGS-rev and pZA-GFPΦT as the template. The PCR product was phosphorylated and ligated to make pZA-GFPΦAGSAGΦT plasmid.

Plasmids harboring *rV* alleles of *t* were created using QuikChange PCR with pT4T as the template and the following primer pairs For/RevtR5K, For/RevtI39V and For/RevT75I to obtain $pT4T^{R5K}$, $pT4T^{I39V}$ and $pT4T^{T75I}$ respectively.

Purification and N-terminal sequencing of T^{his}

The plasmid pETduet-RI-T^{his} was transformed into C43(DE3)*tonA::Tn*10 *slyD::*Kn. The transformants were grown in 3L of LB-Amp at 37^{o}C until A_{550} ~ 0.8. The culture was induced with IPTG for 1hr and the cells were harvested by centrifugation at 7,000 x g for 15 min. The cell pellet was resuspended in 30 ml of French Press buffer (100 mM Tris, pH 8, 1 mM DTT, 1 mM PMSF and 30µl of protease inhibitor cocktail(Sigma)), and the cells were lysed by passing through a French Press cell at 16,000 psi twice. The unlysed cells were removed in a clearing spin at 2,000 x g for 10 min. The membrane fraction was collected by centrifugation of the supernatant of the clearing spin at 100,000 x g for 1hr. The membrane fraction was extracted using the buffer 1% EBB, 0.5 M NaCl and 20 mM HEPES pH 8 overnight at 4^{o}C. Insoluble material was removed by centrifugation at 100,000 x g for 1hr. The soluble fraction was filtered then used as the starting material for IMAC purification using His-trap HP

column (GE/Amersham Pharmacia). The protein was eluted using low pH buffer (1% Ebb, 50 mM NaCl, 20 mM sodium acetate pH 2.5). The pH of the fractions was adjusted to 7 using 1 M NaOH. The purity and the presence of T in each fraction were assessed by SDS-PAGE and Western blot. Fractions containing T^{his} were pooled, concentrated to 500 µl, analyzed using SDS-PAGE, Coomassie stain and western blot. The band recognized by T antiserum was cut out and used for N-terminal sequencing. The N-terminal sequencing was performed by the Protein Chemistry Laboratory of Texas A&M University, Department of Biochemistry and Biophysics.

Results

His tag mutagenesis

To obtain purified T for *in vitro* studies, an allele of *t* that encoded for a T protein with an oligohistidine-tag at its extreme C-terminus was constructed by Ramanculov (108,109). However, lysis mediated by this his-tagged T protein is not saltatory like wild type T-mediated lysis, indicating the holin function of this his-tagged T protein is compromised. Therefore, this allele is not suitable for the overexpression and purification of T for use in further *in vitro* studies. We attempted to generate a more suitable allele encoding a his-tagged T protein by moving the his-tag to sites internal to T. Four different positions were chosen for the insertion of the $Gly_2His_6Gly_2$ sequence, between residues 28 and 29, 51 and 52, 132 and 133 and 148 and 149, to make T^{28his}, T^{51his}, T^{132his} and T^{148his} respectively. The lysis profiles of these alleles are shown in Fig

4.2A. Out of these four alleles, only t^{132his} and t^{148his} alleles caused saltatory lysis, similar to wild type *t*, indicating the holin function of these his-tag-T proteins was not compromised. The alleles t^{28his} and t^{51his} did not cause lysis, and they could not be triggered by the addition of cyanide or DNP (Fig 4.2B). When samples were taken at 20

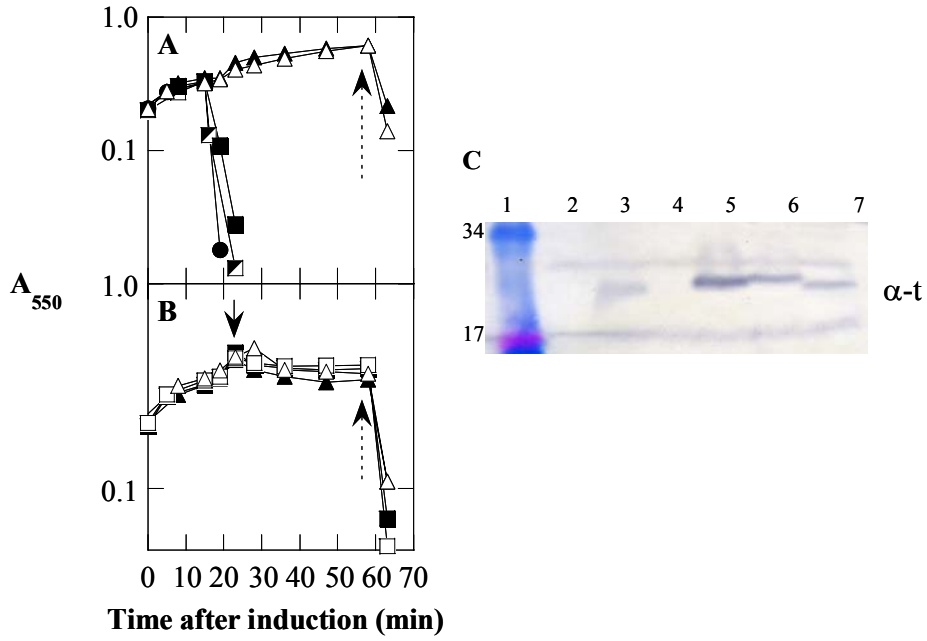

FIG. 4.2. Lysis profile and protein levels of different his-tag insertion alleles of *t*. (A) Lysis profile of different his-tag insertion alleles of *t*. Host CQ21λ*kan*Δ(*SR)* harbored the following plasmids: pT4T, ◩; $pT4T^{132his}$, ■; $pT4T^{148his}$, ● ; $pT4T^{51his}$, ▲; $pT4T^{28his}$ △; were thermo-induced, and the OD was followed as described in the *Materials and Methods***.** (B) Addition of KCN or DNP does not trigger lysis mediated by T^{51his} and T^{28his}. Same host harboring $pT4T^{51his}$, ▲ and △; or $pT4T^{28his}$ ■ and □; was used for experiment as described in (A). Solid arrow indicated 10 mM of either KCN (▲, ■) or DNP (△, □) was added to cultures. Dashed arrow indicated the addition of $CHCl_3$. (C) Western blot of protein accumulation from induction of these alleles 20 minutes after induction Lane 1, molecular weight marker, lane 2, host alone, lane 3, T expressed from pT4T, lane 4, T^{28his} expressed from $pT4T^{28his}$, lane 5, T^{51his} expressed from $pT4T^{51his}$, lane 6, T expressed from $pT4T^{his}$ and lane 7, T expressed from $pT4T^{148his}$.

minutes after induction for analysis by SDS-PAGE, T^{28his} did not accumulate while T^{51his}, T^{132his} and T^{148his} were easily detectable (Fig 4.2C). In fact, the levels of T from the t^{132his} and t^{148his} alleles were higher than the wild type. This is because wild type T causes lysis several minutes earlier than lysis mediated by T^{132his} and T^{148his}. The highest level of T was observed with the non lytic t^{51his} allele. This is not surprising since protein expressed from the t^{51his} allele continues to accumulate past the lysis time of the wild type, t^{132his} and t^{148his} alleles. The allele that was chosen for further cloning, protein over-expression and purification was t^{132his}; henceforth, this will be referred to as t^{his}. The lysis mediated by this T^{his} could be inhibited by antiholin RI, similar to the inhibition observed for wild type T (Fig 4.3).

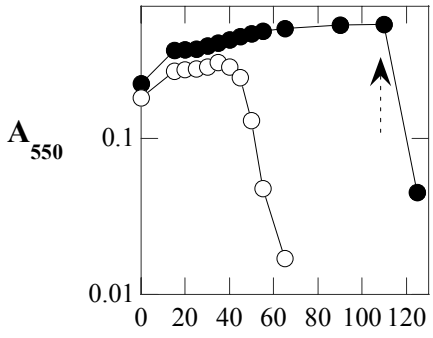

FIG. 4.3. RI blocked lysis mediated by T^{his}. Host CQ21(λ*kan* t^{his}) with or without pPRI were thermally induced, and the culture growth was followed at A_{550}. ● , host with pPRI and ○, host alone. Dashed arrow indicated $CHCl_3$ were added.

Purification of T

Over-expression of t^{his} from a T7 promoter caused cell death soon after induction allowing only a small amount of T to accumulate. For this reason, t^{his} was cloned into a pETduet vector in tandem with *rI*. The pETduet vector possesses two T7 promoters which allow the simultaneous over-expression of two proteins. The growth curve after induction is shown in Fig 4.4A. Even with this system, T^{his} could not be seen on the SDS gel stained with Coomassie, but was observed when the induced cells were subjected to SDS-PAGE and Western blotting as shown in Fig 4.4B. This protein was purified as described in the Materials and Methods with ~ 0.6 mg isolated from 6L of culture.

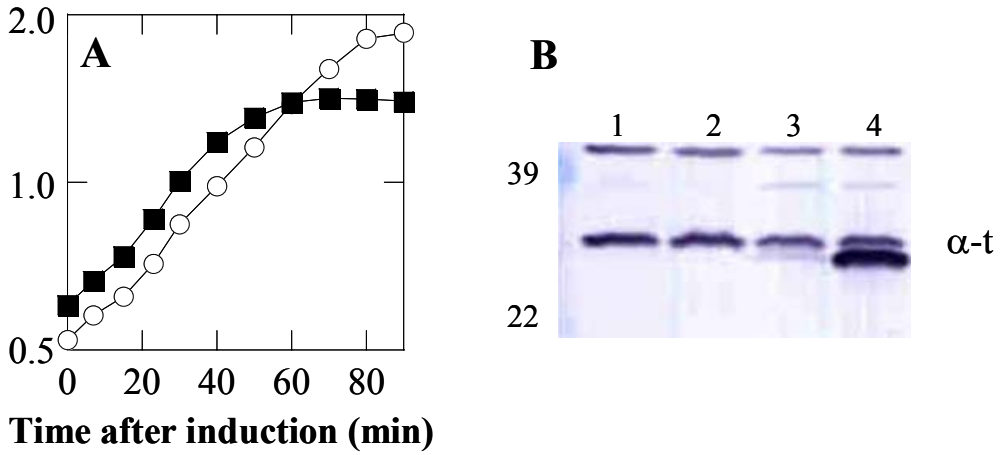

FIG 4.4. Growth curve and Western blot analysis of cells harboring pETduet-RI-T^{his}. (A) Growth curves. ○ induction of pETduet-1. ■, induction of pETduet-RI-T^{his}. (B) Western blot analysis of T using T antibodies. Lanes 1 and 2, pETduet1. Lanes 3 and 4, pETduet-RI-T^{his}. Lanes 1 and 3, uninduced. Lanes 2 and 4, induced.

Because the amount of purified full length T^{his} was not enough to raise a T antiserum, the DNA fragment encoding the CTD of T^{his} was cloned into a pET vector, and used for over-expression and purification as described in the *Materials and Methods* of Chapter II. This protein was also used as the standard to determine the amount of T present in the cell after 60 minutes of T4 wild type infection. According to the gel shown in Fig 4.5, there is approximately 1.5 pmole or ~ 7.7 x 10^{10} T molecules in 1.5 x 10^8 cells at 60 min after infection with T4D. Thus, the number of T molecules per cell is approximately 500.

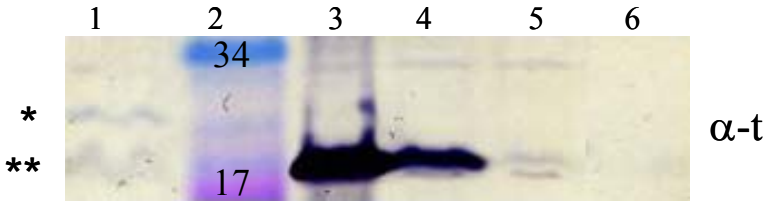

FIG 4.5. Quantification of T in T4D infected cells. Lane 1, T4D infected cells, lane 2, molecular weight marker, lanes 3-5, purified T_{CTD}^{his}. Lane 3, 64 pmol, lane 4, 6.4 pmol, lanes 5, 0.64 pmol. Lane 6, uninfected cells. * full length T, ** T_{CTD}^{his}.

Analysis of N-terminal function

Ramanculov's fusion analysis (108) suggested that T has at least one TMD, with the C-terminal domain from residue 70 in the periplasm and the N-terminal domain (NTD) in the cytoplasm. The 69 residue NTD is long enough to possess either one or two TMDs, as shown in Fig 4.1 B. If T has one TMD, its topology would be N-in and C-out. As a result, the first methionine of T should be deformylated, because its N-terminus is located in the cytoplasm, where the host enzyme deformylase has access to

remove the formyl group of the first methionine. However, if T has a second TMD in the NTD, its topology would be N-out and C-out. There are two possible ways to achieve this. First, both TMDs could be translocated across the membrane by the SecYEG translocon. Assuming T was translocated cotranslationally, the first methionine could not be deformylated. Second, the TMD2 was translocated across the membrane by the SecYEG translocon, and the first TMD could traverse the membrane by a post-translational "flip up" pathway. The post-translational flipping of a TMD into the membrane had been shown for the first TMD of leader peptidase and of S105, the holin of bacteriophage λ (R. White et al., manuscript in preparation). In both cases, N-flip up occurs so fast that the formyl group of the first methionine of these proteins was not removed by the enzyme deformylase. In the case of phage λ holin, the purified S105 protein was not N-terminal sequenceable. The purified S105 could be sequenced only when it was treated with deformylase prior to N-terminal sequencing (R. White et al., manuscript in preparation). The flipping of TMD1 of S105 across the membrane was found be inhibited by the addition of positively charged residues at its N-terminus. The addition of positive charges at the N-terminus also changed holin S105 to an antiholin (44,45), which inhibited S105. The N-terminus of the purified λ antiholin could be sequence without treatment by deformylase (R. White et al., manuscript in preparation). To determine whether the formyl group of the first methionine of T is removed, purified T^{his} was subjected to N-terminal sequencing. The N-terminus of purified T^{his} could be sequenced by Edman degradation, indicating that the protein was deformylated. This suggested that the N-terminus of T was in the cytoplasm.

To further support the idea that the N-terminus of T is in the cytoplasm, positively charged residues were added to the N-terminus of T. Lysis mediated by T^{5R6} or T^{1RR2}, *t* alleles with additional arginines at the N-terminus, was faster than wild type protein (Fig. 4.6A). Since the addition of the positively charged residues would be expected to favor retention of the N-terminus in the cytoplasm, this argues against the idea that the T N-terminus normally residing in the periplasm. However, acceleration of lysis can also occur due to the up-regulation of translation. Thus, Western blot analysis was performed. Protein expressed from these alleles at 10 min after induction showed that both T^{1RR2} and T^{5R6} were easily detected unlike the wild type T (Fig 4.6B). Thus,

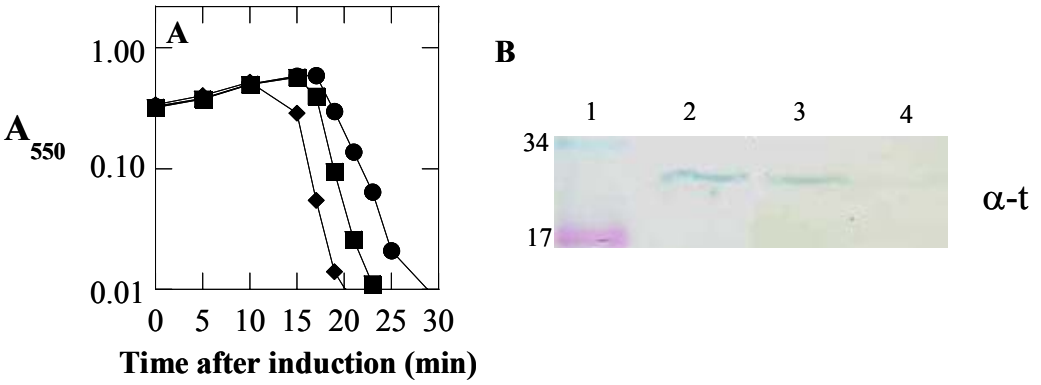

FIG. 4.6. Lysis profile and protein levels of T mutants with additional positive charge at the N-terminus. (A) Lysis profile. Host MC4100(λ*CmΔSR*) harboring pT4T, ●; $pT4T^{5R6}$, ■; $pT4T^{1RR2}$, ◆. (B) Western blot of protein expression at 10 min after induction of CQ21λ*kan*Δ(*SR)* harboring $pT4T^{1RR2}$ (lane 2), $pT4T^{5R6}$ (lane 3) or pT4T (lane 4). Lane 1, molecular weight marker.

the accelerated lysis could be due to higher protein expression. One explanation for this result is that changing the 5' end of *t* gene up regulates the translation of T because a

rare codon was used. When a rare codon is used in an mRNA, the rate of translation shortly after induction is higher than for mRNA with common codons. This is because the pool of tRNA recognizing the rare codon is fully charged. Since only a certain number of holin molecules required for lysis, a higher rate of holin synthesis resulted in faster lysis. Together these data strongly support the idea that T has one TMD with N-in and C-out topology.

We also placed the negatively charged C-myc tag (EQKLISEEDL) and neutral AU1 tag (DTYRYI) between residue 1 and 2 of T^{132his}. Surprisingly, these alleles caused lysis faster than the t^{132his} allele, and they appeared to be insensitive to LIN mediated by RI (Fig 4.7A). SDS-PAGE and Western blot (Fig 4.7B) showed that the protein level of $^{AU1}T^{132his}$ was higher than that of T^{132his}, but the protein level of $^{Cmyc}T^{132his}$ was about the same as that of T^{132his}. The higher protein level of $^{AUI}T^{132his}$ might explain the faster triggering of lysis and, perhaps, the insensitivity to RI. However, the faster lysis phenotype of $^{cmyc}T^{his}$ suggested that the N-terminus plays a functional role in lysis timing.

Analysis of *rV* alleles

The T4*rV* mutants isolated by Krylov in 1965 (74,76) were later sequenced by Dressman and Drake in 1999 (29). These mutants contained mutations in the *t* gene that caused T to become insensitive to LIN. We wanted to check the lysis profile and to test the sensitivity of these mutants toward LIN mediated by RI in our plasmid system. All three known *rV* mutants, t^{R5K}, t^{I39V} and t^{T75I}, lysed faster than wild type *t* (Fig 4.8A). In

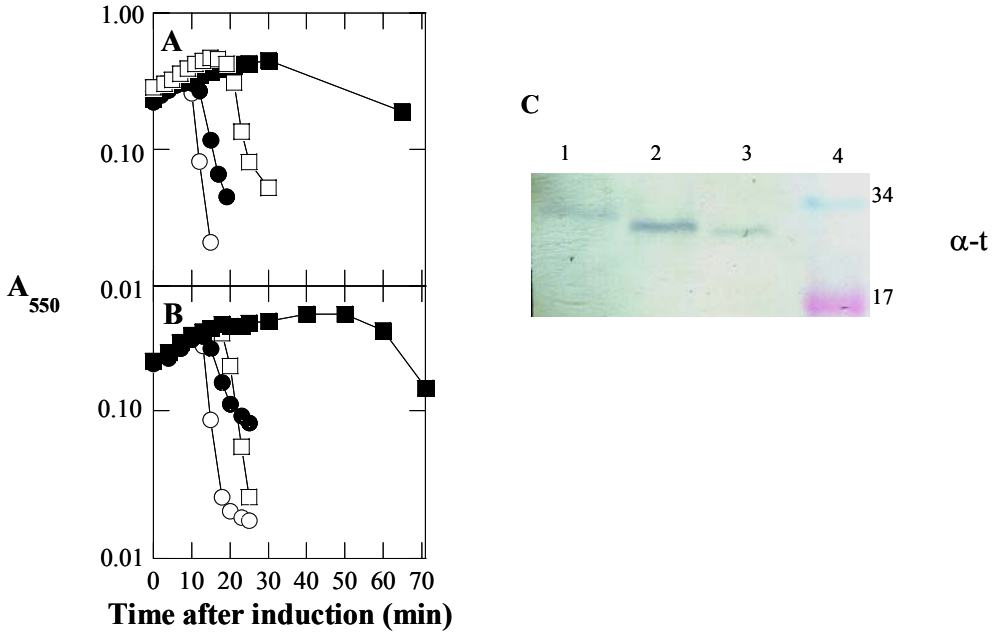

FIG. 4.7. Lysis profile and protein levels of $^{cmyc}T^{his}$ and $^{AUI}T^{his}$. (A) Lysis and LIN of $^{Cmyc}T^{his}$. Host CQ21λ*kan*Δ(*SR)* harboring pT4T^{his} alone, □; pT4This with pZA32-RI, ■; pT4$^{cmyc}T^{his}$ alone, ● ; or pT4$^{cmyc}T^{his}$ with pZA32-RI, ○. (B) Lysis and LIN of $^{AU1}T^{his}$. Same host harboring pT4T^{his} alone or pT4This with pZA32-RI, has the same symbols as in (A); pT4$^{aulT}T^{his}$ alone, ● ; or pT4$^{aulT}T^{his}$ with pZA32-RI, ○. (C) Western blot of protein level of these alleles at 15 min after induction in absence of RI. Lane 1, $^{Cmyc}T^{his}$, lane 2, $^{AUI}T^{hi}$s, lane 3 T^{his} and lane 4, molecular weight marker.

addition, these alleles remained sensitive to LIN mediated by RI, but the length of the LIN period was shorter compared to LIN mediated by RI on wild type T. The protein levels of these mutants were also assessed. Allele t^{R5K} made more protein than the wild type, but the other two mutants made approximately the same amount of protein as wild type T (Figure 4.8B).

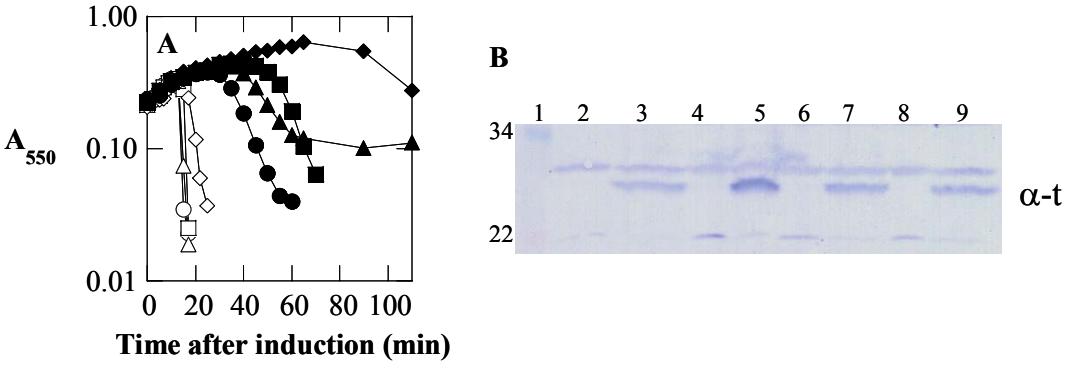

FIG. 4.8. Lysis, lysis inhibition and protein levels of *rV* alleles. (A) Lysis and lysis inhibition of *rV* alleles. Host CQ21λ*kan*Δ(*SR)* harboring pT4T, ◇; $pT4T^{R5K}$, ○; $pT4T^{I39V}$ □; $pT4T^{T75I}$, △. Host CQ21λ*kan*Δ(*SR)* harboring pZA32-RI and either pT4T, ◆; $pT4T^{R5K}$, ● ; $pT4T^{I39V}$, ■; $pT4T^{T75I}$, ▲. (B) Western blot of protein expressions of *rV* alleles compared to wild type *t* at 15 min after induction in absence of RI. Lane 1, molecular weight marker, lanes 2, 4, 6 and 8, uninduced, lane 3, 5, 7 and 9, induced. Lanes 2 and 3, T, lanes 4 and 5, T^{R5K}, lanes 6 and 7, T^{I39V} and lanes 8 and 9, T^{T75I}.

Contribution of the N-terminal domain of T in lysis

The periplasmic domain of T is important for T and RI interaction, and deletion of a C-terminal portion of T from residue 96 to the end of the holin resulted in a *t* allele that still could mediate lysis. In addition, previous sections in this chapter supported the involvement of the N-terminal domain of T in lysis timing. Therefore, we wanted to assess T-mediated lysis in the absence of its N-terminal domain. Deletion of residues 2 to 28 of T resulted in a T mutant that lysed at ~ 100 min after induction, but lysis-mediated by this allele is not as saltatory as lysis mediated by wild type T. The lysis mediated by this mutant still could be inhibited by RI, as shown in Fig 4.9A. The protein level of this mutant is higher than wild type T. This is because the samples were

taken at the lysis time of wild type T. While T synthesis is stopped, $T^{\Delta 2-28}$ continues to accumulate. Thus, this result indicated that protein accumulation prior to lysis was not the problem in this mutant (Fig 4.9B). This result suggested that residues 2-28 might be involved in the timing of the hole formation process. Thus, this region of T (residue 2-128) is not required for lysis but is involved in intrinsic timing and saltatory behavior.

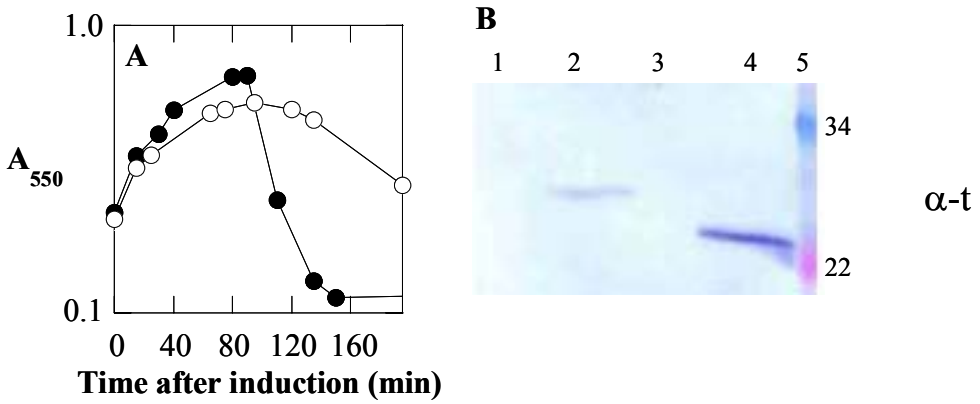

FIG. 4.9. Lysis, lysis inhibition and protein level of $T^{\Delta 2-28}$. (A) Lysis and lysis inhibition of $T^{\Delta 2-28}$. CQ21λ*kan*Δ(*SR)* harboring pT4$T^{\Delta 2-28}$ alone, ● or in the presence of pZA32-RI , ○. (B) Western blot of protein expression of $T^{\Delta 2-28}$ compared to wild type T at time of lysis of T. Lane 1 and 3, uninduced, lane 2 and 4, induced and lane 5, molecular weight marker. Lane 1 and 2, T and lane 3 and 4, $T^{\Delta 2-28}$.

Localization of T in the membrane

The fusion of GFP to a protein of interest is widely used to study protein localization. Fusion of GFP to S105, the λ holin, showed large concentrated patches of GFP on the membrane (R. White et al., manuscript in preparation). However, fusion of GFP to S68, phage 21 holin, showed small patches throughout the cell membrane (Pang,

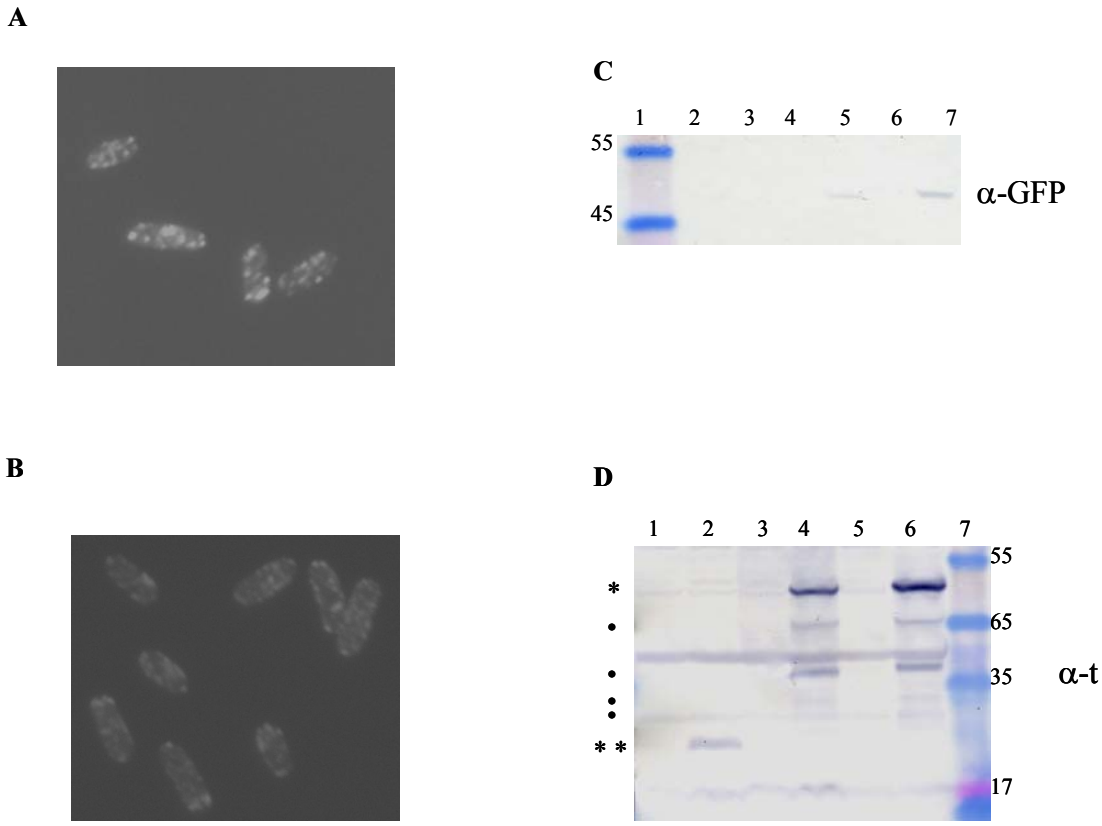

FIG. 4.10. Fluorescence and protein levels of GFPΦT. (A) Fluorescence image of cells expressing GFPΦT. (B) Fluorescence image of cells expressing GFPΦAGSAGΦT. (C) Western blot analysis of fusion protein using GFP antibodies. Lane 1, molecular weight marker, lane 2, 4 and 6, uninduced, lane 3, 5 and 7, induced. Lane 2 and 3, cells expressing T from pZA32-T, lanes 4 and 5, cells expressing GFPΦT from pZA32-GFPΦT and lanes 6 and 7, cells expressing GFPΦAGSAGΦT from pZA32-GFPΦAGSAGΦT. (D) Western blot analysis of fusion protein using T antibodies. Lanes 1, 3 and 5, uninduced, lane 2, 4 and 6, induced. Lane 1 and 2, cells expressing T from pZA32-T, lanes 3 and 4, cells expressing GFPΦT from pZA-GFPΦT, lanes 5 and 6, cells expressing GFPΦAGSAGΦT from pZA32-GFPΦAGSAGΦT and lane 7, molecular weight marker. *, intact fusion protein, **, T and •, cleavage products.

T., personal communication). It was proposed that before forming a hole, holin S105 concentrated into rafts in the membrane known as death rafts (48). Thus, the fluorescent patches observed in S105ΦGFP and S68ΦGFP may represent the death rafts proposed

by Grundling et al. (48). Holin T is similar to S105 in that it forms a big hole in the membrane; thus, we wanted to see if T forms rafts like S105. GFP was fused at the extreme N-terminus of T either with or without a linker (AGSAG). Expression of these fusion proteins caused cell death faster than expression of wild type T. Western blot analysis using GFP antibodies showed that GFPΦT fusion proteins with the correct molecular weight accumulated. Detection using T antibodies indicated that the majority of fusion protein was intact; however, a small amount was cleaved into four smaller species, none of which had the same molecular weight as T alone (Fig 4.10 C and D). Since T antibodies were raised against the purified periplasmic domain of T, it is not likely that the degradation was from the C-terminus of T but rather was from the N-terminus of GFP. In addition, there was more GFPΦT compared to wild type T alone. In *E. coli* cells expressing GFPΦT, many fluorescent patches were observed on the membrane (Fig 4.8A, B). This suggested that death rafts similar to those seen with S105ΦGFP also form with holin GFPΦT.

Discussion

A number of modifications of the N-terminal domain of T resulted in *t* alleles with faster lysis times. In most cases, these modifications also increased the level of holin accumulation. The shorter lysis time of *t* alleles with higher levels of protein expression can be explained using the model proposed by Wang and Young in 2003. According to this model, the pathway to form lesions in the membrane is a transition

from monomers to dimers to oligomers to protein rafts. At some critical holin concentration, a small hole is formed in the middle of the raft which causes a local depolarization. This local depolarization causes a tertiary or quaternary structural change of the holins in the raft and leads to hole formation (139). Therefore, reaching a critical concentration of holin in the membrane seems to be one of several important factors contributing to the timing of lysis. It is reasonable to argue that *t* alleles that up regulate the protein expression levels should have shorter lysis times because they reach the critical protein concentration necessary for lysis faster. However, the same argument cannot be used to explain faster lysis by alleles that have about the same protein expression level as wild type T *in vivo*. These cases may be explained by considering a cytoplasmic element that interacts with the N-terminus of T, thus interfering with the oligomerization process. If modification of the N-terminus of T disrupts the interaction between T and this cytoplasmic element, there is nothing to interfere with T oligomerization, allowing faster hole formation and faster lysis.

Why are these fast lysers insensitive to RI-mediated LIN? In 2001, Ramanculov proposed a model to explain how RI-mediated LIN takes place. In this model, T-mediated lysis can only be inhibited by RI when T is in a form that is called sensitive T or T_s, and these are T_s molecules may be in the monomer form. Once a T molecule participates in the higher oligomer forms, it is no longer sensitive to RI-mediated LIN. If the fast lysing mutants form oligomers faster than RI can form heterodimer with them, these mutants become insensitive toward RI-mediated LIN.

We observed fluorescent patches on the *E. coli* cell membrane when GFPΦT was expressed, indicating death raft formation. Since the GFPΦT fusion protein accumulated at a higher level than wild type T, we do not know how much the fluorescent patches reflect death rafts formed by T in T4 infection. We also observed cleavage products from the fusion protein only when T antibodies were used for protein detection, indicating the protein fusion proteins were degraded from the GFP end. This gives rise to another problem; that is we do no know the contribution of these cleavage products to fluorescent patch formation. To eliminate the possibility patch formation is an over-expression artifact, we need to confirm this result using cells infected with T4*ΔrIgfpΦt e*$^-$, T4 phage with defective endolysin, deletion of *rI* and GFPΦT. Also it would be interesting to see the distribution of GFPΦT in the cell membrane in the presence of RI. S^{68}ΦGFP, the holin of phage 21, gave patches of fluorescence, but in the presence of antiholin, the patches disappeared and a uniform fluorescence was observed on the cell membrane (Pang, T., personal communication). If a similar result is observed in T4 infection, it would support the lysis and lysis inhibition model proposed above. That is, in the absence of antiholin, big rafts of holin form, and in the presence of antiholin, only small rafts form and lysis is inhibited.

CHAPTER V

CONCLUSIONS AND FUTURE DIRECTIONS

The lysis-inhibition phenomenon is one of the "founding" problems of modern molecular genetics, first characterized in the work of Delbrück's Phage Church in the 1940's. Despite its historical prominence, very thorough physiological and genetic investigations, and apparent simplicity in terms of the number of genes involved, six decades have seen very little progress made in terms of understanding this phenomenon at the molecular level. This began to change with the work of Ramanculov et al. (107-110), which established that the T protein of T4 functioned as a holin and that the RI protein could act as an antiholin specific for the T4 holin T. The work in this dissertation has followed on from that work and made a number of advances. First, the work in this dissertation has provided evidence for the following conclusions: (1) RI is a type II integral membrane protein, with an N-terminal TMD acting as a signal anchor and the bulk of the protein in the periplasm; (2) RI is a SAR protein that is released from the cytoplasmic membrane into the periplasm; (3) T and RI interact via their respective periplasmic C-terminal domains; (4) the function of the periplasmic C-terminal domain of RI is sufficient for LIN, and, in fact, is more efficient at this inhibition than wt RI with its SAR domain; (5) the release of the C-terminal domain of RI into the periplasm is required for efficient RI-mediated LIN to occur; (6) the SAR domain also makes RI proteolytically unstable, and the proteolysis is largely mediated by the host periplasmic protease DegP; (7) that T has one transmembrane domain, with its N-terminus in the

cytoplasm; (8) the N-terminal cytoplasmic domain of T is integrally involved in lysis timing of T, and (9) holin T accumulates as oligomeric patches in the membrane in the lytic pathway. Some of these conclusions warrant further discussion.

T-mediated lysis and interaction with RI

T and its relatives stand out from other known holins in terms of size. With 218 residues, T is twice as big as S105, the holin of λ, which has three TMDs, and three times as big as S68, the holin of phage 21, which has 2 TMDs, yet T only has one TMD. Since the large periplasmic C-terminal domain of T interacts with RI, and RI and T are the only *r* proteins that are required for LIN in all host backgrounds, it seems likely that the CTD of T can be regarded as the receptor of the LIN signal. Interestingly, co-expression of secreted periplasmic domain and wild-type holin T delayed T-mediated lysis by ~ 5 min. This indicates that this domain is involved in holin-holin interactions leading to hole-formation. It may be possible to achieve the purification of substantial quantities of the CTDs of both proteins, which have, up to now, been over-produced as inclusion bodies in the cytoplasm of *E. coli*. If secreted CTDs of both RI and T could be purified, the LIN interaction could be open to structural analysis.

Mutations at the N-terminus of T were found to change lysis timing. Insertion of amino acids at the T_{NTD} resulted in *t* alleles that lysed earlier. However, a deletion of the complete cytoplasmic N-terminus resulted in an allele with a later onset of lysis. Even though the rate of T synthesis is up-regulated in the N-terminal insertion alleles, this fact alone cannot be used to account for the acceleration or deceleration of lysis time.

Acceleration of lysis did not occur in just one insertion but in all the insertion mutants, indicating this is not a random event. Perhaps, addition of these amino acids at the N-terminus of T disrupts an inhibitory interaction that normally delays the process of hole formation. This could be a homotypic interaction of the N-terminus of T with itself, or a heterotypic interaction with a cytoplasmic domain of a host protein. When the interference is removed, lesion formation occurs faster, resulting in shorter lysis time. Deletion of the 27 residues at the N-terminus of T caused a significant lysis delay, indicating that the N-terminus may also be involved in facilitating hole-formation, perhaps in the process of oligomerization. These ideas can be tested by following the kinetics of oligomerization of each of these mutants, using pulse-labeling and cross-linking studies.

Properties of RI

The periplasmic C-terminal domain of RI is sufficient for imposing LIN. LIN in T4 infection is a metastable state of lysis inhibition, caused by superinfection events, and collapses if superinfection ceases. Thus, finding the inhibition domain is not sufficient to explain LIN. The simplest way to bring about LIN instability would be to make the inhibitor, the antiholin RI, unstable. Indeed, when the life-time of RI was investigated after the suppression of protein synthesis, it was determined that RI had a very short half-life. Moreover, the proteolytic instability of RI was shown to be dependent on the host periplasmic protease, DegP. Also, the presence of the N-terminal SAR domain, which allows RI to be released in the periplasm, confers sensitivity of RI to DegP.

Mutational analysis could provide clues as to what it is about the SAR domain that attracts the periplasmic protease.

Localization of RI in the periplasm is also required for efficient antiholin function of RI. However, the mechanism by which superinfection activates RI-mediated lysis inhibition is not known. Recall that RI is an early gene product, and T is a late gene product. This means antiholin RI is made before holin T, and if RI is a stable and active protein, then lysis would be permanently inhibited. This problem can be solved by making the life time of active RI very short. When there is no superinfection which equates to the availability of new hosts, T-mediated lysis can proceed. When there is superinfection which equates to the absence of uninfected hosts, a LIN signal is sent into the infected cell. This signal allows RI to stay active longer. When there is no further superinfection, the LIN signal vanishes, and the RI inactivation process is speeded up. Now, without active RI available to mediate LIN, LIN would collapse.

Even though ^{ss}PhoAΦRI$_{CTD}$ and RI^{3L} are more stable than wild-type, we could not transfer these mutant *rI* alleles to the T4 chromosome. There are several possible reasons why they could not be obtained. (1) The PhoA chimera may be such a potent antiholin that it blocks plaque-formation, so our method, which involves screening for plaques, would not work. (2) Even though we predict that T4*rI*^{3L} should make a large, *r* plaque due to partial lost of antiholin function, this may not be the case. In fact, we do not know the plaque morphology of this mutant. Future progress here requires PCR-based control experiments to demonstrate that the recombinant molecules are being formed in the recombination lysates.

The signal for LIN

There is still a lot to be done to elucidate the mechanism of LIN. Most importantly, what is the signal of LIN at the molecular level? There are two possible general kinds of signals from the superinfection event: first, the ectopically-localized genomic T4 DNA, or, second, the internal proteins of the capsid, which total over 300 molecules. In one model, the LIN signal would serve to stabilize active RI, at least temporarily. Thus our ability to cause LIN by over-expressing RI results simply from being able to swamp the proteolytic capacity of the cell, so that RI accumulates in the membrane and periplasm. Assessing RI stability in an *in vitro* reconstitution of superinfection will distinguish which of the two is the signal. This might be feasible using spheroplasts. Inducing *t* in the presence of just a basal level of RI after formation of spheroplasts should result in lysis. If this system works, the next step might be to add the T4 head contents, DNA and proteins, to the spheroplasts, to see if the basal level of RI could be activated to delay lysis.

Another question is what is the level of RI during the infectious cycle either in the presence or absence of superinfection? Currently, it is a major handicap that we cannot detect RI in T4 infection. To answer this question, we need more sensitive RI antibodies. In addition, we also need T4 antibodies that neutralize T4 and prevent it from infecting the cells. With these tools in hand, one can neutralize the infection at any particular time and follow the protein level of RI.

We established the contribution of the N and the C-terminal domain of T in lysis and lysis inhibition, but we do not know the boundary of the one TMD that T possesses.

Because we do not know where the TMD is, we do not know how it participates in the hole formation process. In addition, how does T mediate lysis? Can we visualize the hole after lysis occurs? These questions and more will arise as we make progress on this most ancient phenomenon of classical molecular biology.

REFERENCES

1. **Abedon, S. T.** 1994. Lysis and the interaction between free phages and infected cells, p. 397-405. *In* J. D. Karam (ed.), Molecular biology of Bacteriophage T4. ASM Press, Washington, DC.

2. **Alexeyev, M. F., and H. H. Winkler**. 1999. Membrane topology of the *Rickettsia prowazekii* ATP/ADP translocase revealed by novel dual pho-lac reporters. J. Mol. Biol. **285**:1503-1513.

3. **Anderson, C. W., and J. Eigner**. 1971. Breakdown and exclusion of superinfecting T-even bacteriophage in *Escherichia coli*. J. Virol. **8**:869-886.

4. **Anderson, C. W., J. R. Williamson, and J. Eigner**. 1971. Localization of parental deoxyribonucleic acid from superinfecting T4 bacteriophage in *Escherichia coli*. J. Virol. **8**:887-893.

5. **Benzer, S.** 1955. Fine structure of a genetic region in bacteriophage. Proc. Natl. Acad. Sci. USA **41**:344-354.

6. **Benzer, S.** 1957. The elementary unit of heredity, p. 70-93. *In* W. D. McElroy and B. Glass (ed.), The chemical basic of heredity. The Johns Hopkins Press, Baltimore, MD.

7. **Bernhardt, T. G., W. D. Roof, and R. Young**. 2000. Genetic evidence that the bacteriophage ϕX174 lysis protein inhibits cell wall synthesis. Proc. Natl. Acad. Sci. USA **97**:4297-4302.

8. **Bernhardt, T. G., D. K. Struck, and R. Young**. 2001. The lysis protein E of phi X174 is a specific inhibitor of the MraY-catalyzed step in peptidoglycan synthesis. J. Biol. Chem. **276**:6093-6097.

9. **Bernhardt, T. G., I. N. Wang, D. K. Struck, and R. Young**. 2001. A protein antibiotic in the phage Qbeta virion: diversity in lysis targets. Science **292**:2326-2329.

10. **Bernhardt, T. G., I. N. Wang, D. K. Struck, and R. Young**. 2002. Breaking free: "protein antibiotics" and phage lysis. Res. Microbiol. **153**:493-501.

11. **Bienkowska-Szewczyk, K., B. Lipinska, and A. Taylor**. 1981. The *R* gene product of bacteriophage λ is the murein transglycosylase. Mol. Genet. Genomics **184**:111-114.

12. **Black, L. W., and C. Ahmad-Zadeh**. 1971. Internal proteins of bacteriophage T4D: their characterization and relation to head structure and assembly. J. Mol. Biol. **57**:71-92.

13. **Blasi, U., C-Y. Chang, M. T. Zagotta, K. Nam, and R. Young**. 1990. The lethal λS gene encodes its own inhibitor. EMBO J. **9**:981-989.

14. **Bode, W.** 1967. Lysis Inhibition in *Escherichia coli* infected with bacteriophage T4. J. Virol. **1**:948-955.

15. **Brock, T. D.** 1990. The emergence of bacterial genetic. Cold Spring Harbor Laboratory Press, Cold Spring Harbor, NY.

16. **Broom-Smith, J. K., and B. G. Spatt**. 1986. A vector for the construction of translational fusions to TEM beta-lactamase and the analysis of protein export signals and membrane protein topology. Gene **49**:341-349.

17. **Cairns, J., G. S. Stent, and J. D. Watson** 1966. Phage and the origins of molecular biology. Cold Spring Harbor Laboratory of Quantative Biology, Cold Spring Harbor, NY.

18. **Campbell, A. M.** 1969. Episomes. Harper and Row, New York, NY.

19. **Champe, S. P.** 1963. Bacteriophage reproduction. Annu. Rev. Microbiol. **17**:87-114.

20. **Cheng, X., X. Zhang, J. W. Pflugrath, and F. W. Studier**. 1994. The structure of bacteriophage T7 lysozyme, a zinc amidase and an inhibitor of T7 RNA polymerase. Proc. Natl. Acad. Sci. USA **91**:4034-4038.

21. **Childs, J. D.** 1973. Superinfection exclusion by incomplete genome of bacteriophage T4. J. Virol. **11**:1-8.

22. **Coombs, D. H., and F. Arisaka**. 1994. T4 tail structure and function, p. 259-281. *In* J. D. Karam (ed.), Molecular biology of bacteriophage T4. ASM Press, Washington, DC.

23. **Cordonnier, C., and G. Bernardi**. 1965. Localization of *E. coli* endonuclease I. Biochem. Biophys. Res. Commun. **20**:555-559.

24. **Cornett, J. B., and M. Vallee.** 1973. The map position of the immunity (*imm*) gene of bacteriophage T4. Virology **51**:506-508.

25. **Daegelen, P., and E. Brody.** 1990. The *rIIA* gene of bacteriophage T4. I. Its DNA sequence and discovery of a new open reading frame between genes *60* and *rIIA*. Genetics **125**:237-248.

26. **Delbrück, M.** 1942. Interference between bacterial viruses: I. Interference between two bacterial viruses acting on the same host, and the mechanism of virus growth. Arch. Biochem. Biophys. **264**:1238-1244.

27. **Doermann, A. H.** 1948. Lysis and lysis inhibition of *Escherichia coli* bacteriophage. J. Bacteriol. **55**:257-276.

28. **Doermann, A. H.** 1952. The intracellular growth of bacteriophages. I. Liberation of intracellular bacteriophage T4 by premature lysis with another phage or with cyanide. J. Gen. Physiol. **35**:645-656.

29. **Dressman, H. K., and J. W. Drake**. 1999. Lysis and lysis inhibition in bacteriophage T4: *rV* mutations reside in the holin *t* gene. J. Bacteriol. **181**:4391-4396.

30. **Driukas, A., and R. Nivinskas**. 2003. Studies on the expression of gene *rIII* and *30.9* of bacteriophage T4 *in vivo*. Biologijia **3**:13-15.

31. **Duckworth, D. H**. 1971. Inhibition of T4 bacteriophage multiplication by superinfecting ghost and the development of tolerance after bacteriophage infection. J. Virol. **7**:8-14.

32. **Duckworth, D. H**. 1974. Who discovered bacteriophage? Bacteriological Reviews **40**:793-802.

33. **Eiserling, F. A.** 1983. Structure of T4 Virion, p. 11-24. *In* C. K. Mathews, E. Kutter, G. Mosig, and P. B. Berget (ed.), Bacteriophage T4. ASM Press, Washington, DC.

34. **Eiserling, F. A., and L. W. Black**. 1994. Pathways in T4 Morphogenesis, p. 209-212. *In* J. D. Karam (ed.), Molecular biology of bacteriophage T4. ASM Press, Washington, DC.

35. **Emrich, J.** 1968. Lysis of T4-infected bacteria in the absence of lysozyme. Virology **35**:158-165.

36. **Emrich, J., and G. Streisinger**. 1968. The role of phage lysozyme in the life cycle of phage T4. Virology **36**:387-391.

37. **Ennis, H. L., and K. D. Kievitt**. 1973. Association of the RIIA protein with the bacterial membrane. Proc. Natl. Acad. Sci. USA **70**:1468-1472.

38. **Evrard, C., J. Fastrez, and J. P. Declercq**. 1998. Crystal structure of the lysozyme from bacteriophage lambda and its relationship with V and C-type lysozymes. J. Mol. Biol. **76**:151-164.

39. **Fastrez, J.** 1996. Phage lysozymes, p. 35-64. *In* P. Jollès (ed.), Lysozymes: Model enzymes in biochemistry and biology. Birkhäuser Verlag, Basel.

40. **Fürste, J. P., W. Pansegrau, R. Frank, H. Blöcker, P. Scholz, M. Bagdasarian, and E. Lanka**. 1989. Molecular cloning of the plasmid RP4 primase region in a multi-host-range tacP expression vector. Gene **48**:119-131.

41. **Furukawa, H., and S. Mizushima**. 1982. Roles of cell surface components of *Escherichia coli* K-12 in bacteriophage T4 infection: interaction of tail core with phospholipids. J. Bacteriol. **150**:916-924.

42. **Goldberg, E., L. Grinius, and L. Letellier**. 1994. Recognition, attachment and injection, p. 347-356. *In* J. D. Karam (ed.), Molecular biology of bacteriophage T4. ASM Press, Washington, DC.

43. **Goldberg, E. B.** 1980. Bacteriophage nucleic acid penetration, p. 115-141. *In* L. L. P. L. Randall (ed.), Virus receptors. Receptor and recognition. Chapman & Hall, Ltd., London.

44. **Graschopf, A., and U. Blasi**. 1999. Functional assembly of the lambda S holin requires periplasmic localization of its N-terminus. Arch. Microbiol. **172**:31-39.

45. **Graschopf, A., and U. Blasi**. 1999. Molecular function of the dual-start motif in the lambda S holin. Mol. Microbiol. **33**:569-582.

46. **Grundling, A., U. Blasi, and R. Young**. 2000. Biochemical and genetic evidence for three transmembrane domains in the class I holin, lambda S. J. Biol. Chem. **275**:769-776.

47. **Grundling, A., U. Blasi, and R. Young**. 2000. Genetic and biochemical analysis of dimer and oligomer interactions of the lambda S holin. J. Bacteriol. **182**:6082-6090.

48. **Grundling, A., M. D. Manson, and R. Young**. 2001. Holins kill without warning. Proc. Natl. Acad. Sci. USA **98**:9348-9352.

49. **Hausman, R.** 1988. The T7 Group, p. 259-289. *In* R. Calendar (ed.), The bacteriophages. Plenum Press, New York, NY.

50. **Herriott, R. M., and J. L. Barlow**. 1957. Protein coats or "ghosts" of coli phage T2. II. The biological functions. J. Gen. Physiol. **41**:307-331.

51. **Hershey, A. D.** 1946. Mutation in bacteriophage with respect to the type of plaque. Genetics **31**:620-640.

52. **Hershey, A. D.** 1946. Spontaneous mutation in bacterial virus. Cold Spring Harb. Symp. Quant. Biol. **11**:67-77.

53. **Ho, K.** 2001. Bacteriophage therapy for bacterial infections. Rekindling a memory from the pre-antibiotics era. Perspectives in Biology and Medicine **44**:1-16.

54. **Ho, S. N., H. D. Hunt, R. M. Horton, J. K. Pullen, and L. R. Pease.** 1989. Site-directed mutagenesis by overlap extension using the polymerase chain reaction. Gene **77**:51-59.

55. **Höltje, J-V.** 1998. Growth of the stress-bearing and shape-maintaining murein sacculus of *Escherichia coli*. Microbiology and Molecular Biology Reviews **62**:181-203.

56. **Inouye, M., N. Arnheim, and R. Sternglanz**. 1973. Bacteriophage T7 lysozyme is an N-acetylmuramyl-L-alanine amidase. J. Biol. Chem. **248**:7247-7252.

57. **Isaac, D. D., J. S. Pinkner, S. J. Hultgren, and T. J. Silhavy**. 2005. The extracytoplasmic adaptor protein CpxP is degraded with substrate by DegP. Proc. Natl. Acad. Sci. USA **102**:17775-17779.

58. **Israeli, M., and M. Artman**. 1970. Leakage of b-galactosidase from phage-infected *Escherichia coli*: A re-evaluation. J. Gen. Virol. **7**:137-142.

59. **Jacob, F., and C. R. Fuerst**. 1958. The mechanism of lysis by phage studied with defective lysogenic bacteria. J. Gen. Physiol **18**:518-526.

60. **Jacobson, R. H., X. J. Zhang, R. F. DuBose, and B. W. Matthews**. 1994. Three-dimensional structure of beta-galactosidase from *E. coli*. Nature **369**:761-766.

61. **Josslin, R.** 1970. The lysis mechanism of phage T4: mutants affecting lysis. Virology **40**:719-726.

62. **Josslin, R.** 1971. Physiological studies on the *t* gene defect in T4-infected *Escherichia coli*. Virology **44**:101-107.

63. **Kai, T., H. Ueno, Y. Otsuka, W. Morimoto, and T. Yonesaki**. 1999. Gene *61.3* of bacteriophage T4 is the spackle gene. Virology **260**:254-259.

64. **Kanamaru, S., P. G. Leiman, V. A. Kostyuchenko, P. R. Chipman, V. V. Mesyanzhinov, F. Arisaka, and M. G. Rossman**. 2002. Structure of the cell puncturing device of bacteriophage T4. Nature **415**:553-557.

65. **Kao, S-H., and W. H. McClain**. 1980. Baseplate protein of bacteriophage T4 with both structural and lytic function. J. Virol. **34**:95-103.

66. **Kao, S-H., and W. H. McClain**. 1980. Role of bacteriophage T4 gene *5* and gene *s* products in cell lysis. J. Virol. **34**:104-107.

67. **Kim, D. Y., and K. K. Kim**. 2005. Structure and function of HtrA family proteins, the key players in protein quality control. J. Biochem. Mol. Biol. **38**:266-274.

68. **Koch, G., and W. J. Dreyer**. 1957. Characterization of an enzyme of phage T2 as a lysozyme. Virology **6**:291-293.

69. **Koch, G., and E. M. Jordan**. 1957. Killing of *E. coli* B by phage free T2 lysate. Biochim. Biophys. Acta **25**:437.

70. **Kolesky, S., M. Ouhammouch, E. N. Brody, and E. P. Geiduschek**. 1999. Sigma competition: the contest between bacteriophage T4 middle and late transcription. J. Mol. Biol. **291**:267-281.

71. **Kolisnychenko, V., G. Plunkett III, C. D. Herring, T. Fehér, J. Pósfai, F. R. Blattner, and G. Pósfai.** 2002. Engineering a reduced *Escherichia coli* genome. Genome Research **12**:640-647.

72. **Kolmar, H., P. R. Waller, and R. T. Sauer**. 1996. The DegP and DegQ periplasmic endoproteases of *Escherichia coli*: specificity for cleavage sites and substrate conformation. J. Bacteriol. **178**:5925-5929.

73. **Krojer, T., M. Garrido-Franco, R. Huber, M. Ehrmann, and T. Clausen**. 2002. Crystal structure of DegP (HtrA) reveals a new protease-chaperone machine. Nature **416**:455-459.

74. **Krylov, V. N.** 1966. A new *r* gene of bacteriophage T4B? Microb. Genet. Bull. **24**:4-5.

75. **Krylov, V. N., and N. K. Yanknovsky**. 1975. Mutation of the new gene *stIII* of bacteriophage T4B suppressing the lysis defect of gene *stII* and a gene *e* mutant. J. Virol. **15**:22-26.

76. **Krylov, V. N., and A. Zapadnaya**. 1965. Bacteriophage T4B *r* mutations sensitive to temperture (*rts*). Genetic **1**:7-11.

77. **Kutter, E., B. Guttman, and K. Carlson**. 1994. The transition form host to phage metabolism after T4 infection, p. 343-356. *In* J. D. Karam (ed.), Molecular biology of bacteriophage T4. ASM Press, Washington, DC.

78. **Kutter, E., T. Stidham, B. Guttman, E. Kutter, D. Batts, S. Peterson, T. D. Javakhishvili, F. Arisaka, V. Mesyanzhinov, W. Rüger, and G. Mosig**. 1994. Genomic map of bacteriophage T4, p. 491-518. *In* J. D. Karam (ed.), Molecular biology of bacteriophage T4. ASM, Washington, DC.

79. **Lederberg, J.** 1952. Lysogenicity in *E. coli* K-12. Genetics **36**:560-573.

80. **Lipinska, B., M. Zylicz, and C. Georgopoulos**. 1990. The HtrA (DegP) protein, essential for *Escherichia coli* survival at high temperatures, is an endopeptidase. J. Bacteriol. **172**:1791-1797.

81. **Loessner, M. J., G. Wendlinger, and S. Scherer**. 1995. Heterogeneous endolysins in *Listeria monocytogenes* bacteriophages: a new class of enzymes and evidence for conserved holin genes within the siphoviral lysis cassettes. Mol. Microbiol. **16**:1231-1241.

82. **Los, M., G. Wegrzyn, and P. Neubauer**. 2003. A role for bacteriophage T4 *rI* gene function in the control of phage development during pseudolysogeny and in slowly growing host cells. Res. Microbiol. **154**:547-552.

83. **Lu, M. J., and U. Henning**. 1989. The immunity (*imm*) gene of *Escherichia coli* bacteriophage T4. J. Virol. **63**:3472-3478.

84. **Lu, M. J., and U. Henning**. 1992. Lysis protein T of bacteriophage T4. Mol. Gen. Genet. **235**:253-258.

85. **Lu, M. J., Y. D. Stierhof, and U. Henning**. 1993. Location and unusual membrane topology of the immunity protein of the *Escherichia coli* phage T4. J. Virol. **67**:4905-4913.

86. **Lutz, R., and H. Bujard.** 1997. Independent and tight regulation of transcriptional units in *Escherichia coli* via the LacR/O, the TetR/O and AraC/I1-I2 regulatory elements. Nucleic Acids Res. **25**:1205-1210.

87. **Lwoff, A.** 1953. Lysogeny. Bacteriological Reviews **17**:269-337.

88. **Mathew, B. W.** 1996. Structural and genetic analysis of the folding and function of T4 lysozyme. FASEB J. **10**:35-41.

89. **Mathews, C. K.** 1994. An overview of the T4 developmental program, p. 1-8. *In* J. D. Karam (ed.), Molecular biology of bacteriophage T4. ASM Press, Washington, DC.

90. **McPheeters, D. S., A. Christensen, E. T. Young, G. Stormo, and L. Gold**. 1986. Translational regulation of expression of the bacteriophage T4 lysozyme gene. Nucleic Acids Res. **14**:5813-5826.

91. **Meerman, H. J., and G. Georgious**. 1994. Construction and characterization of a set of *E. coli* strains deficient in all known loci affecting the proteolytic stability of secreted recombinant proteins. Bio/Technology **12**:1107-1110.

92. **Miller, E. S., E. Kutter, G. Mosig, F. Arisaka, T. Kunisawa, and W. Ruger**. 2003. Bacteriophage T4 genome. Microbiology and Molecular Biology Reviews **67**:86-156.

93. **Model, P., and M. Russel**. 1988. Filamentous bacteriophage, p. 375-456. *In* R. Calendar (ed.), The bacteriophages. Plenum Press, New York, NY.

94. **Moody, M. F.** 1973. Sheath of bacteriophage T4. 3. Contraction mechanism deduced from partially contracted sheaths. J. Mol. Biol. **80**:613-635.

95. **Mosig, G., and F. Eiserling**. 2006. T4 and related phages: Structure and development, p. 225-267. *In* R. Calendar (ed.), The bacteriophages, Oxford University Press, Inc., New York, NY.

96. **Mukai, F., G. Streisinger, and B. Miller**. 1967. The mechanism of lysis in phage T4-infected cells. Virology **33**:398-404.

97. **Murray, N. E., W. J. Brammar, and K. Murray**. 1977. Lambdoid phages that simplify the recovery of in vitro recombinants. Mol. Gen. Genet. **150**:53-61.

98. **Nakagawa, H., F. Arisaka, and S-I. Ishii**. 1985. Isolation and characterization of the bacteriophage T4 tail-associated lysozyme. J. Virol. **54**:460-466.

99. **Nene, V., and R. E. Glass**. 1981. Direct measurement of absolute suppressor efficiency. Bioscience Reports **1**:571-574.

100. **Paddison, P., S. T. Abedon, H. K. Dressman, K. Gailbreath, J. Tracy, E. Mosser, J. Neitzel, B. Guttman, and E. Kutter**. 1998. The roles of the bacteriophage T4 *r* genes in lysis inhibition and fine-structure genetics: A new perspective. Genetics **148**:1539-1550.

101. **Park, J. T.** 2001. Identification of a dedicated recycling pathway for anhydro-N-acetylmuramic acid and N-acetylglucosamine derived from *Escherichia coli* cell wall murein. J. Bacteriol. **183**:3842-3847.

102. **Park, T., D. K. Struck, J. F. Deaton, and R. Young**. 2006. Topological dynamics of holins in programmed bacterial lysis. Proc. Natl. Acad. Sci. USA **103**:19713-19718.

103. **Peterson, R. F, K. D. Kievitt, and H. L. Ennis**. 1972. Membrane protein synthesis after infection of *Escherichia coli* B with phage T4: the RIIB protein. Virology **50**:520-527.

104. **Pribnow, D., D. C. Sigurdson, L. Gold, B. S. Singer, C. Napoli, J. Brosius, T. J. Dull, and H. F. Noller**. 1981. *rII* cistron of bacteriophage T4. DNA sequence around the intercistronic divide and position of genetic landmark. J. Mol. Biol. **149**:337-376.

105. **Raab, R., G. Neal, J. Garrett, R. Grimaila, R. Fusselman, and R. Young**. 1986. Mutational analysis of bacteriophage lambda lysis gene *S*. J. Bacteriol. **167**:1035-1042.

106. **Raab, R., G. Neal, C. Sohaskey, J. Smith, and R. Young**. 1988. Dominance in lambda S mutations and evidence for translational control. J. Mol. Biol. **199**:95-105.

107. **Ramanculov, E.** 2001. Bacteriophage T4 Lysis and Lysis Inhibition: A molecular perspective. Ph.D. dissertation Texas A&M University, College Station.

108. **Ramanculov, E., and R. Young**. 2001. Genetic analysis of the T4 holin: timing and topology. Gene **265**:25-36.

109. **Ramanculov, E., and R. Young**. 2001. Functional analysis of the phage T4 holin in a lambda context. Mol. Genet. Genomics **265**:345-353.

110. **Ramanculov, E., and R. Young**. 2001. An ancient player unmasked: T4 *rI* encodes a t-specific antiholin. Mol. Microbiol. **41**:575-583.

111. **Raudonikiene, A., and R. Nivinskas**. 1992. Gene *rIII* is the nearest downstream neighbour of bacteriophage T4 gene *31*. Gene **114**:85-90.

112. **Raudonikiene, A., and R. Nivinskas**. 1993. The sequences of gene *rIII* of bacteriophage T4 and its mutants. Gene **134**:135-136.

113. **Riede, I**. 1987. Lysis gene *t* of T-even bacteriophage: Evidence that colicins and bacteriophage genes have common ancestors. J. Bacteriol. **169**:2956-2961.

114. **Riede, I.** 1987. Receptor specificity of the short tail fibers (gp*12*) of T-even type *Escherichia coli* phages. Mol. Gen. Genet. **206**:110-115.

115. **Rutberg, B., and L. Rutberg**. 1965. Role of superinfecting phage in lysis inhibition with phage T4 in *Escherichia coli*. J. Bacteriol. **90**:891-894.

116. **Rutberg, L., and B. Rutberg**. 1964. On the expression of the *rII* mutation of T-even bacteriophages in *Escherichia coli* strain B. Virology **22**:280-281.

117. **Salton, M. R**. 1957. The properties of lysozyme and its action on microorganisms. Bacteriological Reviews **21**:82-99.

118. **Shapira, A., E. Giberman, and A. Kohn.** 1974. Recoverable potassium fluxes variations following adsorption of T4 phage and their ghosts on *Escherichia coli* B. J. Gen. Virol. **23**:159-171.

119. **Shinedling, S., D. Parma, and L. Gold**. 1987. Wild-type Bacteriophage T4 is restricted by the lambda *rex* genes. J. Virol. **61**:3790-3794.

120. **Siegele, D. A., and J. C. Hu**. 1997. Gene expression from plasmids containing the *ara*BAD promoter at subsaturating inducer concentrations represents mixed populations. Proc. Natl. Acad. Sci. USA **94**:8168-8172.

121. **Silhavy, T. J., and M. L. Berman**. 1984. Bacterial strains, p. xi-xiii. *In* T. J. Silhavy and M. L. Berman (ed.), Experiments with gene fusions. Cold Spring Harbor Laboratory Press, Cold Spring Harbor, NY.

122. **Silver, S., E. Levine, and P. M. Spielman**. 1968. Cation fluxes and permeability changes accompanying bacteriophage infection of *Escherichia coli*. J. Virol. **2**:763-771.

123. **Simon, L. D., and T. F. Anderson**. 1967. The infection of *Escherichia coli* by T2 and T4 bacteriophage as seen in the electron microscope. I. Attachment and penetration. Virology **32**:279-297.

124. **Singer, B. S., S. T. Shinedling, and L. Gold**. 1983. The *rII* genes: a history and a prospectus, p. 327-333. *In* C. K. Mathews, E. M. Kutter, G. Mosig, and P. B. Berget (ed.), Bacteriophage T4. ASM, Washington, DC.

125. **Slavcev, R. A., and S. Hayes**. 2004. Overexpression of *rexA* nullifies T4*rII* exclusion in *Escherichia coli* K(λ) lysogen. Can. J. Microbiol. **50**:133-136.

126. **Smith, D. L., and R. Young.** 1998. Oligohistidine tag mutagenesis of the λ holin gene. J. Bacteriol. **180**:4199-4211.

127. **Snyder, L., and G. Kaufmann**. 1994. T4 phage exclusion mechanism, p. 391-396. *In* J. D. Karam (ed.), Molecular biology of bacteriophage T4. ASM Press, Washington, DC.

128. **Snyder, L., and K. McWilliams**. 1989. The *rex* genes of bacteriophage lambda can inhibit cell function without phage superinfection. Gene **81**:17-24.

129. **Stent, G. S.** 1963. The Twort-D'Herelle phenomenon, p. 1-21. *In* R. Emerson, D. Kenedy, R. B. Park, G. Beadle, and D. M. Whiaker (ed.), Molecular biology of bacterial virus. W. H. Freeman and Company, San Francisco and London.

130. **Strauch, K. L., and J. Beckwith**. 1988. An *Escherichia coli* mutation preventing degradation of abnormal periplasmic proteins. Proc. Natl. Acad. Sci. USA **85**:1576-1580.

131. **Strauch, K. L., K. Johnson, and J. Beckwith**. 1989. Characterization of *degP*, a gene required for proteolysis in the cell envelope and essential for growth of E*scherichia coli* at high temperature. J. Bacteriol. **171**:2689-2696.

132. **Streisinger, G., F. Mukai, W. J. Dreyer, B. Miller, and S. Horiuchi**. 1961. Mutations affecting the lysozyme of phage T4. Cold Spring Harb. Symp. Quant. Biol. **26**:25-30.

133. **Tran, T. A., D. K. Struck, and R. Young**. 2005. Periplasmic domains define holin-antiholin interactions in T4 lysis inhibition. J. Bacteriol. **187**:6631-6640.

134. **Tsugita, A., and M. Inouye**. 1968. Complete primary structure of phage lysozyme from *Escherichia coli* T4. J. Mol. Biol. **37**:201-212.

135. **Vallee, M., and J. B. Cornett**. 1972. A new gene of bacteriophage T4 determining immunity against superinfecting ghost and phage T4-infected *Escherichia coli*. Virology **48**:777-784.

136. **Vallee, M., J. B. Cornett, and H. Bernstein**. 1972. The action of bacteriophage T4 ghost on *Escherichia coli* and the immunity to this action developed in cells preinfected with T4. Virology **48**:766-776.

137. **van Wezenbeek, P. M., T. J. Hulsebos, and J. G. Schoenmaker** 1980. Nucleotide sequence of the filamentous bacteriophage M13 DNA genome: Comparison with phage fd. Gene **11**:129-148.

138. **Visconti, N.** 1953. Resistance to lysis from without in bacteria infected with T2 bacteriophage. J. Bacteriol. **66**:247-253.

139. **Wang, I. N., J. Deaton, and R. Young**. 2003. Sizing the holin lesion with an endolysin-β-galactosidase fusion. J. Bacteriol. **185**:779-787.

140. **Wang, I. N., A. E. Dykhuizen, and L. B. Slobodkin**. 1996. The evolution of phage lysis timing. Evolution Ecology **10**:545-558.

141. **Wang, I. N., D. L. Smith, and R. Young**. 2000. Holins: the protein clocks of bacteriophage infections. Annu. Rev. Microbiol. **54**:799-825.

142. **Weaver, L. H., and B. W. Matthews**. 1987. Structure of bacteriophage T4 lysozyme refined at 1.7 Å resolution. J. Mol. Biol. **193**:189-199.

143. **Weintraub, S. B, and F. R. Frankle.** 1972. Identification of the T4*rIIB* gene product as a membrane protein. J. Mol. Biol. **70**:589-615.

144. **Xu, M., A. Arulandu, D. K. Struck, S. Swanson, J. C. Sacchettini, and R. Young**. 2005. Disulfide isomerization after membrane release of its SAR domain activates P1 lysozyme. Science **307**:113-117.

145. **Xu, M., D. K. Struck, J. Deaton, I. N. Wang, and R. Young**. 2004. A signal-arrest-release sequence mediates export and control of the phage P1 endolysin. Proc. Natl. Acad. Sci. USA **101**:6415-6420.

146. **Young, R.** 1992. Bacteriophage lysis: mechanism and regulation. Microbiol. Rev. **56**:430-481.

147. **Young, R.** 2000. Phages will out: strategies of host cell lysis. Trends. Microbiol. **8**:120-128.

148. **Young, R.** 2002. Bacteriophage holins: deadly diversity. J. Mol. Microbiol. Biotechnol. **4**:21-36.

149. **Zagotta, M. T., and D. B. Wilson**. 1990. Oligomerization of the bacteriophage lambda S protein in the inner membrane of *Escherichia coli*. J. Bacteriol. **172**:912-921.

VITA

Tram Anh Thi Tran received her Bachelor of Science degree in biology and chemistry from Stephen F. Austin State University in the fall of 1998. In spring of 1999, she entered the Biotechnology program at the same university and received the Master of Science degree in 2001. In the fall of 2000, she started her doctorate study in biochemistry at Texas A&M University and received her Ph.D. in the spring of 2007. Her research focuses on the mechanism of bacteriophage T4 lysis and lysis inhibition.

Ms. Tran may be reached at Texas A&M University, TAMU 2128, Bio/Bio 315, College Station, TX 77843. Her e-mail address is anhtran@neo.tamu.edu